Politecnico di Torino

Department of Mechanical and Aerospace Engineering

Master of Science in Automotive Engineering

Master's Thesis:

Development of a Fuel Cell Electric Vehicle Powertrain for Airport Applications

Academic supervisor:
Andrea Tonoli

Academic co-supervisor:
José María López Martínez

Candidate:
Gabriele Segale s282580

Academic Year 2022-2023

Aim

What is described in this Master thesis is a part of a project of development and adaptation into Fuel Cell Electric Vehicle (FCEV) of an off-road Plug-in Hybrid Electric Vehicle (PHEV) present at the research centre of the Polytechnic University of Madrid, called INSIA, with the goal of change the conventional powertrain of an airport "Follow me" vehicle into the new hybrid one to test, evaluate and validated it. The parts of the development described in this thesis are the analysis of powertrain and driving mission data, the dimensioning of components and the fine-tuning of the control algorithms for the energy management strategy. This project aims to generate knowledge, for every sector and entity involved, related to the topic of hydrogen as power source, fuel cell vehicles and viability, convenience and effectiveness of this solution for a particular class of vehicle: the airport "Follow me" vehicle, for assistance and guiding of aircraft on runways.

This project is subsidised by the Spanish government and directed by the Community of Madrid (CM) and CIEMAT (Centre for Energy, Environmental and Technological Research), in cooperation with different institutions such as the Technical University of Madrid (UPM) and the Adolfo Suarez Madrid-Barajas airport, managed by the AENA group. This airport hybrid electric vehicle using fuel cells is to be realised in a prototype manner, with the aim of replicating the performance of the current conventional vehicle in operation and demonstrating that it can be not only an effective solution within the runways of Madrid airport, with the idea of conceptually replacing the current "Follow me" car with diesel internal combustion engine, but also beneficial in terms of environmental impacts.

The activity in which the research centre INSIA is participating, more specifically its Environmental Impact and Traction Systems

Department, is part of the "GreenH2" project and is a public grant competition promoted by CM and CIEMAT, called "Pilas de combustible: diseño, construcción y operación de una instalación para la realización de ensayos de trenes de potencia que integren pilas de combustible en el sector naval y aéreo". Within it, various activities are promoted for the climate safeguard and to comply with the 2050 European programme of decarbonisation, including the one that INSIA-UPM joined, which specifically concerns the "development of a powertrain for port and/or airport applications". The research centre, having joined the project, contacted AENA, the Spanish public company that manages airports and their infrastructures throughout the country, to collaborate on this initiative.

The objective of this activity, therefore, will be to present the first substantial steps in the long project of development and adaptation of this airport FCEV prototype, explaining the main results obtained in the various phases and the methods used to achieve them. Even though the project has not yet been completed, since it is scheduled for completion in 2025, what present in this thesis can be useful to understand which is the process of design and management of FCEV powertrain elements and its features, advantages and disadvantages with respect to the current combustion powertrain.

Methodology

The thesis will be developed in 6 different Chapters, each of them with specific objectives for composing the overall activity of literature and market research, powertrain data analysis, component dimensioning, design and fine-tuning of the EMS and results analysis. The Chapters will be the following:

- *Chapter 1*: a general introduction related to basic aspects which will be analysed, which concern the environmental issues that society is dealing with today, measures that have been taken at public and private level and commitment that each protagonist of this activity will provide. The type of vehicle the project is aimed at will be presented and it will be explained why an alternative solution is studied. Finally, a brief theoretical outline revising the literature on the functioning and composition of fuel cells and FCEVs, with main advantages and disadvantages, will be covered as state of the art.
- *Chapter 2*: current market situation for the airport sector, with a focus on electromobility and in particular on FCEVs. Will be analysed the airport sector's need to invest more in electromobility solutions, defining main environmental and legislative causes. Results that are expected in the future will be briefly presented. Finally, solutions currently existing in the airport sector will be reviewed, both with regard to BEVs and FCEVs.
- *Chapter 3:* analysis of the vehicle's driving mission and powertrain data coming from sensors placed inside the real "Follow me" car. Will be treated the processing of these data, with the relevant calculations performed, and the actual analysis using two different approaches: based on the single driving mission or on the entire operative day. Results of them make possible to outline the characteristics of the vehicle currently in use, as well as forming the basis for the definition of FCEV powertrain requirements.

- *Chapter 4:* definition of performance, power, energy and consumption requirements of the hybrid powertrain, in order to obtain the proper sizing and selection of the elements composing it. Thanks to the data analysis, will be explained the requirements of the FCEV propulsion system, necessary to recreate the performance of the original ICE vehicle. With them, it will be possible to present the expected vehicle architecture, with all its characteristics and also the ones of all the elements that will compose it. Finally, will be specified which actual components will be selected from the market for future purchase, installation and setting up.
- *Chapter 5:* creation and fine-tuning of the energy management strategy which will be implemented in the FCEV. After a brief theoretical overview of EMSs, the one that will be used within the FCEV control unit will be explained in detail, considering its nature, composition and goals. The methodology used for its creation and fine-tuning will be presented, as well as its state-flow structure and the algorithms that make up its operation.
- *Chapter 6:* presentation of the results obtained so far from simulations with the longitudinal dynamics model of the FCEV "Follow me" with the EMS tailor-made for its control. Comparison with the results obtained with the same simulations carried out with a BEV "Follow me", to show some differences between the two architectures. Finally, a summary of the results achieved so far during the course of the activity is shown, as well as an analysis of the objectives achieved and the next steps of the project.

Table of Content

List of Figures

List of Tables

Nomenclature

Symbol	Description
EV	Electric vehicle
BEV	Battery electric vehicle
HEV	Hybrid electric vehicle
PHEV	Plug-in hybrid electric vehicle
FCEV	Fuel cell electric vehicle
ICE	Internal combustion engine
GPS	Global positioning system
GNSS	Global navigation satellite system
IMU	Inertial measurement unit
CAN	Controller area network
SD	Secure digital
RTC	Real-time clock
EMS	Energy management strategy
UN	United nations
COP21	21th climate conference of Paris
SDG	Sustainable development goal
GHG	Green-house gas
GSE	Ground support equipment
PAC	Plan of action
DC	Direct current
AC	Alternate current
PWM	Pulse width modulation
SPM	Synchronouys permanent magnet
LV	Low voltage
HV	High voltage
EM/eM	Electric motor
PMS	Permanent magnets synchronous
FC	Fuel cell
PEM	Proton exchange membrane

PEMFC	Proton exchange membrane fuel cell
ESS	Energy storage system
BoP	Balance of Plant
MEA	Membrane electrode assembly
AAI	Airport authority of India
RE	Range Extender
LF	Load Follower
HM	Hybrid Mode
P-ReFCEV	Plug-in Range-Extender Fuel Cell Vehicle
FEMS	"Follow me" Energy Management Strategy
BTM	Battery Traction Mode
HTM	Hybrid Traction Mode
HRM	Hybrid Regeneration Mode
BCM	Battery Charging Mode
PDB	Power Distribution Box
HIL	Hardware-in-the-loop

Chapter 1: Introduction

In this chapter will be given a general and complete introduction related to the basic aspects which will be analysed in this thesis.

They concern the environmental issues that society is dealing with today, the measures that have been taken at public and private level and the commitment that each protagonist of this activity will provide. The type of vehicle the project is aimed at will be presented and it will be explained why an alternative solution is being studied. Finally, a brief theoretical outline, revising the literature, on the functioning and composition of fuel cells and FCEVs, with their main advantages and disadvantages, will be covered as state of the art.

1.1. Sustainability goals for each sector

1.1.1. Agreements for climate protection

The United Nations (UN) Paris Climate Conference (COP21) in December 2015 concluded with the first universal and legally binding agreement on climate change, setting out a global framework to avoid dangerous climate change by keeping global warming well below 2°C. In this context, the EU confirmed to the international community its target to reduce greenhouse gas emissions by 40 per cent by 2030. Based on this agreement, the UN endorsed a set of targets for growth (United Nations Development Program, 2021) [4]. There are 17 goals, called Sustainable Development Goals (SDGs), to eliminate poverty and address social, economic and environmental issues on the planet. The 17 SDGs were developed based on three main components of the concept of sustainability: social, economic and ecological. These goals can be adopted by any country and organization for its own sustainable plans [5]. The Paris Agreement legally binds the participating countries to act against global warming, and consequently they have defined strategies to reduce greenhouse gas (GHG) emissions in all their sectors. The Spanish government promotes compliance with these objectives through its draft laws on climate change and energy transition.

1.1.2. Outline of the GreenH2 project

The participation of the CM in the execution of the Complementary Renewable Energy and Hydrogen Plan is carried out through the project "Strategic Positioning of The Community of Madrid in R+D+I in Green Hydrogen and Fuel Cells" (abbreviated as GreenH2), led by CIEMAT and carried out in cooperation with different institutions, like the ones presented in the following subsections. Among the various activities promoted, the one referred to in the following thesis is the LIA7 "Hydrogen uses in the heavy transport, aviation and shipping sectors". For the activity in question, it was necessary to choose an airport vehicle among all those circulating between the airport runways, to proceed with the development of its powertrain in the form of fuel cell propulsion and the creation of an effective prototype. To choose an appropriate vehicle for the activity, was necessary to consider several aspects, trying to select a candidate for which a conversion to a sustainable propulsion system would bring a great benefit. Moreover, since the creation of the prototype includes the entire vehicle, also considering the adaptation of one vehicle already present in the establishment is crucial, since it can reduce the economic effort and time required for its production. The airport support vehicle "Follow me" was chosen at the end, because it is used extensively within the airport, has a high operating time and travels long distances each day. In terms of use, a "Follow me" is most often used at low speed or idling, conditions which generate a high level of pollution. These characteristics make it an ideal candidate for a fuel cell propulsion system, enabling environmentally useful results. Furthermore, the architecture of the "Follow me" vehicle at Adolfo Suárez Madrid-Barajas airport is very similar to that of a vehicle already present at INSIA, both of comparable size and with four-wheel drive, which can be used for the adaptation and creation of the hybrid propulsion system.

1.1.3. Commitment of AENA

The research centre, having joined the project, contacted AENA, the Spanish public company that manages airports and their infrastructures throughout the country, to collaborate on this initiative. This company manages 46 airports in Spain and collaborates directly or indirectly in the management of 23 others in different countries around the world [1][2]. Of the total global GHG emissions, the aviation sector accounts for approximately 2.5%. However, 95% of these emissions are generated by aircraft, while the rest are attributable to other fields of airports, involving numerous agents in the whole picture [2]. This 5% therefore also includes the various GSE vehicles, also the "Follow me" on which this activity is directed. Although the greatest effort is therefore focused on the energy efficiency of aircraft and its direct systems, it is important to achieve sustainability goals by working on every field. To give an example of how airports are dealing with the problem, AENA in its PAC (Climate Action Plan), in addition to the actions aimed at sustainable aviation, which have a (hypothetical) weight of 55% in what is the goal of reducing GHG emissions, there are many more initiatives. These include fields such as renewable energy production, air conditioning, use of biofuels, car sharing, promotion of public transport, optimisation of logistics, public information and, of course, GSE vehicles electrification [2]. This field, albeit in its own small way, can contribute to global decarbonisation. Furthermore, AENA relies on scientific research and university collaborations to expand knowledge on the possibilities of alternative energy sources, including hydrogen. In the near future, when the technology will be more mature and the infrastructure will be more in place throughout the country, this type of solution may be exploited by the company's airports to continue and consolidate the path towards decarbonisation.

1.1.4. Commitment of airport Adolfo Suárez Madrid-Barajas

Regarding the specific case of Madrid Airport, which has provided its "Follow me" vehicle, part of its Ground Support Equipment (GSE), for the measurements needed to develop the project, AENA has implemented its own climate action plan "Plan de acción climática (PAC)" for its airports, in line with the SDGs promoted by the United Nations. This plan has the goal of airports achieving carbon neutrality in 2026 and zero emissions (carbon-free) in 2040. In addition, in Spain there are 8 airports in AENA that are submitted to the ACA (Airport Carbon Accreditation) programme, the only global programme with institutional support for carbon certification, always in line with the COP21 commitments. ACA independently assesses and recognises airports that are at different stages of their journey towards comprehensive carbon emission reductions [6]. Obviously, Adolfo Suarez Madrid-Barajas airport is one of the 8 airports regularly enrolled in the programme and consequently aligns its strategic model with the 17 UN SDGs, with a particular commitment to SDG number 13: Climate Action.

Figure 1: Sustainable Development Goals of the 2030 Agenda of United Nations [2].

1.1.5. Commitment of INSIA

INSIA, for its part, will offer its own vehicle, designed by the research centre itself, called in the past "Innvextran", for the realisation of this new project. This particular vehicle, built for a past activity, is an off-road four-wheel-drive vehicle, featuring a special Plug-in Series-Hybrid powertrain, with a 30kW electric motor and a generator powered by a 1.0L gasoline engine. Built on the basis of an IVECO Massif in Santana Motor's facilities in Linares

(Spain), the Innvextran has 76 hp and is capable of achieving a continuous torque of 200 Nm and a range in electric mode of around 60 km. Its creation was financed by another national public-private cooperation programme, called "Plan nacional de investigación científica, desarrollo e innovación tecnológica 2008-2011", in which participated INSIA and other two partners, Mecacontrol and Cetmet. The idea of this project was to create a functional prototype of an off-road range-extender hybrid, so that such a car would go into production in small series, allowing different configurations to meet the different needs of possible customers. It is currently in the process of being legalised and available to major brands that want to take an interest in its commercialisation. [7].

Figure 2: Off-road Plug-in Series-Hybrid Electric Vehicle "Innvextran" [7]

The vehicle structure consists of the main components listed in the following Table 1:

Component	Specification	Model
Liquid-cooled AC induction motor	30kW rated power and 320Vdc nominal capacity	A200-250 by MES-DEA
$LiFePO_4$ DC battery	3Vdc single cell nominal capacity for a total of 320Vdc	WB-LY100 AHA by Santana
Battery charger	320Vdc nominal capacity	PAP3200 by Powerfinn
Motor controller	400V nominal capacity	EV/HEV-MC 230/400 by Kolektor

Traction inverter module	PMW modulation	TIM 300W by MES-DEA
Gasoline engine	3 cylinders 0.962L 20.9kW rated power	WG972 by Kubota
Liquid-cooled SPM generator	160Vdc nominal capacity for 45kW continuous output power @7000tpm	By Kolektor
Control unit for various safety components control		ESX LT by STW Mobile Machine

Table 1: Main components composing the architecture of the Innvextran

In order to give an outlook of the actual propulsion system and driveline present in the vehicle to be adapted, the following scheme (Figure 3) is proposed.

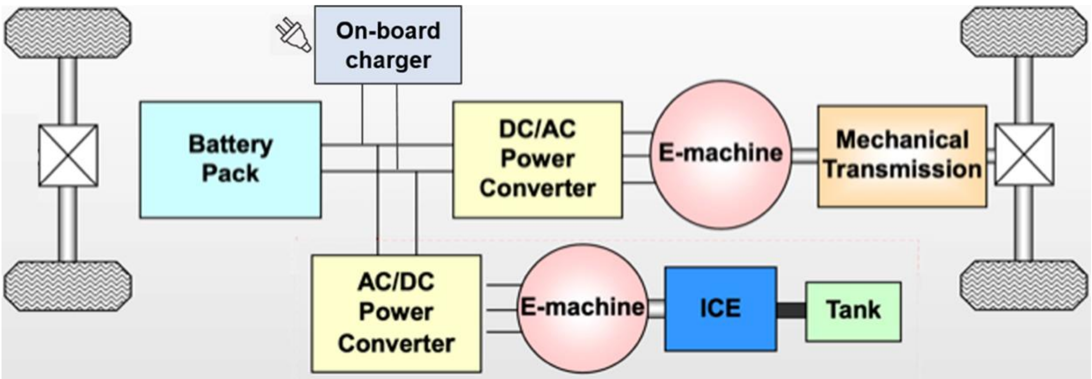

Figure 3: Representative scheme of the Plug-in Series-HEV architecture with its main elements [8]

In that model is possible to see the 4WD driveline the mechanical transmission and wheels. As far as traction system is concerned, there is the main propulsion electric line consisting of the E-machine working as motor and the battery, which is flanked by the thermal hybrid unit consisting of the E-machine working as generator and ICE.

1.2 "Follow me" vehicle

1.2.1. Vehicle function

Madrid Airport has made its airport GSE vehicle available to undergo the series of measurements to collect data for the powertrain on which the simulations will be carried out: it is a Ford Ranger Diesel Euro 6, shown below in Figure 4. Such a GSE vehicle is called "Follow me" and performs the functions of aircraft marshalling, i.e. the set of codified and internationally standardised procedures for visual communication between pilots and ground personnel at an airport. The marshallers often give directions to the pilot by driving this particular vehicle, which is conventionally yellow, or with a recognisable chequered pattern. Such cars are not required by law at airports but are now part of the standard marshalling service at larger ones and are usually purchased from external suppliers, through public competitions, being road vehicles that can be easily adapted to the airport task through third-party companies.

Figure 4: The Ford Ranger used in Madrid airport as "Follow me" vehicle [1]

Specifically, they perform the function of guiding the aircraft and its pilot, once the landing is complete, to its final destination within the airport, especially in conditions where the airport is unfamiliar to the pilot, or in adverse weather conditions, when visibility drops below 150 metres. If a pilot were to get lost or take too long to complete landing operations, this could put other flights at risk, as well as delay the airport's schedule, resulting in higher costs and major inconvenience to passengers and workers. They are equipped with an audio-visual device and a screen with a large illuminated "FOLLOW ME" sign, which is lit up when operating as a guide, so that it is visible to the pilot and can communicate messages to him, while the driver of the vehicle communicates with the pilot himself and with the airport control tower [9]. While they are not engaged with any aircraft, these vehicles perform another function: that of checking the runway, verifying its condition and giving directions to other vehicles and personnel. They therefore control the state of the tarmac, the presence of objects or the occurrence of emergency or unusual situations, which could endanger the movement of aircraft or other service vehicles. They are also used as guides for construction vehicles in the event of necessary repairs, as these work vehicles are usually contracted and are unfamiliar with the rules, structure and safety of the airport.

1.2.2. Possible vehicle's typologies

There is no law defining the segment, type and characteristics of this type of vehicle, so there have been various choices at every airport around the world in recent years. As mentioned earlier, a "Follow me" car is usually a road vehicle purchased by the airport, which would be intended for road use, that is then simply adapted to perform its marshalling function, with the addition of audio-visual communication systems. In this sense, the solutions are many and can vary between:

- Small segment: for example, Smart Fortwo in Austrian airport of Zeltweg or in the German airport of Stuttgart [10].
- Medium segment: the majority of the solutions used.
- Pick-up: like the vehicle used in Madrid airport and many others.
- Commercial vehicles: for example, Volkswagen Multivan in German airport of Hamburg [11].
- Hypercars: for example, Porsche Cayman in the German airport of Hannover or Lamborghini Huracan EVO in the Italian airport of Bologna [12].

The same applies to the type of powertrain and power source, with the main solution until recent years always being the diesel combustion car, both in terms of availability and simplicity.

Figure 5: Examples of "Follow me" vehicles used in other airports [10][12]

1.2.3. Vehicle driving mission´s features

Within the various airport GSE vehicles, AENA mentions that the "Follow me" one travels between 150 and 300km each day, depending on the size of the airport, reaching the end of its useful life within the runways in about 6 years. In addition, according to airport safety regulations, the maximum speed of these vehicles in their movement area is limited to 30km/h, while in other areas within the airport complex it can be higher, at the discretion of the signalling [13]. Most "Follow me" vehicles driving mission consequently consist of short periods of high-load operation followed by extended periods of low-load, idle or engine OFF, before or after completing their task with the airplane, to give directions, to check tracks or to move personnel. In particular, idling in those vehicles is a common practice, primarily as a convenience to the operator to maintain the equipment in a ready mode and avoid lengthy warm-up periods, especially in cold climates. Such methods of operation consequently lead to "Follow me" cars being driven for a high amount of time of total use at low revs or in idling, consuming a lot of fuel and generating high emissions. This operation is extremely inefficient for an ICE, when the current goal of decarbonisation is progressing very rapidly towards a zero-emission goal in 2040. Precisely for this reason, this type of airport vehicle has in recent years undergone a powertrain change towards electromobility or alternative sources.

1.3. State of art of fuel cell electric vehicle

1.3.1. Carbon-free energy sources

As the interest and concern about dangerous climate situation find in society nowadays an increases, every sector, including the airport one, is trying to make its contribution in the fight to limit damages and reverse the trend. As far as ground mobility is concerned, increased efficiency, biofuels and electrification are the strategies currently being employed at every opportunity, with the last gaining in importance continuously as technology grows over the years. With regard to GHG emissions, it is well known that the transport sector is responsible for about 1/3 of the total, due to the characteristics of the fossil fuels still widely used today and the efficiency limits of the technology that is able to exploit them. The search for non-polluting energy sources in this area can be a solution in the short and long term for the climate, especially when it comes to electricity produced in a renewable or low-emitting manner. These resources can be widely used also for airport GSE, varying between the different types of typologies that are present on the market.

1.3.2. Fuel Cell Electric Vehicle and Energy Storage Systems

One type of electric vehicle is the hydrogen Fuel Cell Electric Vehicles (FCEV), where an electric motor is used to provide the driving power, instead of an internal combustion engine. However, these electric vehicles do not require external charging to supply batteries with the energy needed for traction, but are able to produce it directly on board, thanks to fuel cells (FC). In these cells, hydrogen as fuel together with air give rise to an electrochemical reaction, which can be described as inverse electrolysis, without causing any combustion, to generate electricity as traction energy and water as the only product for exhaust. This type of propulsion has several advantages, as will be discussed more precisely later and compared to the pure electric vehicle, this typology can achieve a more extended range with a shorter charging time. [14]. Nevertheless, it has also some drawbacks: the energy and specific power of a FC gives lower values than those produced by a combustion engine and such systems have slow dynamics and when faced with fast transients, such as start-ups, accelerations or climbing, they struggle to follow the energy demands of the vehicle. As a result, fuel cells are not the type of technology that is capable, on its own, of taking over the complete task of moving a vehicle of the typical weight and size of a road vehicle.In fact, FCEVs contain in the architecture an energy-storage system (ESS) to provide the dynamic power and extend the life of FCs, as well as to store regenerative braking energy, which FCs cannot do because they are monodirectional, can't store energy inside. The most common ESS is the battery, but ultracapacitors or a combination of the two is also sometimes considered. An FC ultracapacitor vehicle is, however, the least desirable vehicle choice of the three, due to the relatively high powertrain cost and low fuel economy, resulting from the high vehicle mass. This result is due to the low energy density of ultracapacitors, if compared to recent growth of battery performances. In addition, the difficulty in controlling charging and discharging currents and the increase in recharging time are other aspects to the disadvantage of this type of ESS [15]. As far as the mixed solution is concerned, battery FC and battery-ultracapacitor FC vehicles are very close competitors. The battery solution is generally less expensive, less complex and easier to manage, which is why it is preferred [14][15].

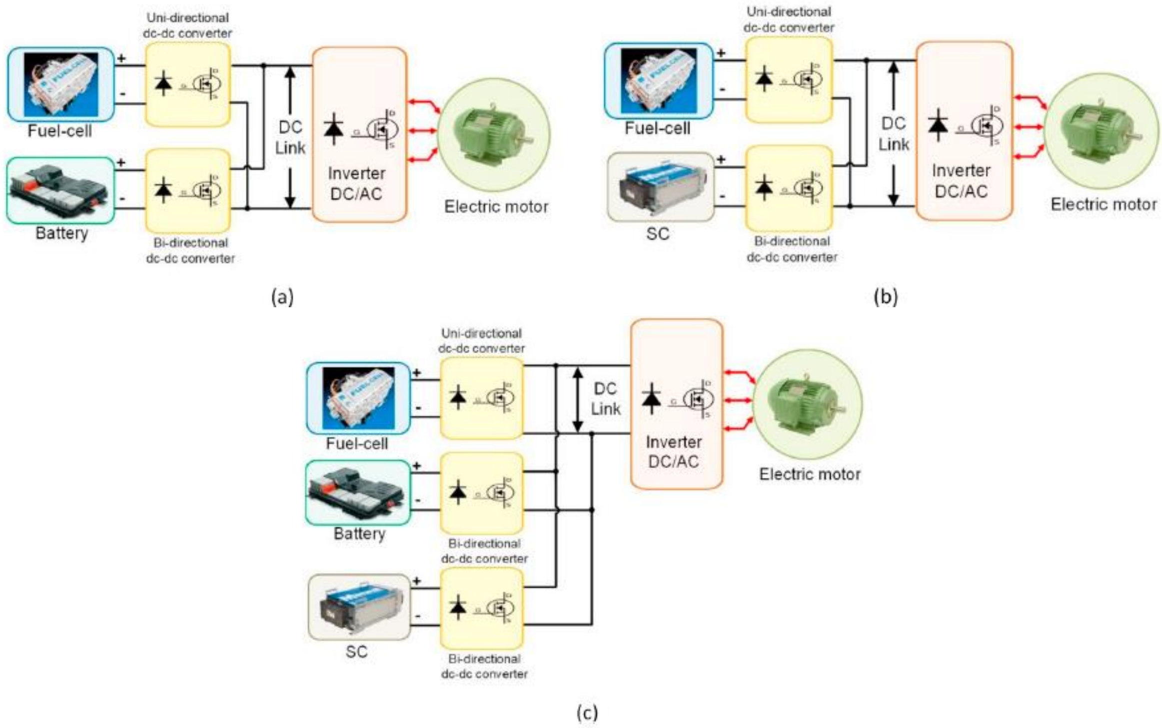

Figure 6: FC electric vehicle configurations: (a) FC battery solution, (b) FC supercapacitor solution, and (c) FC battery-supercapacitor solution [14]

1.3.3. Proton Exchange Membrane fuel cell

There are different types of FCs depending on their composition, characteristics and the materials used to make them. For automotive applications, where the energies required by a FC range from a few to a few hundred kW, PEM (Proton Exchange Membrane) fuel cells are the most effective technology, due to their low operating temperature, noise, faster start-up capability, lower mass and higher power density. The basic PEM fuel cell stack consists of membrane electrode assemblies (MEA) covered by two bipolar plates, anodes and cathodes on both sides, where electricity is generated by electrochemical redox reactions when hydrogen and air are supplied [16]. More technically, the fuel cell is supplied with hydrogen at the anode, the negative terminal, and oxygen at the cathode, the positive one. Molecules of H_2 are dissociated through a platinum-based catalytic reaction and each hydrogen atom loses its only electron, converting in a hydrogen proton H^+. Since the electron cannot pass through the membrane, it passes through the electrical circuit and creates an electrical current. The hydrogen protons migrate from the anode through the membrane, finding oxygen molecules at the cathode and combining to form water molecules. The fuel cell is an energy converter, not an energy source, it converts the chemical energy of a fuel (H_2) directly into electricity and heat.

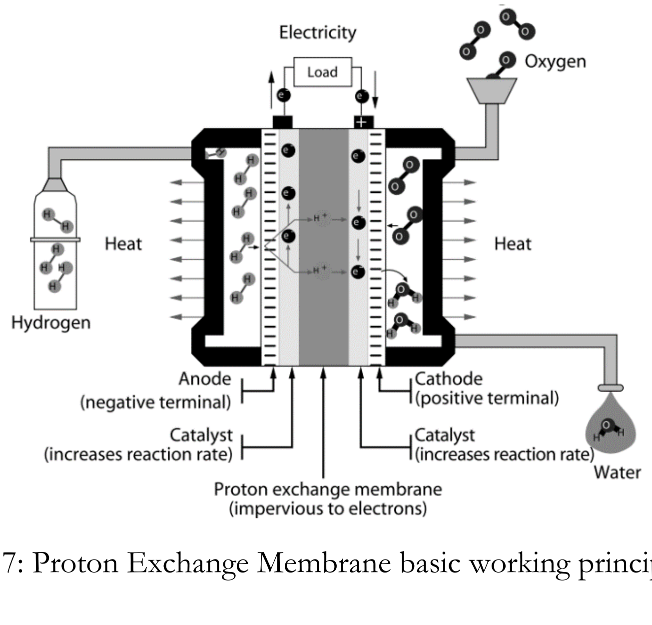

Figure 7: Proton Exchange Membrane basic working principle [15]

The choice of the type of FC is always a compromise between its characteristics, advantages and drawbacks, which can be summarized in the following Table 2:

Type	Acronym	Electrolyte	Temperature	Output power	Applications
Alkaline	AFC	Potassium hydroxide	60–250°C	10-100kW	Transport, stationary
Proton exchange membrane	PEMFC	Solid polymer membrane	80°C	1-250kW	Transport, stationary, portable power
Direct methanol	DMFC	Polymer membrane	80°C	100W-1kW	Portable power, stationary, transport
Phosphoric acid	PAFC	Phosphoric acid	200°C	50kW-1MW	Stationary distributed generation
Molten carbonate	MCFC	Alkali metal carbonates	600-800°C	1kW-1MW	Stationary large distributed generation
Solid oxide	SOFC	Ceramic	800-1000 °C	1kW-3MW	Stationary large distributed generation

Table 2: Summary of typologies and features of fuel cell technologies

Given the characteristics of the airport GSE vehicle under consideration, the powertrain that will be composed will include PEMFC. The main advantages of this type of fuel cell, considering the specific automobile application, are the low operating temperature, which means that the cell does not need a long time to warm up before starting to be fully operational to generate electricity, the high specific power, which can reach 1kW/kg and the low weight, compared to the others. Drawbacks can be the necessity of membranes to be kept in a good degree of hydration in order to proceed with the chemical conversion, otherwise membrane deterioration is the consequence, durability issues, which must be kept under control to reach a satisfactory lifetime, for what regards the transportation sector expectative and the high cost of the catalyst, which usually is platinum.

1.3.4. Fuel cell vehicle architecture

From a structural viewpoint, an FCEV can be considered as a type of BEV, because this vehicle can also be equipped with batteries or supercapacitors as ESS. Thus, FCEVs can be considered as a type of series hybrid vehicle, in which the fuel cell acts as an electrical generator that uses hydrogen and is series-paralleled with the battery. The on board fuel cell produces electricity, which can be used to provide traction power or can be stored in the ESS for future use. Fuel cell vehicles can be classified according to many criteria such as the fuel storage method (pressurized or liquid H_2), the power system structure or the battery size (plug-in or non-plug-in). Currently, the commercial FCEVs Honda Clarity, Toyota Mirai, and Hyundai Nexo have a power architecture which relies on H_2 stored at 700bar and small batteries (they are non-plug-in). In Figure 8 below is shown an example of FCEV architecture.

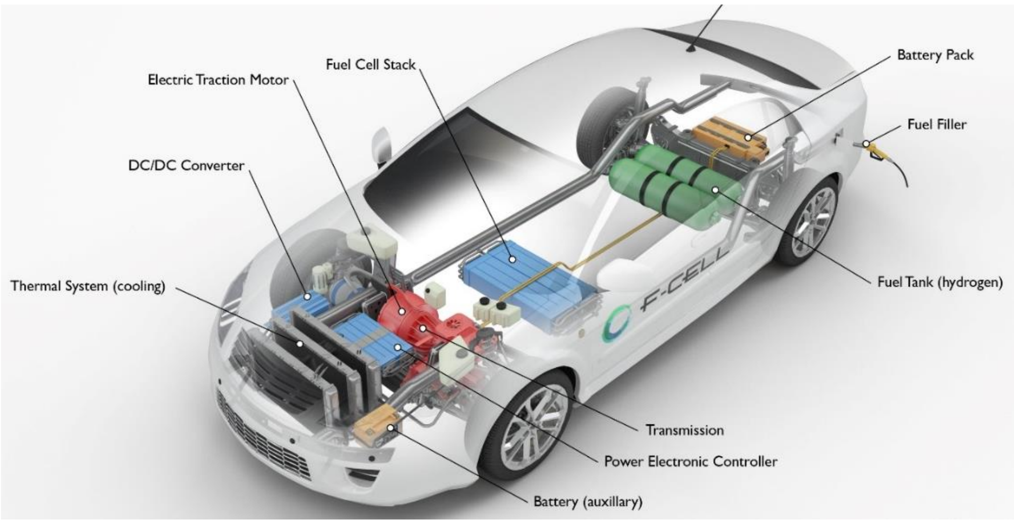

Figure 8: Key components of a hydrogen Fuel Cell Electric Vehicle [16]

The main and mandatory elements composing this type of vehicle are presented as follow, even if is important to underline that several different structures are possible, including many more component, depending on purposes, requirements, ideas and design:

- *Fuel cell system*: composed by the FC stack, usually PEM type, associated with a nominal power and the balance of plant (BoP), namely all the auxiliary elements (fuel reformer, heat exchangers, air management systems, pumps, valves, sensors, fittings and piping) and the compressor needed to turn a fuel cell into a useful chemical converter. Usually, the BoP is composed by three parts: cathode side, anode side and cooling. To provide high-pressure air to the fuel cell, is present a compressor in the cathode side, together with a heat exchanger, working as a intercooler, and a humidifier system to increase the cathode inlet humidity, using the water which comes out at the exhaust. The *anode side* includes the supply of hydrogen, regulated by a pressure valve to adapt the pressure of the storage system to the one used inside the stack, and can be present or not a recirculation pump, together with a mass flow meter to measure the H_2 consumption, a pressure sensor to measure inlet H_2 pressure and a purge valve, to periodically remove the excess liquid water and impurities in the cell. In the *cathode side* the electrons and positively charged hydrogen ions combine with oxygen to form water, gaseous and in form of droplets, which flows out of the cell thanks to flow channels. The heat exchanger is used as *cooling system*, which can be of two different types, depending on the power level of the FC stack and consequently needs for cooling, which are air or liquid, useful to keep the system temperature inside the operating range.

- *High voltage battery:* bidirectional high-voltage ESS which allows regenerative braking energy and assists the vehicle during high-power demands. Batteries are usually of the lithium-ion type with a nominal voltage around 400 and 700 Vdc. This voltage value also defines the nominal voltage of the HV bus, for the connection of high voltage systems operating in the powertrain. Usually the battery also provide the threshold power for the FC start-up, through a dedicated DC/DC converter to adapt the HV of the battery to the input level for the stack.
- *FC monodirectional DC/DC converter:* the fuel cell is connected to the DC bus via a DC/DC converter, which is usually a boost-type, to increase the output voltage of the fuel cell to the nominal voltage of the DC bus.
- *Battery bidirectional DC/DC converter:* realizing the voltage matching between the battery and the DC bus and manage the bidirectional flow of energy to provide power transient and to recover and store braking energy. In battery discharge mode, the bidirectional converter works in boost-mode, while when in battery charging mode, the bidirectional converter works in buck-mode.
- *Electric motor and power electronic controller:* using power from the fuel cell and the traction battery pack, this electric motor, usually of AC induction or IPM typologies, drives the vehicle's wheels. The power electronic controller manages the flow of electrical energy delivered by the fuel cell and the battery, controlling the speed of the electric motor and the torque production.

- *Hydrogen fuel tank:* stores the H_2 gas on-board as fuel, automotive applications generally settle for vessels operating at 700 or 350bar, with a capacity around 4-6kg of hydrogen and a weight of the vessel around 100kg. Actually, there are five types of vessels (from I to V) for hydrogen which can be used in FCEV, depending on the materials and compositions of their structures and therefore defining increasing performance features. Most common nowadays are type III or IV, made by a metallic or plastic liner fully wrapped with carbon or fiberglass, which can ensure an adequate lighter weight and reinforced structure.
- *On-board charger:* to enable the vehicle battery to be charged, if the power of the FC not allow a strategy in which the hydrogen part can fully maintain the state of charge between acceptable limits, an on-board charger is connected to the high voltage bus. This element converts the AC current, coming from the charging station, into DC stored by the battery. A charger with a minimum voltage higher than that of the battery is required, in order to prevent the flow of current being directed in the opposite direction.

1.3.5. Advantages on efficiency

FCEVs are advantageous in terms of energy efficiency, compared to combustion vehicles. Considering a standard 60% efficiency in hydrogen production, transmission and supply, supposing that the fuel cell system efficiency floats around 40 and 60% is a reasonable approximation [18]. For a tank-to-wheel efficiency of 80%, which is the value of a standard FCEV, the total well-to-wheel efficiency for the whole life cycle of a fuel cell vehicle is therefore around 27%. Considering different typologies of powertrains, FCEVs have the highest overall well-to-wheel efficiency, together with BEVs, while the conventional ICE vehicle has an efficiency of only 14% [19]. Electrification can therefore significantly improve the overall well-to-wheel efficiency.

1.3.6. Advantages on global emissions

This gain in efficiency also translates into a reduction in emissions, both global and local. For an engine using fuel cells, GHG emissions are zero during utilization, while for a combustion vehicle they reach up to 80% of total well-to-wheel GHG emissions. This translates into a high advantage for an airport when it has to comply with limits and regulations. In any case, even in the least efficient cases of hydrogen production, i.e. when energy derived from natural gas combustion, coal or grid power [19], well-to-wheel GHG emissions still see a reduction of between 6% and 23%, compared to internal combustion vehicles [19][20][21].

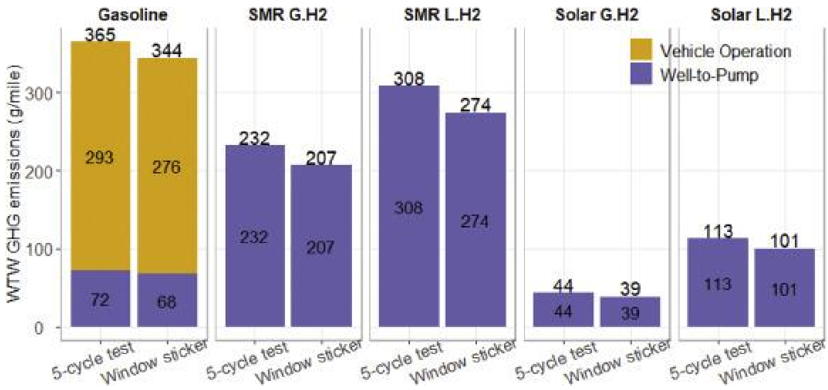

Figure 9: WTW GHG emissions for gasoline vehicle (Mazda 3) and FCEV (Toyota Mirai) [19]. (SMR G.H2 refers to gas steam reforming gaseous hydrogen production, L.H2 to liquid hydrogen; Solar G.H2 refers to thermic solar gaseous hydrogen production, L.H2 for liquid hydrogen; the same applies to Figure 6 and 7)

1.3.7. Advantages on local emissions

As far as local emissions are concerned, having water as the only product of the conversion, also these emissions for a FCEVs are zero. If the assessment is extended to the well-to-wheel analysis, this solution is still advantageous: always considering the least efficient case of H_2 production and delivery, the reduction is between 50% and 80% for CO emissions, while for hydrogen produced from renewable sources or with the appropriate low-emitting energy mix, the NOx emission reduction can vary between 30% and 70% [20][21][22]. These reductions are already very high nowadays and considering the technological developments that will surely be produced in the coming years, which will improve the efficiencies of all hydrogen production routes and delivery infrastructures, these reductions are bound to increase. These reductions are already very high nowadays and considering the technological developments that will surely be produced in the coming years, which will improve the efficiencies of all hydrogen production routes and delivery infrastructures, these reductions are bound to increase. In the figures below (Figure 10 and 11) are shown WTW CO and NOx emissions for FCEV with different hydrogen productions.

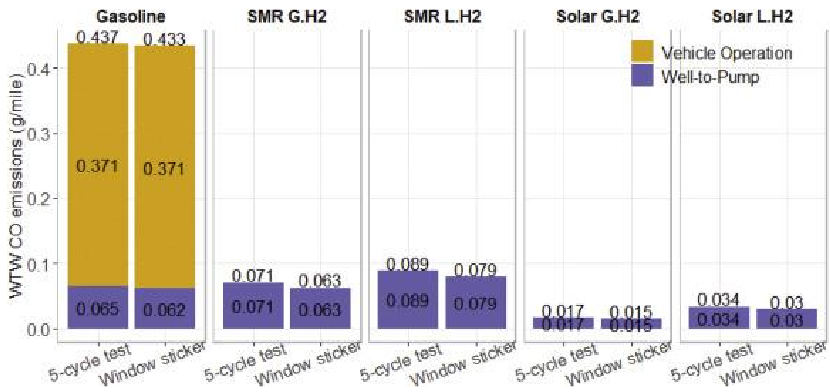

Figure 10: WTW CO emissions for gasoline vehicle (Mazda 3) and FCEV (Toyota Mirai) [19]

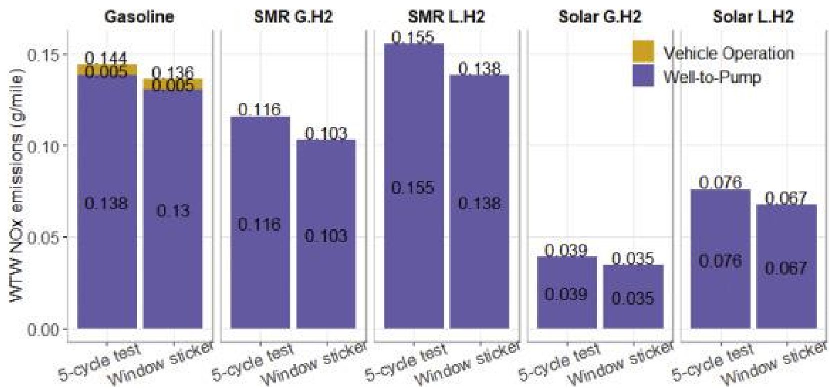

Figure 11: WTW NOx emissions for gasoline vehicle (Mazda 3) and FCEV (Toyota Mirai) [19]

1.3.8. Comparison with Battery Electric Vehicle

As for the comparison with a Battery Electric Vehicle (BEV), it is well known that tank-to-wheel emissions are zero in both cases, all emissions being attributable to the manufacture of the vehicles and the production of their energy traction sources [23]. Throughout the life cycle, achievable reductions in GHG emissions are generally equal, depending very much on the type of energy production, efficiency of infrastructures in the manufacturing sites, delivery and supply techniques and intensity of power required [24]. It is again important to emphasise that these results can only be achieved with low-impact energy production, otherwise the environmental impact for the production of BEVs and FCEVs can be greater than for normal ICEs [23]. In the following Figure 12 is shown a comparison between GHG emission for BEV and FCEV.

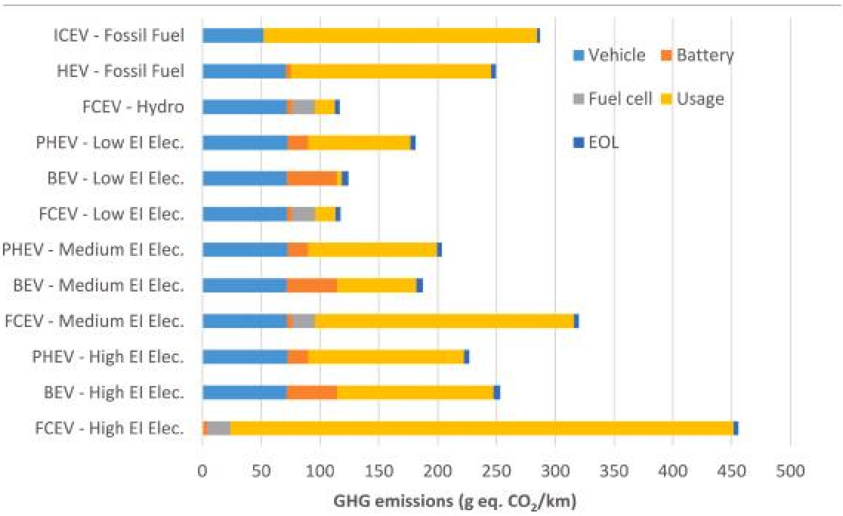

Figure 12: Life cycle GHG emissions by vehicle type for low, medium and high electricity grid emission intensity (EI) scenarios at 150.000 km vehicle mileage [23]. (EOL: end-of-life, referred to emissions from the waste disposal and treatment of products.)

Chapter 2: Market analysis for the airport case

This chapter will present the current market situation for the airport sector, with a focus on electromobility and in particular on FCEVs.

The airport sector's need to invest more in electromobility solutions will be analysed, defining the main environmental and legislative causes. The results that are expected in the short future, in form of advantages and disadvantages, will be briefly presented. Finally, the solutions currently existing in the airport sector for its GSE vehicles will be reviewed, both with regard to battery electric and fuel cell electric vehicles.

2.1. Electromobility developments in airports

2.1.1. Growth of airports sector and its emissions

Electrically driven vehicles, replacing the use of ICEs and fossil fuels, are now widely studied and gradually being applied in any sector, whether private or public. In the airport one, thanks to the growing interest and pressures towards climate issues that are driving countries and industry to generate climate protection policies, plans and projects, developments towards electromobility are finding an easy and rapid diffusion. As a result, airports are also experiencing a natural electrification process in recent years: the development of electromobility is an urgent task for industry, which is facing increasing pressure to reduce their gas emissions. This pressure is not only related to current emissions, but also to the expected growth of the sector in the coming years. Today there are more than 40.000 airports in the world, serving more than 4 billion passengers a year. The effects of COVID-19 have greatly reduced their activity, lowering these numbers till its half, but the values are already expected to return to previous ones in few years and growth will begin [25]. As far as global pollution is concerned, the climate impact of aviation accounts for 3.5% of the total, about 920 million tonnes of CO_2(e) in 2019, and forecasts say that by 2050 emissions could triple without intervention. [26]. According to the latest estimates, the aviation sector will increase by an average of 4.3% per annum with regard to cargo and people transported over the next 20 years [27].

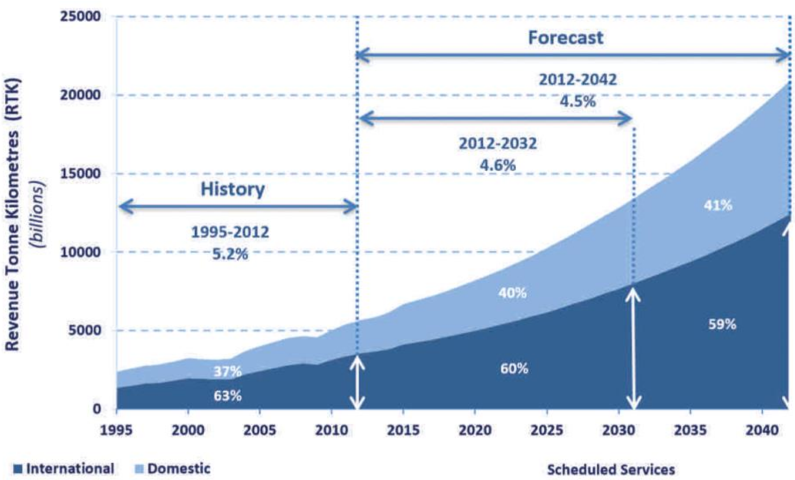

Figure 13: Expected growth path for aviation sector, quantified in metric tonnes of revenue load carried for one kilometre [27]

The growth of the sector will obviously lead to an increase in the number of airports, the surface area of existing ones, the number of aircraft, their flights and thus their service. Consequently, the number of ground vehicles circulating at the airports will grow proportionally, as will their emissions. As this growth continues, the requirement for more efficient, more reliable and environmentally friendly solutions will gradually increase for both airborne and ground operations.

2.1.2. Sources of pollution and possible solutions

Airport pollution can come from a wide variety of sources including aircraft engines, infrastructures and auxiliary power units, pollutants created by the high volume of people moving around the facilities and also from ground transport for GSE vehicles. Aircraft engines generally combust fuel efficiently, and jet exhausts have very low smoke emissions. However, pollutant emissions from aircraft at ground level are increasing with aircraft movements and, in addition, a large amount of air pollution around airports is also generated by surface traffic. Vehicles travelling to and from airports are regarded in most analyses as the biggest contributor to local concentrations of pollutants, especially where airports are located in or near major urban centers. Consequently, airports are required to complete a series of environmental improvements, encompassing all areas in which they can intervene, such as electrification of building systems, generation of renewable energy on-site, improvements on energy and water efficiency, increase of the efficiency of airplanes, smart organization of the logistic and also conversion of their ground fleets to electric vehicles (EVs); GSE vehicles may include aircraft tugs, start-up assistance units, forklifts, tractors, air conditioning units, ground power units, baggage tugs, belt loaders, fuel or hydrant trucks, catering trucks, water trucks, toilet trucks and airport marshalling vehicles, such as the "Follow me" one.

The development of electromobility usually has two different approaches: the development of electromobility within the airport (Airside) and the development of electromobility in the transport of passengers to and from the airport (Landside). In both cases, airports are recommended to gradually replace internal combustion vehicles with electric vehicles or, as a temporary alternative, with other vehicles with alternative propulsion [28]. Following fuels can be alternative options to conventional gasoline or diesel ones: mixtures with ethanol, mixtures with biodiesel, natural gas (compressed or liquefied), liquefied petroleum gas (propane), methanol and hydrogen.

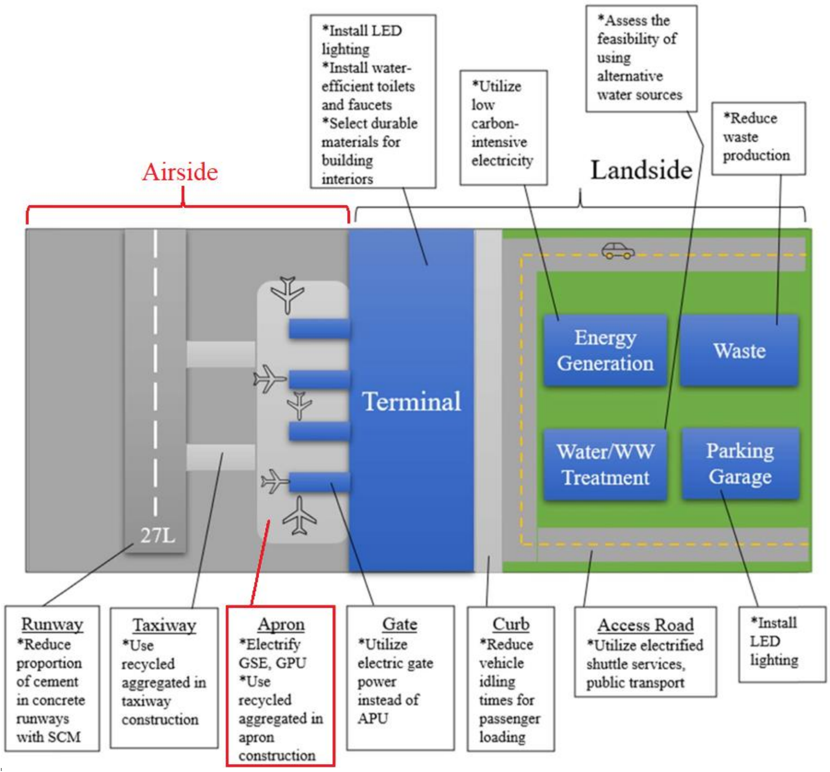

Figure 14: Suggested best practices for improving airport environmental sustainability [24]

2.1.3. Advantages and drawbacks of electric vehicles

Regarding the use of electric vehicles, the main advantages are:

- EVs have *high efficiency*, can convert approximately 75% of the chemical energy stored in the batteries to power the wheels [16]. An ICE can only convert less than 20% of the energy stored in gasoline. Moreover, in stop-and-go operations, EVs are even more efficient since electricity is not consumed while the vehicle is stopped (no idling).
- *Complete tank-to-wheel emission reduction*. Nevertheless, is difficult to evaluate the well-to-wheel emission impact, depending on how the energy is produced, such a vehicle may pollute less or more overall.
- As far as the *performance, acceleration, speed and handling* of an EV are concerned, they are equal to those of a conventional ICE.
- *Level of noise pollution*: electric vehicles are much quieter than conventional petrol- or diesel-powered vehicles. This is particularly useful in an airport environment where noise can be annoying for passengers and airport staff.

- They require *less maintenance*, replacements and have fewer moving parts, which results in reduced interventions and lower operating capital.

However, it is known that EVs have several drawbacks:

- *Limited battery storage capacity* and may present a limited possibility for towing vehicles over long distances, finding difficult to be used in certain operations, such as towing an aircraft between gates or high loads on high inclined routes.
- Another issue is *autonomy*, which results in a more frequent need for recharging than refueling ICE vehicles. Moreover, the recharging time can vary greatly, depending on the presence of adequate fast-charging stations and is longer than the time needed to refuel a combustion vehicle. In fact, even the best cases of quick charging, it can take up to 15 minutes. This results in the need to develop appropriate logistics and charging time management plans, involving the entire GSE vehicle fleet, or portion of them.
- Another issue is the need for adequate *electricity supply infrastructure* at airports and the associated costs. Charging infrastructure can be very costly for an airport without a sufficient existing electricity network. Most support vehicles can be recharged easily from conventional Type I and Type II recharging stations, but at the cost of an operation that can take up to eight hours. A good number of fast recharging stations are required to meet demand, especially during peak air travel periods [29].

2.1.4. Advantages and drawbacks of fuel cell vehicles

With regard to hydrogen vehicles, possible benefits are:

- In terms of *emissions* have been discussed in the previous paragraph. For example, most updated analysis shows a possible reduction of pollutant derived from the use of a complete hydrogen fleet of GSEs around 25, even 50% with the conversion of vehicles up to higher power levels [30].
- *Level of noise pollution*: in the same way as BEVs, quietness which can offer these typologies of vehicle is useful in airport environments.
- *Rapid recharging*: FC vehicles can be recharged within minutes, very similar to ICE powered vehicles, making them suitable for use in an airport environment where downtime must be minimised.

On the other hand, although vehicle using this fuel are increasingly being developed and spreading, knowing the energy and environmental advantages of this technology, they nevertheless still have a quantity of disadvantages, mainly due to the technology's early stage of development:

- *Hydrogen production* is not always environmental convenient if high-consuming and polluting techniques are used. Also, preliminary cost comparisons between hydrogen and diesel have been investigated: results showed that, despite the already mature technical level of PEM systems, its cost is not yet lower than common fuel version, but it might be affordable in the next few years [30].
- *Distribution and supply infrastructures* are currently very limited, due to low demand and high cost, as hydrogen requires large and heavy containers with efficient and energy-demanding insulation systems to be stored in the stations. The country with the largest number of hydrogens refuelling stations is Japan, with a value of 154. In Europe as a whole, this number only reaches 161, with Germany alone having 91 [31].
- *Transport and related infrastructure* are also poor, due to the lack of demand of this type of fuel and the high difficulties in transporting gases at high pressures or for refrigerated liquids.

Thinking about these difficulties and numbers, which affect the possibilities of a whole country, it is easy to understand how complex it can be for an airport to have an adequate infrastructure to manage a fleet of vehicles using fuel cells. However, the technology is currently in an early stage of development and is set to see its possibilities increase exponentially in the coming years, decreasing its costs and branching out.

2.2. Existing solutions in airports

2.2.1. Electric solutions

As mentioned in the previous chapter, the general growth of the airport sector will lead to an increase in pollution and GHG emissions. To contribute to their decrease, one solution that will be employed is to act on the vehicle fleet that makes up the GSE vehicles, such as increasing powertrain efficiency, electrification or the use of biofuels or alternative sources. In recent years, electrification and the use of hydrogen and fuel cell technologies have been investigated as one of the best possible solutions to reduce pollution, since vehicles powered by such energy sources avoid GHG emissions and local pollutants such as CO, HCs and NOx. As far as AENA is concerned, the beginning of the use of electric vehicles in its GSE fleet dates back to 2011, when the company introduced 33 electric vehicles for use at its airports, with the long-term goal of replacing the entire fleet of 1.200 vehicles. [32]. In the rest of the world's airports, there are many examples of fleet electrification that can be documented, some of which are mentioned below

- In Germany, *Stuttgart airport* purchased six electric ground handling vehicles, built six charging devices and all their buses are powered by electricity [33]. In Munich airport, approximatively the 20% of the 1.250 handling vehicles, machines and equipment are already electric [34].
- In Austria, yet in 2019 the airport's vehicle fleet of *Vienna* consisted of 380 electric vehicles and is constantly expanding.
- In England, the *London Gatwick Airport* began testing autonomous electric vehicles in the airport area in 2018, used to transport employees between different locations inside the airport [35].
- In USA, the largest part of the vehicle fleet at *JFK Airport in New York* is already electric [36].
- In Canada, *Montreal-Trudeau Airport* has 12 electric vehicles, while *James Armstrong Richardson Airport* in Winnipeg has turned four luggage vehicles into electric ones [37].
- In India, the *Kolkata Airport* has five electric transporter and the adoption of electric vehicles is part of a recent broader plan signed by the Airport Authority of India (AAI) [38].

Precisely regarding the case of the "Follow me" vehicle, *Alicante-Elche Airport* was the first in which AENA used a 100% electric vehicle to service its runway [39]. As a result of this addition, a fast charging point was also installed in the marshallers unit, having to cope with the low autonomy of about 200km after a single charge of the vehicle, considering that this quantity can be driven in only one day during periods with increased air traffic. Other documented examples of EVs used for this function include those at the *Airport in Genoa*, where are used three Citroën Ami [40] and at *TAG Farnborough Airport*, where in 2015 three 100% electric Renault Zoe were purchased for the same purpose [41].

Figure 15: the three Citroën Ami full electric used as "Follow me" at Genova airport [40]

2.2.2. Fuel cell solutions

Besides, fuel cells are suited to overcome some drawbacks of battery powered motors, such as limited operation time, long time to recharge and high costs of disposal and replacement. Several airports worldwide have already introduced and experimented hydrogen vehicles in their airside and landside. Hydrogen stations have also been installed in several airports to be able to offer the possibility of on-site hydrogen refueling, rather than resorting to complete tank changes or refilling at locations further away from the operational area [30]. Hereafter some relevant example of hydrogen solutions:

- In Germany, the *Frankfurt Airport* is implementing collaborations for hybrid fuel cell/battery baggage transporter for usage on airport apron areas [42]. Munich airport and many more are undertaking feasibility studies for the implementation of hydrogen and fuel cells. In particular, this last German airport can be considered as forefront for hydrogen technology for this sector: the current fleet of airport vehicles has already been composed by some hydrogen-powered vehicles, equipped with internal combustion engines using liquid or gaseous hydrogen, instead of fossil fuels. Some other buses for transporting passengers and lifters for baggage are instead equipped with an electric traction system powered by fuel cells. Moreover, fuel is supplied directly inside the airport: gaseous hydrogen is produced autonomously on-site using high-pressure electrolysis, while liquid hydrogen is being delivered from a nearby liquefaction plant [43].

- A similar program was developed in Canada at the *Vancouver Airport* in 2006, leading to the purchase of some buses and tractors for luggage equipped with fuel cells [42].
- In United States, in 2015 at *Memphis International Airport* in Tennessee, 15 operating fuel cell GSE unit were inserted in the airport, while *Albany International Airport* launched the first FC cargo tuggers in 2018 [44].
- In Spain, first investigations about the replacements of diesel fleet with FCEVs go back to 2006, when IBERIA in collaboration with the University of Madrid Carlos III design a prototype of FC electric conveyor, which transports and elevates the load to the storage compartment of the aircraft [45].

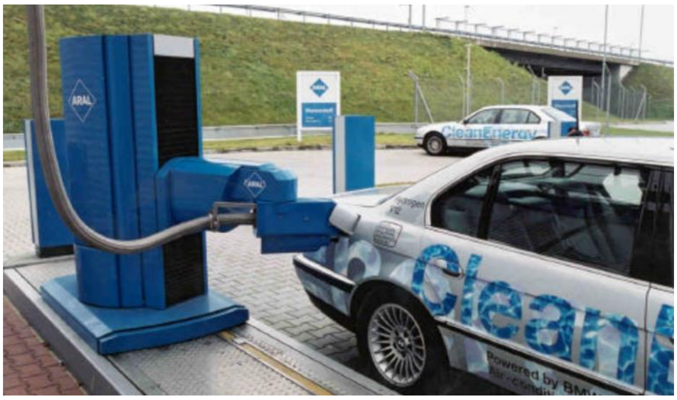

Figure 16: Liquid hydrogen robot dispenser present in the Munich airport [44]

For what regards the specific case of the "Follow me" vehicle, nowadays no FCEV solutions are documented, present on the market or inside airports. As said in this introduction, this type of vehicle is not special, actually is a common road vehicle, for passenger or commercial purposed and therefore no special cases have ever been designed using fuel cells. Currently, exist less than ten FCEV which can be bought or rented, at high prices, thereby airports are not prone to rely on these available car models [46]. Nevertheless, the need to decarbonize and reduce GHG emissions in airports also prompts the study of these types of solutions, as is activity case. Considering the driving cycle characteristics of this type of GSE vehicle, it is easy to foresee that in the future its propulsion will be provided by an electric powertrain, pure- or fuel cells-based. In general, the use of hydrogen vehicles at airports is expected to continue growing in the coming years. According to a 2019 report by the International Energy Agency (IEA), the global hydrogen vehicle fleet is expected to increase from about 340.000 in 2018 to about 2.5 million in 2030 and up to 19 million in 2050. Furthermore, it is estimated that the global hydrogen vehicle market could reach USD 278 billion by 2027, with a compound annual growth rate of 37.8% from 2020 to 2027 [46]. However, the growth of hydrogen vehicles at airports will also depend on the availability and competitiveness of hydrogen technologies compared to other clean energy sources and the development of hydrogen refueling infrastructure in the future.

Chapter 3: "Follow me" Vehicle Data Analysis

In this chapter will be treated the analysis of the vehicle's driving mission and powertrain data coming from the sensors placed inside the real "Follow me" car.

Data were retrieved through the use of sensors, the characteristics of which will be briefly presented, as well as the data they can acquire. The processing of the same with the relevant calculations performed, useful for the actual analysis, will be addressed in this chapter. Finally, in the final and main part, will be treated the analysis of these data collected using two different approaches: based on the single driving mission or on the entire operative day. The results of these two analyses make it possible to outline the characteristics of the "Follow me" vehicle currently in use, as well as forming the basis for the definition of FCEV powertrain requirements.

3.1. Vehicle sensor data

3.1.1. Conventional "Follow me" vehicle

In order to obtain a proper dimensioning of the FC powertrain components for the "Follow me" hydrogen vehicle, is necessary to define correct speed, torque, power, energy and consumption requirements. These needs are necessary in preliminary phase to create a proper model to carry out sets of simulations for the component sizing. Real driving mission data are mandatory to define a set of representative driving missions, describing usual and realistic cases of vehicle use, but also special cases or with special characteristics to subject the powertrain model to more demanding cases as well. Moreover, are necessary to define the correct sizing for the different components present inside the powertrain, after a correct and complete analysis. Real driving cycles data can be collected thanks to the concrete operation of the vehicle, in this case could be provided thanks to AENA and the Ford Ranger "Follow me" car currently operating along the runways of the Adolfo Suarez Madrid-Barajas airport. The Ford is a 4WD with a diesel combustion engine with the following main characteristics:

Identification of the propulsion system	
Compression ignition engine	
Engine identification code	Bc2x
Engine manufacturer	OM936 LA6.3
Maximum power (kW)	125
Maximum torque (Nm)	500 @ 2000rpm
Displacement (cm^3) / nº cylinders	1996 / 4 in line
Fuel type	Diesel
CO2 emissions (g/km)	245
Emission standard	Euro VI AR
Identification of chassis and body	
Completed vehicle type approval number	E5*2007/46*0080*07

MOM/MMTA (kg)	2320/3270
Total height (mm)	1815
Overall width (mm)	1860
N° axles and wheels	2 axles / 04 wheels
Wheelbase (mm)	3220
Tyre dimensions	225/70 R16

Table 3: Technical specifications of the Ford Ranger "Follow me" vehicle

3.1.2. Vehicle instrumentation

These data for the analysis can be stored inside memories thanks to the utilization of sensors connected directly to the vehicle bus CAN, then analysed with proper software in order to extract meaningful conclusions. Data collection on the Ford Ranger was performed over the course of some weeks, using two sensors placed inside the vehicle, able to store GPS data over positions, speeds or accelerations of the vehicle and CAN driveline data relative to engine functioning, pedals utilization and fuel consumption. More specifically, these two sensors are:

- GPS-to-CAN with 3D inertial sensor and UDR: GPS module which produces GNSS position and 3D inertial (IMU) data (via a gyroscope and accelerometer) and outputs it via configurable CAN bus frames. The IMU provides three accelerations and three gyroscope readings. For automotive applications, the module supports a sensor-fusion model using information from both the GNSS and IMU to provide improved positioning information, particularly in places with GNSS-denied conditions and outages [48]. Specifically, these data are represented in the following Table 4:

Sensor validity	Number of satellites	Time stamps	Time validity			
Positioning	Longitude	Latitude	Altitude	Position accuracy	Distance covered	Distance accuracy

Angle	Roll	Pitch	Heading	Roll accuracy	Pitch accuracy	Heading accuracy
Speed	Speed value	Speed accuracy				
Acceleration	Acceleration x value	Acceleration y value	Acceleration z value			
Angular rate	Angular rate x value	Angular rate y value	Angular rate z value			

Table 4: List of data collected with the GPS-to-CAN sensor

- CAN bus data logger (SD + RTC): module which records timestamped CAN data to an extractable memory (SD card). The frequency of data acquisition is 10 Hz. This sensor collect data from the driveline and sent them, together with GPS ones, to the memory to easily extract them. Specifically, driveline data are represented in the following Table 5:

Vehicle functioning	Coolant temperature	Engine oil temperature	Throttle position	Inlet manifold air flow rate
Velocity	Vehicle speed	Engine rpm		
External	Intake air temperature	Absolute barometer pressure	Ambient air temperature	
Fuel	Fuel tank level	Engine fuel rate		
Engine performance	Engine load	Demanded engine torque	Actual engine torque	Reference engine torque

Table 5: List of data collected with the CAN bus data logger

Not all sensor data are useful for defining the powertrain requirements of this study, so some have been discarded and only certain data were analyzed. Along the 49 days that the vehicle housed the sensors, from 16 September to 03 November 2022, there were generated

297 raw files, each of them created from the moment the contact was given to switch ON the vehicle, until it was switched OFF. In this sense, each raw file corresponds to a specific driving cycle. This means that approximately 6 times a day the vehicle was given the ignition contact with the key (i.e., the car performed a driving mission), but this does not mean that each of them was related to an operational use along the airport runways. The first files were related to tests carried out in the INSIA center to check its operation, others were related to moving the vehicle for refueling or special uses, and others were related to switching ON the quadrille without starting the engine. Therefore, of all these detections, only 72.4% were considered for an initial analysis, which still corresponds to a high and satisfactory number of cases for what concerns sizing and dimensioning.

3.2. Data processing

To obtain analytically and statistically interesting data, which were able to comprehensively describe the vehicle's driving mission characteristics and requirements, the raw data obtained from the sensors were further processed with the MATLAB® software. The objective of this treatment was to obtain average and meaningful values found in each work cycle (i.e., each raw file) and in each day of utilization, to have an overall view of the vehicle requirements. Specifically, all the data calculated for each of the files were the following:

- *Characteristic times*: total time, time in motion (where speed of the vehicle is higher than 0), its percentage, idle time and its percentage.
- *Distance* travelled.
- *Altitude* variation.
- Characteristic *speeds*: maximum velocity, maximum engine rpm, average velocity and average motion velocity (where speed of the vehicle is higher than 0).
- Horizontal *acceleration*.
- *Engine data*: maximum torque, average torque, maximum power, average power and average motion power (where speed of the vehicle is higher than 0).
- *Energy data*: average energy and average motion energy (where speed of the vehicle is higher than 0).
- *Fuel consumption*: average in liter per hours and in kilometers per liters, total in liters.
- *Energy consumption*: considering average energy and average motion one.

The sense of calculating data "in motion" was useful to obtain indications of the average demands of the vehicle at the moment it is actually moving, i.e. isolating from the calculations the large amount of time when it is in idle, as will be shown later. The total time was calculated by considering the sensor detection interval of 10Hz. Vehicle acceleration was obtained by deriving the horizontal displacement values. The altitude variation was obtained by considering the highest and lowest altitude value detected during the movement, appropriately filtered with adequate altitude accuracy and altitude precision data. With data on actual engine torque T_{act}, reference engine torque T_{ref} and engine rpm, the vehicle's power could be calculated, instant by instant:

$$P\ [kW] = \frac{T_{act} * T_{ref}\,[Nm] \times RPM\left[\frac{rad}{s}\right]}{1000}$$

With these values was possible to calculate the different values of power: maximum, average and average in motion. The vehicle's reference torque was taken from its data sheet, which was 420 Nm [49]. Knowing the usage time for each driving cycle, it was then possible to calculate the vehicle's energy, instant by instant:

$$E\ [kWh] = P\ [kW] \cdot \frac{t_{total}\ [s]}{3600s}$$

With these values was possible to calculate the different values of energy: average and average in motion. Knowing the engine fuel rate at each instant, the total time and the distance travelled, case by case, it was possible to calculate the average and total fuel consumption:

$$FC\ [l] = fc\ \left[\frac{l}{h}\right] \cdot t\ [h]$$

$$fc\ [km/l] = \frac{distance\ [km]}{FC\ [l]}$$

Combining the value of average energy along the driving mission and relative value of distance covered, was finally possible to collect data about the energy consumption. As last analysis, the latitude and longitude data could be converted into .kml files for reading them within the Google® Earth software. In this way, for each use of the vehicle (i.e., for each driving mission) it was possible to have its actual GPS footprint, thus being able to observe it on a case-by-case basis, if necessary. The following Figure 17 and 18 from Google® Earth show all the overlapped driving missions in GPS data, carried out by the vehicle during the survey period. As can be seen, they trace the roads that make up the airport complex, limited only to them, since the vehicle is used for aircraft marshalling and the non-representative files were not considered in this preliminary analysis.

Figure 17: Overlay of all GPS footprints of the 'Follow me' vehicle inside the Adolfo Suarez Madrid-Barajas airport

Figure 18: Overlay of all GPS footprints of the 'Follow me' vehicle inside the Adolfo Suarez Madrid-Barajas airport oriented to show the relative position with respect the city of Madrid.

3.3. Data analysis

The data produced by the various driving missions of the vehicle over the days of observation were analysed in two distinct ways, in order to obtain values to define the initial requirements. The two are:

- Based on the *individual diving mission*: in other words, based on the individual file emitted by the vehicle at the time of use. This type of analysis is useful to give a local indication of the vehicle's demands from the moment it was used until the end of the driving cycle (i.e., switch ON – switch OFF). Such an analysis has been particularly useful for obtaining performance data and maximum values, such as speed, acceleration, torque, power and altitude variation.
- Based on the *whole operative day:* This type of analysis proved to be mandatory since a "Follow me" vehicle should, in theory, always be available throughout the day to respond to any need. Consequently, dimensioning solely on the basis of individual driving cycles would be insufficient, as these do not consider the overall utilisation of the vehicle. A full day of operations was composed, on average, by 6 driving missions, developed during the course of the same day at irregular intervals dictated by the needs of the airport. This type of analysis is useful to give an overall indication of the demands on the vehicle over the course of a typical day, especially with regard to energy values, consumption, times and distances travelled.

3.3.1. Data analysis based on driving missions

By using the calculations for each of the files considered in the data processing, it was possible to obtain a series of values to give a qualitative indication of the vehicle's needs. The Table 6 on the next page shows these values, presenting the minimum, median, average and maximum. They are nothing more than the minimum and maximum values found during all driving missions, the average of all surveys and the median for statistical purposes and to understand the distributions of all the values. There were 216 driving missions included in the final calculation, between the 03 of October to the 03 of November 2022, properly filtered to include only the adequate ones. All these values will be then discussed and eventually compared with the data in the vehicle's technical sheet, in order to explain why were chosen and which considerations can lead, also showing some charts when necessary.

Data	Minimum Value	Median Value	Average value	Maximum value
Total time [min]	4.97	72.72	80.08	248.75
Time in motion [min]	0.00		34.92	124.90
Time in motion [%]	0.00	51.20	43.79	-
Idle time [min]	0.03		44.81	177.21
Idle time [%]	0.51	48.81	56.2	-
Distance [km]	1.10	14.09	17.55	68.17
Altitude variation [m]	2.70	20.35	22.63	71.09
Maximum vehicle speed [km/h]	37.00	79.00	79.24	134.00
Average vehicle speed [km/h]	8.12	14.64	18.99	53.14
Average motion vehicle speed [km/h]	2.11	30.87	32.84	67.38
Maximum engine RPM	86.59		2869.59	3947.70
Maximum acceleration [m/s^2]	0.03		3.07	9.70
Maximum acceleration [g]	0.00		0.31	0.99
Maximum engine torque [Nm]	126.00		397.87	429.20
Average engine torque [Nm]	28.36		62.3	168.41
Maximum power [kW]	3.18	106.34	106.93	172.14
Average power [kW]	2.38	7.23	9.72	35.24
Average motion power [kW]	5.58	11.76	12.9	39.10
Average energy [kWh]	0.42	7.72	6.64	26.94
Average motion energy [kWh]	0.38	5.26	6.59	24.35
Fuel consumption [l/h]	0.20		1.78	5.89
Fuel consumption [km/l]	0.04		9.89	15.62
Total fuel consumption [l]	4.43		1.81	5.58
Energy consumption [kWh/km]	0.30		0.53	1.68
Motion energy consumption [kWh/km]	0.27		0.39	0.72

Table 6: Summary of all representative values of vehicle's driving cycles requirements

The *total time* represents how much time elapses from the beginning to the end of the driving mission, showing that on average the vehicle is used for 80 minutes, and most are below this average. For more meaningful time data, values over a whole day will be more useful. The *time in motion* and the *time in idle* give a real indication of what the proportions of real usage of the vehicle are, effectively showing what was previously said: the part of time when the vehicle is stationary but with the engine running is very high, more than 50%. It may serve to confirm what discussed in the introduction: the idea of the very low efficiency with which such a GSE vehicle is used, consuming large amounts of fuel without actually generating traction but generating huge amounts of pollution, globally and locally. In this direction, a vehicle capable of producing only H_2O as exhaust product would produce a rather considerable decrease in environmental impact, while keeping its mode of use and performances unchanged.

Similarly to total time, the *distance* values represents how long were the driving mission. Again, for more meaningful distance data, values over a whole day will be more useful. The *altitude variation* (Figure 19) shows how this type of vehicle moves in flat paths with almost no gradients, typically corresponding to the topography of airport runways. Such a profile implies a low need for maximum torque to move on paths with high gradients, in addition to that required for maximum acceleration, even if the vehicle used is a pick-up with a great off-road capacity. The maximum values are found when the vehicle moves from one terminal to the other, as there is a difference in height between the two of about 50 metres.

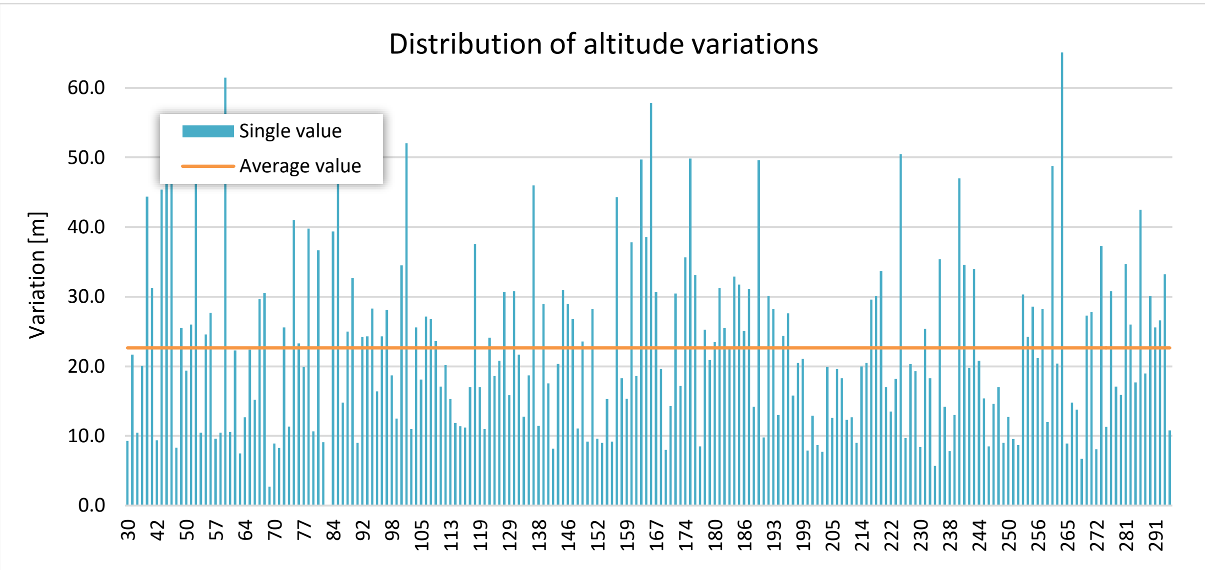

Figure 19: Distribution of altitude variations for the "Follow me" Ford Ranger driving cycles and comparison with the average value

The *maximum speed* values show that in many driving missions the vehicle reaches high speeds, demonstrating a tendency to move quickly, with a certain urgency, when it has to reach the operative zone. However, it happens not often, maximum speed was 16.6% above 100 km/h and only 4.6% above 120 km/h. The *average speed*, on the other hand, is low, obviously dictated by the high idle time where the speed is zero. In fact, it was interesting to have data on *average moving speed*, i.e. excluding stationary operation from the calculation, in order to actually understand how fast the vehicle tends to move most of the time around the tracks. Since the speed limit on runways is 30 km/h, it is logical that the average moving speed is low too and corresponds to this value, while it rises especially on very short driving missions or off the airside. As far as accelerations are concerned, the analysis to be made is very peculiar. The *maximum acceleration* values found, albeit in a few cases, are very high, in fact accelerations of more than 10 m/s^2 could be found in hyper cars, certainly not in a vehicle equipped with a 125 kW engine. The Ford Ranger data sheet reports a 0-100 km/h acceleration in 9.8 s, which corresponds to an acceleration of 2.87 m/s^2 (0.29 g) [49]. These excessive values are due to inaccuracies in the satellite GPS data, as CAN data were not used to calculate accelerations, since they had a high order of magnitude of 1 m/s. Due to the low accuracy of them, a maximum acceleration value higher than the maximum found in the data sheet was detected in 50.9% of the cases, which is too high to be considered reliable. Consequently, as far as maximum acceleration is concerned, requirements will be defined on the basis of experience rather than on driving missions' data.

Talking about pure powertrain performances, the *engine torque* values are consistent with those dictated by the vehicle data sheet, which speak of a maximum of 420 Nm [49]. As far as the *power* values are concerned, a profile of 170 kW as peak power and 40 kW as continuous power is outlined, although the latter could be assumed to be even lower, averaging 12.9 kW. This high difference is dictated by the fact that most of the time the average speed of the vehicle is low, generating low power for its movement. As proof on consistency, the first graph on the following page (Figure 20) shows that the average motion power values are always higher than the average ones and their distribution is correlated, presenting the same trend. Their difference increases as much as the time in motion within the driving cycle is high. Speaking of *average energy*, a demand of 7 kWh is obtained as average for driving missions, with maximum values reaching almost 30 kWh. As for distance and time, values over a whole day will be more useful. The second graph on the following page (Figure 21) shows the opposite with respect to power: average energy values are always higher than average motion values, while their distribution remains correlated, presenting the same trend. The reason is that since energy is calculated on a time-base and the movement time is less than the total, the resulting energy will be lower. Their difference increases as much the idle time within the driving cycle is high, as opposed to power.

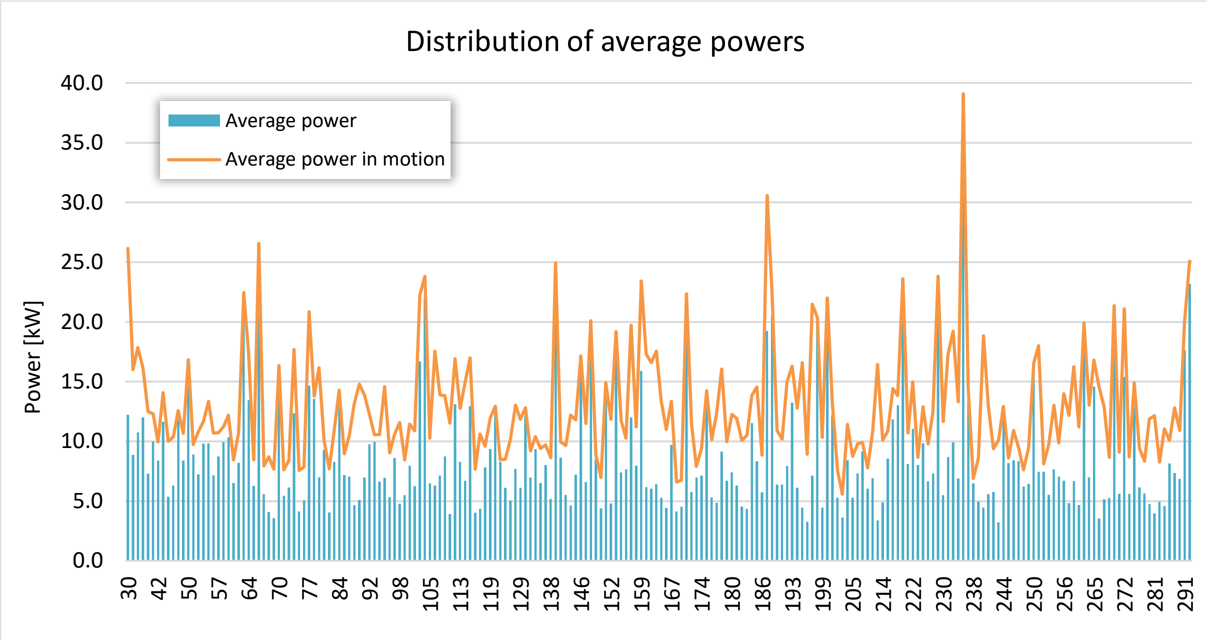

Figure 20: Distribution of average power for the "Follow me" Ford Ranger driving cycles and comparison with the average motion power

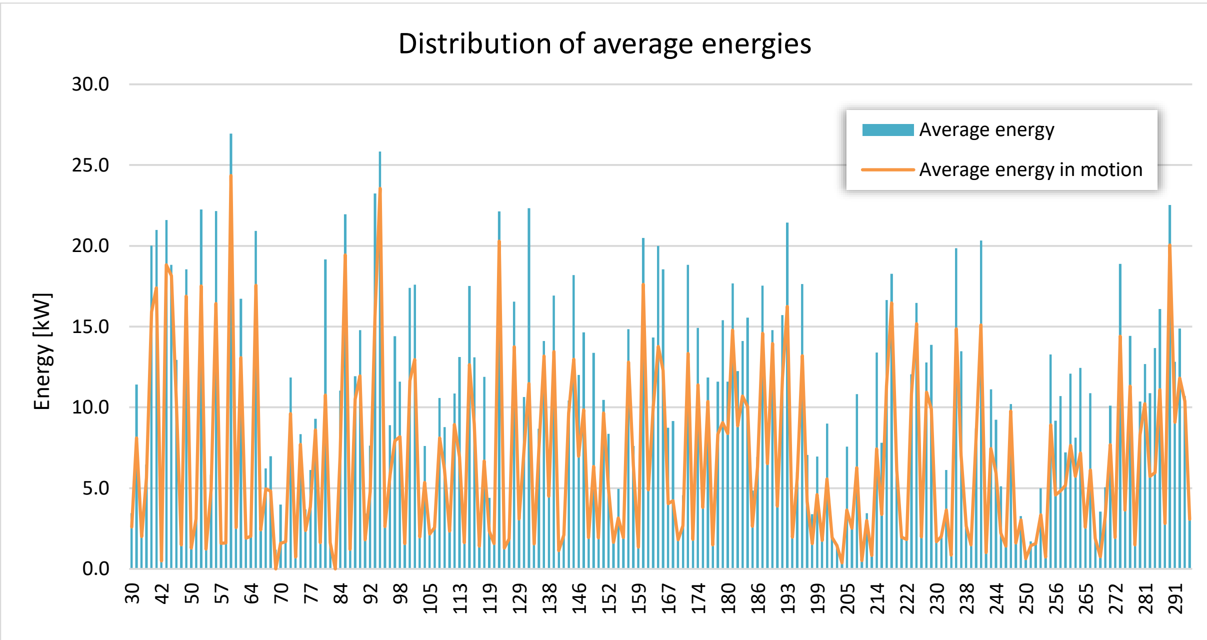

Figure 21: Distribution of average energy for the "Follow me" Ford Ranger driving cycles and comparison with the average motion energy

The data on *average fuel consumption* are representative of how the vehicle has higher consumption, above the ones as reference indicated on the data sheet, since its operation at low speeds and high idle times are prevalent. For the Ford Ranger in question, where theory speaks of average consumption in combined cycles between 6.9 and 7.2 l/100km [49], in 92.6% of driving missions it consumes more, with an average of just below 11 l/100km. The *total consumption* shows that, on average, the vehicle consumes 2.3% of its tank capacity (which is equal to 80 l [49], a big capacity probably selected to decrease de necessity of refuelling moments) when carrying out a driving mission, with a maximum of 7%. In this case again, it will be interesting to calculate what the fuel requirement will be in relation to the tank capacity over a whole operating day. Lastly, *average energy consumption*s are also analysed, since correspond to a value that is used in electrically driven vehicles to define their utilization. Again, these consumptions are high, above the ones found in a conventional electric vehicle, which are around 0.2 kWh/km in urban use and around 0.3 kWh/km in extra-urban use [50]. What can be said it that this type of use is energy-consuming for the vehicle, more so than road transport use, as driving missions are long and there is a lot of idle time. In addition, if regenerative braking were possible, its efficiency would be greatly reduced, as the times in which braking energy is produced would be very few, to the detriment of predominantly stationary use.

Fuel consumption [l/h]	Energy Consumption [kWh/km]
5.89	0.63
4.77	0.47
4.53	0.74
4.51	0.49
4.48	0.55
4.34	0.47
4.34	0.42
4.22	0.46
3.98	0.45
3.93	0.39
3.93	0.40
3.78	0.44
3.68	0.48
3.62	0.44
3.54	0.34
3.48	0.45
3.48	0.44
3.43	0.51
3.33	0.44
3.20	0.51

Fuel consumption [l/h]	Energy Consumption [kWh/km]
0.44	1.68
0.56	0.88
0.61	0.71
0.61	1.13
0.67	1.13
0.72	0.85
0.74	0.71
0.75	0.97
0.78	0.84
0.80	0.66
0.80	0.66
0.81	0.66
0.85	0.64
0.85	0.71
0.90	0.54
0.91	0.67
0.91	0.56
0.93	1.06
0.93	0.85
0.94	0.39

Figure 22: Comparison between fuel and energy consumption for the "Follow me" Ford Ranger driving missions. On the left: overall 20 highest values of fuel consumption and related values of energy consumption. On the right: overall 20 lowest values of fuel consumption and related values of energy consumption.

It is interesting to comment what is shown in the previous Figure 22, comparing the fuel consumption and energy consumption values for the 20 driving missions with the highest and lowest average fuel consumption values, respectively, as an example. Generally, high fuel consumption corresponds to low energy demands in relation to the distance travelled, since large distances are covered for the same amount of energy consumed. In these terms, energy consumption can be seen as energy efficiency, giving an indication of how useful the energy consumed was in moving the vehicle. In driving missions characterised by high idle time, even if little fuel is consumed, the energy efficiency is always low, as this energy is consumed without travelling. In the following Figure 23, attention is once again drawn to the relationship between idle time and vehicle energy consumption, showing how they generally present the same trend. In other words, the more the vehicle is used at low efficiency, the higher the energy consumption tends to be in relation to the distance travelled in the driving mission.

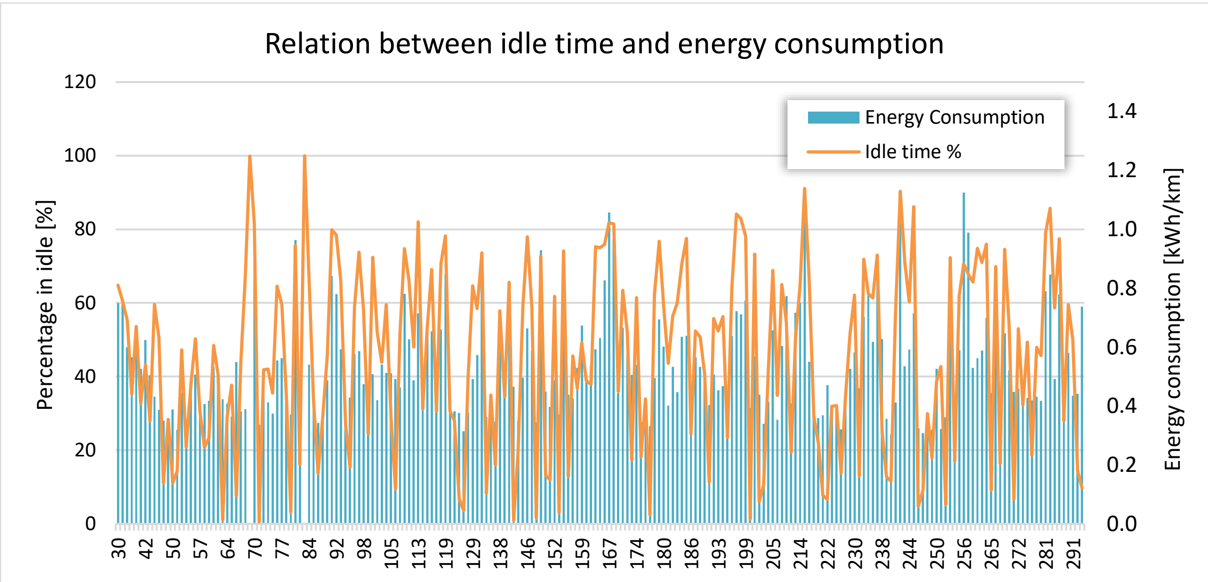

Figure 23: Distribution of energy consumption for the "Follow me" Ford Ranger driving cycles and comparison with the percentage of idle time

Finally, in order to have a more in-depth overview of power and energy, boxplots have been made for some of the quantities. As far as maximum power is concerned, its distribution is shifted in favour of high values with a high frequency, but it still maintains a very high variability, depending on the maximum speeds that are reached in the various driving missions. It is a different story for the motion, where most measurements are concentrated in the low values and its variability remains limited, being dependent on the average speed in motion, which in the course of the driving missions is almost always in the range of 25 km/h to 35 km/h. For what regards energy, results are also concentrated in the lower values, albeit with a higher variability. These considerations can be seen graphically in the Figure 24 below, obtained using MATLAB® software.

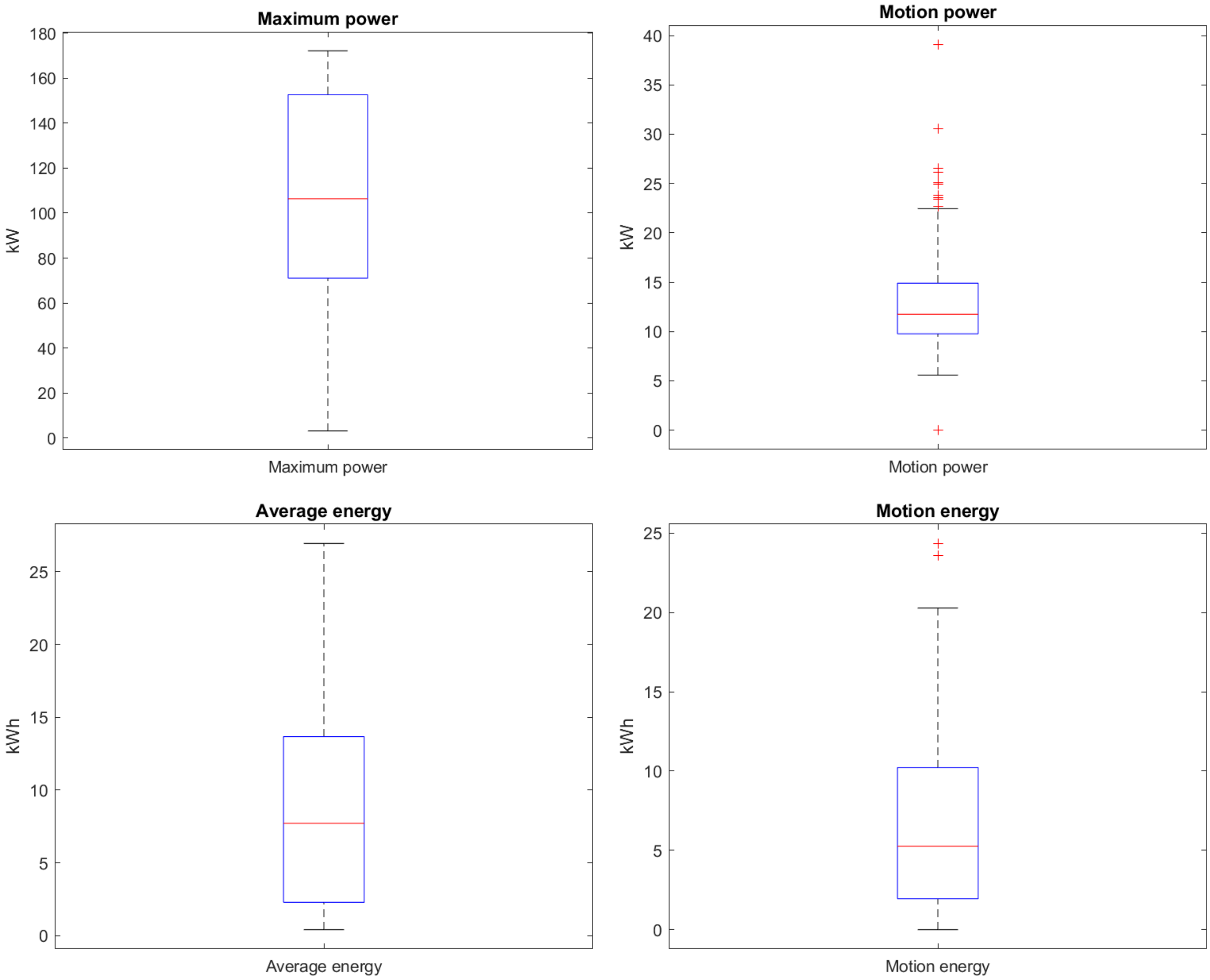

Figure 24: Boxplot representation for whole "Follow me" Ford Ranger driving cycles data of power and energy quantities

3.3.2. Data analysis based on operative days

By summing up the data for each of the files considered in the data processing organized in same days, it was possible to obtain the same previous values to give a qualitative indication of the vehicle's needs, but with a view above a whole operative day. The Table 7 on the next page shows main representative values, presenting the minimum, average and maximum. Of the 216 driving missions included in the final calculation, data for 32 operative days were carried out, varying their composition between only two driving missions till including 10 of them. All these values will be again discussed and eventually compared with the data in the vehicle's technical sheet, in order to explain which considerations can lead, also showing some charts when necessary.

Data	Minimum Value	Average value	Maximum value
Total time [h]	0.74	8.93	15.12
Time in motion [%]	24.48	44.97	86.49
Idle time [%]	13.52	55.02	75.52
Distance [km]	15.92	117.38	256.31
Average energy [kWh]	9.16	59.18	107.40
Average motion energy [kWh]	7.63	44.28	87.04
Fuel consumption [l/h]	0.87	1.46	3.67
Total fuel consumption [l]	1.84	12.13	22.84
Energy consumption [kWh/km]	0.40	0.53	0.76
Motion energy consumption [kWh/km]	0.31	0.39	0.55

Table 7: Summary of all representative values of vehicle's operative day requirements

The *total time* for a whole day has a very high variation, from less than one hour till more than 2/3 of a day in continuous operation. Otherwise, the average shows how the time is quite high, which could be a problem for electric-propelled vehicles, considering the low capacity and high recharging time. With storage systems not adequate to supply enough energy, this type of powertrain could suffer, or at least need of wiser utilization to not income in possibility to not being available when requested. The *time in motion* and the *time in idle* give the same indication of what was found in the previous analysis: more than half of operative day is spent in idle. With regard to the *distance* travelled, the data reflect what was said by AENA, namely that such a vehicle travels with great variability between a few and 250 km in a working day, thus varying greatly depending on requirements. As for the total time, the lower autonomy of electrified vehicles and the need for recharging could produce problems that must be considered. However, FCEVs do not need to be recharged, as their energy management manages to keep the battery at an adequate charge level at all times. The refuelling of hydrogen takes a fairly limited amount of time, in the order of minutes, which is slightly more than what is required for combustion vehicles. Compared to a purely battery-electric solution, this allows the problem of recharging to be overcome, while issues concerning the need for adequate capacity must continue to be considered. In the Figure 25 below, similarly on what done for the altitude variation in Figure 19, the distribution of operative time values is graphed to show their variability. Moreover, in the Figure 26 in next page, in the same way the distribution of covered distance each day shows the variability of this data.

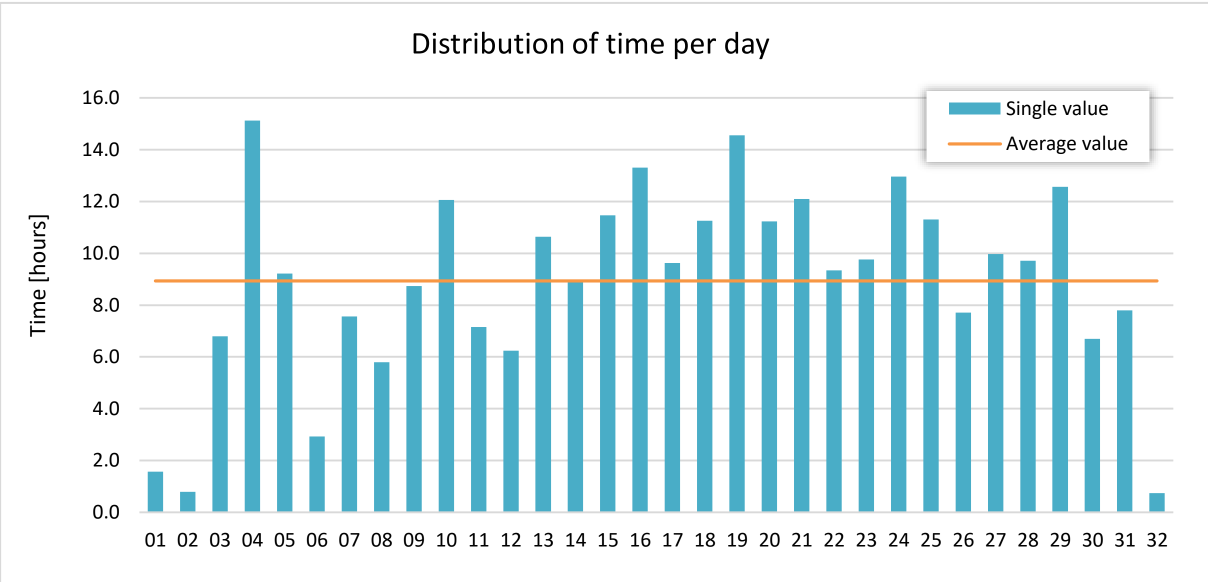

Figure 25: Distribution of operational time each day for the "Follow me" Ford Ranger driving and comparison with the average value

As far as *average energy* is concerned, the amount of it which is required from the vehicle in a day operation is equivalent to what a battery can give, in a complete discharge cycle, of the type generally used in a conventional electric vehicle. Indeed, Today's EV batteries can provide a capacity from 28.9 kWh (in the Mini Cooper SE, for an EPA range of 110 miles) to roughly 200 kWh (in the coming 2022 GMC Hummer EV pickup, which is expected to have a range of 350 miles), with a whole average of 66 kWh. Considering that, although in rare cases, the vehicle can consume energy quantities of up to 100 kWh in a single day, a "Follow me" car can be considered as a particularly energy-intensive vehicle [51]. In Figure

27 in next page, similarly as shown in Figure 20, average motion power values are always higher than the average ones and their distribution is correlated, presenting the same trend. Their difference increases as much as the time in motion within the operative day is high.

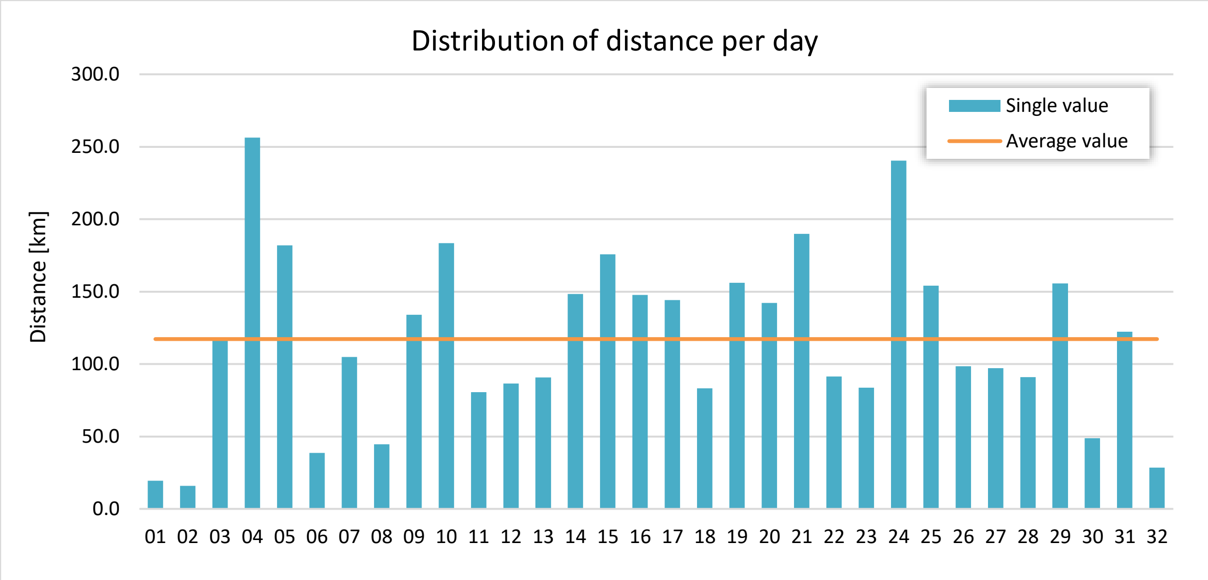

Figure 26: Distribution of distance covered each day for the "Follow me" Ford Ranger driving and comparison with the average value

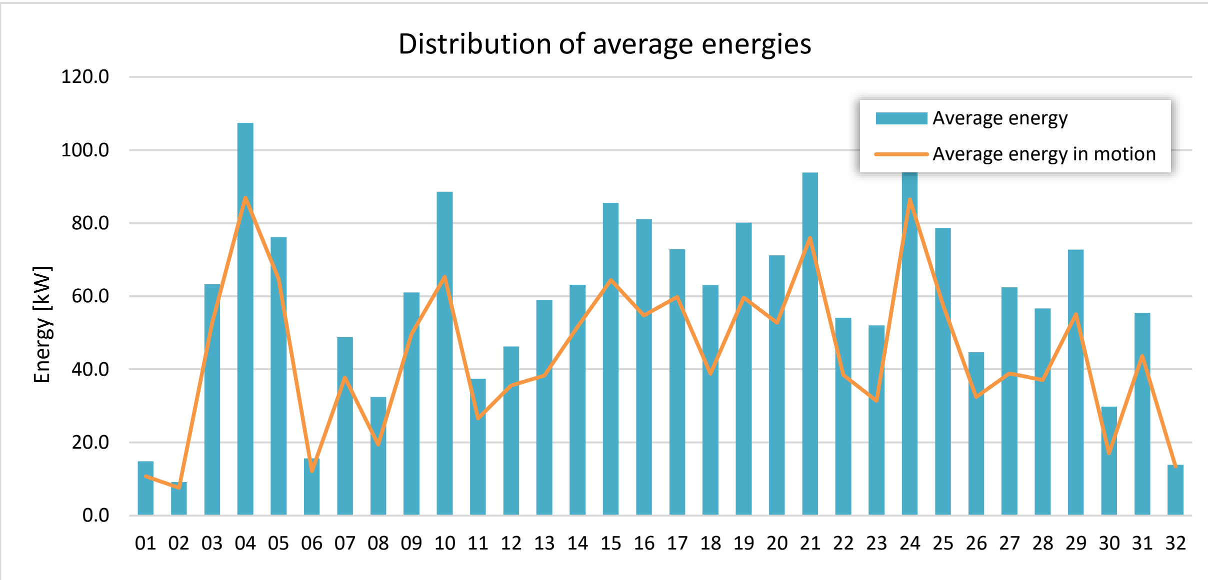

Figure 27: Distribution of average energy for the "Follow me" Ford Ranger days of operation and comparison with the average motion energy

Data on *average fuel consumption* and *energy consumption* are still representative of how the vehicle has high consumptions, since operation at low speeds and high idle times are prevalent. The *total consumption* shows that, on average, the vehicle consumes in a day 15.1% of its tank capacity (which is equal to 80 l [49]), with a maximum of 28.8%. This means that a tank, wisely chosen big for this purpose, needs to be refuelled every 6 days, on average, or each 3 days in worst case, which does not correspond to a problematic demand in terms of having the vehicle in an operational state all the times. Likewise shown in Figure 23, the Figure 28 below shows that the vehicle is energy-consuming as much as driving missions are long and full of idle time.

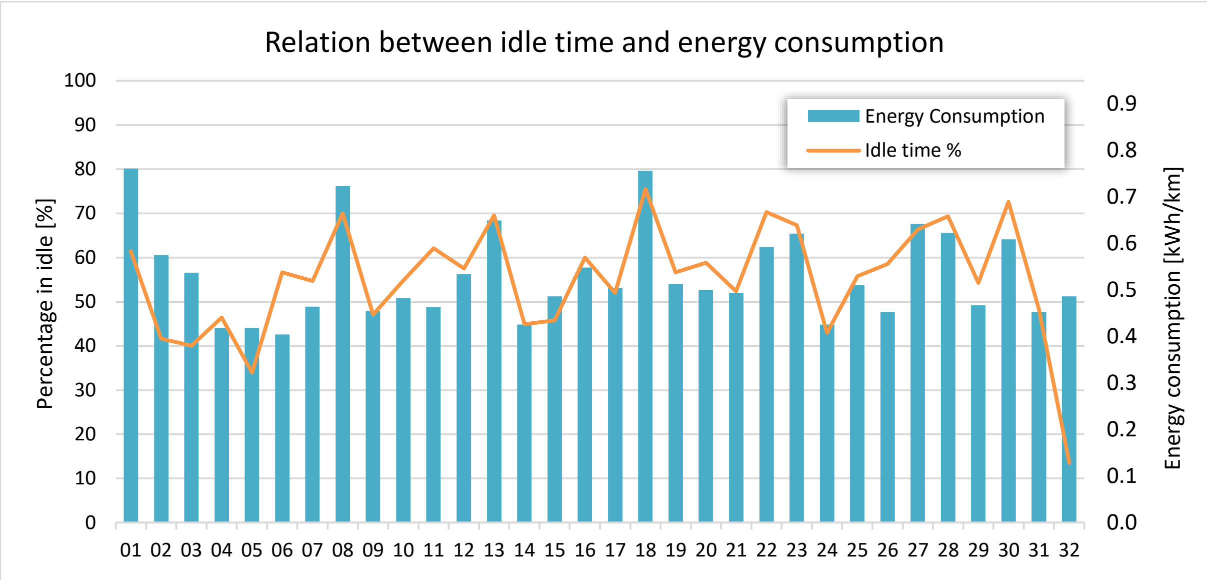

Figure 28: Distribution of energy consumption for the "Follow me" Ford Ranger days of operation and comparison with the percentage of idle time

3.3.3. "Follow me" features summary evaluation

In conclusion, wanting to create a general summary of the results obtained through the analysis of the data available from the "Follow me" vehicle, both with regard to a single driving mission and an entire operational day, the following Table 8 is created. It summarizes and evaluates which characteristics are required and provided by the airport vehicle under examination and thus which will be those to be replicated in the FCEV.

Feature	Evaluation
Time of utilization	High average operating time, high variability and prevalent (55%) idle use
Distance covered	High distances travelled, with great variability according to needs
Altitude variation	Use of the vehicle on almost flat routes with very limited gradients
Maximum vehicle speed	Moderately high speed (100 km/h) reached in 1/6 of the driving mission, while peaks (> 120 km/) only less than 5%
Average vehicle speed	Low average speed (30 km/h), almost similar to what expected in urban use
Maximum power needed	High power values (150 kW) achieved in 1/3 of the cases
Average power needed	Low average power for vehicle movement, near 20 kW with peaks of 40 kW
Average energy needed	High amount of energy required each day (average of 60 kWh), equivalent to the whole capacity of a standard EVs battery
Fuel consumption	High fuel consumption, higher than the vehicle would have in an urban use
Energy consumption	High energy consumption, higher than what a normal EV would have, even in the worst energy-demanding cases

Table 8: Summary of real "Follow me" vehicle features and evaluation with respect to needs

Chapter 4: Powertrain Components Selection

In this chapter, the definition of performance, power, energy and consumption requirements of the hybrid powertrain, in order to obtain the proper sizing and selection of the elements composing it, will be carried out.

Thanks to the data analysis, will be explained the requirements of the FCEV propulsion system, necessary to recreate the performance of the original operating ICE vehicle. With them, it will be possible to present the expected vehicle architecture, with all its characteristics and also the ones of all the elements that will compose it, basing on the results of appropriate simulations using longitudinal vehicle models. Finally, will be specified which actual components will be selected from the market for future purchase, installation and setting up in the final prototype.

4.1. Definitions of vehicle requirements

Once the behaviour of the "Follow me" vehicle has been analysed and, consequently, the characteristics it must possess for proper utilisation have been defined, the requirements for FC powertrain components must be decided, in order to size them and select from the market. These components have to be found individually from what the market offers, specific values have to be outlined in order to research and subsequently purchase from the various manufacturers. Since it is not possible to resort to an unlimited budget and is present a limit for the purchase of all the elements, an evaluation must obviously always be made when defining requirements, considering not only the performance, but also the cost of the various elements. Although some have relatively low and competitive prices and there are many alternatives on the market (such as for battery and electric motor), for the FC system, with fewer solutions and high prices, the final choice will necessarily have to pass through compromises. Below, first concrete requirements for the powertrain elements are outlined. However, for the electric motor, it is not yet appropriate to draw them up definitively, since further analyses will have to be carried out, for reasons which will be presented later.

4.1.1. Sizing of battery and high voltage DC bus

The average energy and power values found in the data analysis give an indication of what is the proper high voltage sizing. Wanting to provide the vehicle with a hydrogen traction capacity of around 10 to 30 kW, having to reach power peaks of 120 kW and having to meet am high average daily energy demand of around 60 kWh, with daily peaks of up to 100 kWh, a nominal 400 V battery (i.e., in between 250 and 500 V) seems to be adequate. This value also defines the voltage of the vehicle's HV bus, which connects all high-voltage systems operating in the powertrain, such as power converters and inverters. It is possible to find batteries with a voltage of around 400 V that can withstand charging and discharging currents in line with those of the EM to be selected, as well as having a satisfactory capacity, probably less than the 60 kWh envisaged, but still sufficient for a full day's operation. Obviously, a higher capacity battery could also be considered (i.e., the 700/800 V solution), providing more easily a better performance and greater autonomy, to cover with margin also the longest days and to allow to work with lower currents. However, such a solution would be too expensive for the activity and by raising the voltage value, then will be more difficult to find an electric motor with power values around 120 kW, as well as having to raise the range of voltage values for the other HV components, with problems relating to safety, HV circuit management effort and their price.

4.1.2. Sizing of hybridization unit relevance

Another issue to be addressed for the prototype in question is whether or not to install a recharging system: in other words, to define whether or not to opt for a plug-in solution. Indeed, given the low power by the hydrogen power supply, as will be further analysed in subsection 4.1.4., the final FCEV powertrain seems to take on a structure that can be traced back to that of a Range-Extender (RE) hybrid with the possibility to recharge the battery from recharging infrastructures.

- *RE:* in such a hybrid, the secondary power source is primarily used to enable the vehicle to increase the range that would normally be achieved, with the same vehicle, by presenting only the primary power source. The hybrid unit power usually in this case is equal to the average power of a reference cycle representative of the real usage of the vehicle, like the 13 kW which comes out from the data analysis. In this case, the primary source can be seen as the battery, while the secondary source and intended for the RE function is the hydrogen. In such an architecture, this would mean that the FC would not be able to allow the battery to have a CS profile, but rather a CD one, as it would not be able to safely deliver a sufficient level of energy at all times to keep the battery within an adequate charge level. Another consideration to be made in favour of this architecture is the comparison between the price of hydrogen and the price of electricity for a vehicle. While this will probably be less relevant in the future, there is currently a substantial price difference in relation to the energy supplied for the two energy sources. Hydrogen is more expensive than electricity and this could lead to a preference for recharging the vehicle in a plug-in solution rather than refilling the hydrogen tank more frequently. However, a non-rechargeable solution, with the FC allowing the vehicle to be self-sufficient in terms of battery charging, is not entirely dispatchable. Such a possibility will depend very much on the type of energy management strategy that will be implemented in the vehicle, either for or against certain objectives, such as hydrogen consumption or battery sustaining. Therefore, the decision on the presence of a recharging point in the vehicle is postponed to later evaluations, only when simulations with already functioning EMSs will be able to give actual indications on the convenience of one solution over another.

- *LF:* Another possibility could be implementing a Load-Follower (LF) hybrid, where the hybrid unit must be able to provide a power which can cover all the continuous maximum power condition. In this typology, the hybrid unit is bigger and with bigger contribution in the traction of the vehicle, also allowing the possibility of a CS profile and avoiding the presence of an OBC for battery external charging. However, in the case of a complete maximum continuous power supply, for the real usage of the "Follow me" vehicle in question the range of the FC power should be near 30 kW, target which seems to be difficult to reach, considering the high price of FC systems.

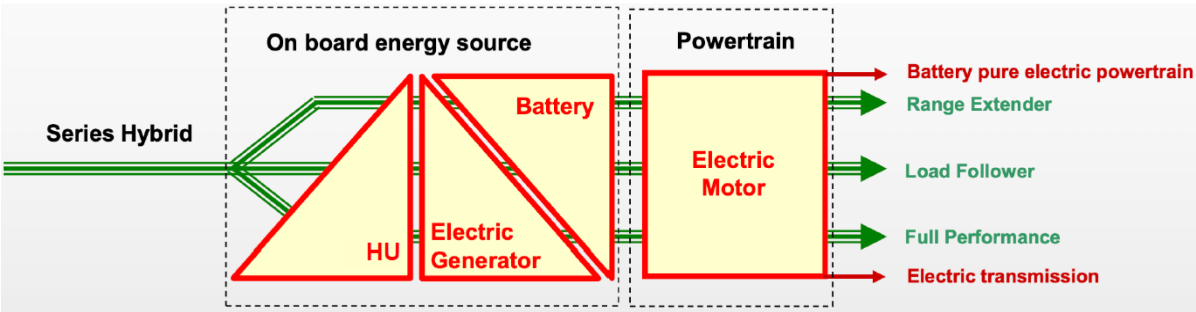

Figure 29: typologies of simple hybrid electric vehicles [61]

4.1.3. Sizing of electric motor

Apart from the type of motor, which considering the variety on offer and the better performance it can offer, a synchronous permanent magnet motor will be probably selected, the crucial characteristics it must have are different: peak power, continuous power, peak torque, speed range and input voltage range:

- *Peak power*: having detected several times during the cycles, as maximum power, a value of 120 kW, and wanting to exclude cases where peaks of more than 150 kW are reached, since they correspond to speeds above 120 km/h, the EM must be able to deliver this level of power. In reality, the cases in which the maximum power exceeds 120 kW have been many, more than 50%, but in order to achieve an adequate price-performance compromise and taking into account a high difference between peak and continuous, as will be analysed in the next section, an EM capable of delivering a maximum of 120 kW and thus reaching at least an hypothetic speed of 100 km/h is the most viable solution. Speeds much higher than this value may be considered superfluous for operational purposes, since along the runways the "Follow me" vehicles circulate with limits of 30 km/h and only reach maximum speeds when travelling outside the airside, to reach another terminal or to return to service stations.

- *Continuous power*: the analysis showed that this value is very low, in the region of 13 kW. There is a high difference between peak and continuous since the majority of utilisation is conducted in idle or at low speeds, with high peaks being reached several times but only for a very limited portion of use. If the solutions on the market have to be analysed, the value that must be compulsorily satisfied is the peak one, while the continuous will in any case be satisfied, considering that EMs in the order of 120 kW peak always have a continuous value which reach at least a few dozen of kW.
- *Peak torque*: the definition of the requirement cannot be made without simulations, since its value necessarily depends on the characteristics of the vehicle in which the motor is to be placed, rather than on the vehicle from which the data was taken. There is no high difference between the "Follow me" Ford Ranger and the Iveco Massif where the FCEV powertrain will be implemented in terms of dimensions and masses involved. However, as they are, respectively, a front-wheel-drive and an all-wheel-drive vehicle, with different gearbox and differential ratios, further analysis must be performed. The analysis of the data yielded values with peaks of 420 Nm, which is the maximum torque of the vehicle in the airport, but it is easy to assume that, by providing an engine with lower peak power values, torque values will also be lower. Nevertheless, what may be the proper torque requirement for the vehicle can be obtained by means of appropriate simulations, where it is possible to define the needs under conditions of high acceleration and high gradients.
- *Speed range*: having to change the type of motor, from a combustion motor that necessarily uses gear ratios to reach high speeds, to an electric motor with power and torque characteristics with a greater and single speed range, it is necessary to define this value. There are different solutions on the market in terms of maximum speed with the desired power value, depending on the technical characteristics of the electric motor, between 4000 and 10000 rpm. Consequently, in the same way as can be done for peak torque, appropriate maximum speed values can be obtained by means of simulations, still under conditions of strong acceleration and steep slopes.
- *Input voltage range*: the voltage value that the electric motor uses for traction is defined by the battery and what the HV BUS can handle, i.e. expected 400 V nominal. Consequently, the motor must be able to operate with voltage values in the range of 250 and 500 V. It must be considered that the power and torque values for an electric

motor are dependent on the supply voltage, so they may vary, albeit to a limited extent.

4.1.4. Sizing of hydrogen tank

In this case, there are basically two solutions: refillable and non-refillable hydrogen tanks.

- *Refillable tanks* are larger and more expensive, providing greater autonomy and avoiding the need to remove them manually when they become empty.
- *Non-refillable tanks* tend to be smaller in volume and price, as their removal must be quick and easy and their replacement economically not demanding.

As far as this activity is concerned, given the lack of hydrogen refuelling stations in the proximity of the research centre and the lack of need for high autonomy, it is complicated to use a refillable hydrogen tank. Indeed, for the length of tests that will actually be carried out on the vehicle once the FC powertrain is installed, a tank capable guaranteeing several hundred kilometres of autonomy would be unnecessary. In addition, for refuelling with a fixed tank, this would entail moving from the site every time the tank became empty. In Spain there are 11 hydrogen refuelling stations, two within the Community of Madrid, the closest to INSIA is at a distance of 10 km. For these reasons, the choice has been to use non-refillable tanks, to be changed whenever they run out of hydrogen. This choice, in any case, does not affect the results of this thesis, as the presence of rechargeable or non-rechargeable tanks in the vehicle is a factor that does not affect its EMS formulation.

As far as sizing is concerned, theory speaks of a range of around 100 km per kg of hydrogen as fuel. This means that, assuming a worst-case scenario, i.e. operating days in which distances of 300 km are covered, a 3 kg tank would be exhausted. Current hydrogen vehicles on the market have tanks in the range of 4-6 kg, so the expected range is around 300-600 km, as the data sheets for these vehicles also state. This would translate, in the case of a "Follow me" vehicle, to the consumption of the entire tank on longer operative days, or 30-40% of the same if one considers the average distance measured in the data analysis. These values are slightly higher to those seen for the Ford Ranger used at the airport, showing that between diesel and hydrogen propulsion there is a difference in the frequency of need for recharging/refuelling. A tank in the order of the above-mentioned kilograms, like the ones of current vehicles on the market, can therefore be considered sufficient for the purpose. The weight of the hydrogen tank should be limited, since the heavier and bulkier the tank, the heavier the vehicle and the more complex the supply system. In any case, this size for this prototype will depend on the possibilities offered by the market, which generally tend not to exceed a weight of between 4 and 6 kg for reasons of space, weight cost and management, but in reality will be shown that it will be impractical to resort to such a voluminous solution. Wanting to define a minimum, maintaining the value of 100 km/kgH_2 as capacity of hydrogen as fuel, a tank of at least 1 kg should be present in a "Follow me" vehicle, in order to provide an acceptable extension of the electric range.

4.1.5. Sizing of fuel cell system

The hydrogen part of the traction system is the real protagonist of this activity, so it would be a priority to procure a fuel cell with sufficiently high performance values, in order to be as interesting as possible, from the point of view of hydrogen research. However, despite this premise, the fuel cell system in the prototype vehicle will not have a high power output, mainly for budget reasons. Nevertheless, the results that can be achieved with a power-limited engine in a hybrid FC-battery system are interesting and valid, as they present similarities between logical and operational processes regarding operation and energy management, for any power level. As the FC is sized according to the power level, the average power values define the requirements for the fuel cell system. Having measured an average power close to 10 kW, considering idle time, and 13 kW, considering only movement, the FC must be able to match at least this power level. In reality, the average power reaches values of up to 39 kW in certain driving cycles, in short cycles where the speed is always high. As said before, should be very interesting the idea of procuring and studying a FC capable of fully satisfying the average power demand even in the worst or unusual cases, in order to be able to fully operate continuously and autonomously, always within an appropriate efficiency range. In addition, considering that FC systems are normally supplied with net power from which the power required from its BoP for the power supply is already subtracted, having a power of 10 kW would mean having a net power that is only about double what the system loses for its own operation. This means having a system with low efficiency, as well as being inconvenient for production purposes for automotive surrounds, with the consequent possible difficulty of finding commercial solutions with such low power. However, the solution of higher power is not viable for this activity, for two fundamental reasons: the first is that, as before, such high average power cycles tend to be unconventional, and not related to purely operational purposes; the second, of a practical nature, is that, if a cost-performance balance were to be made, a FC capable of achieving more than 30 kW would require a very high expense, would occupy an excessive volume and, since it would not be possible to use an on-board refuelling system, that capacity would be wasted for the hydrogen consumption in question. This last sentence is because non refuelling solutions tend to be smaller, allowing for a small quantity of hydrogen as fuel and making the solution of having a FC with high power and therefore consumption impractical: the hydrogen tank would be exhausted very quickly. Consequently, the wisest choice is to resort to a fuel cell system with a power rating of between 10 and 20 kW, going higher to satisfy transient, if necessary, with the energy provided by the battery. With such a power level, the FC will be able to cover the typical energy demands of continuous operation and also be able to recharge the battery, to increase its range, under certain conditions. As expressed earlier in subsection 4.1.1., whether the FC will be able to enable the vehicle to have an RE architecture can only be found in more advanced stages of the analysis, in the fine-tuning part of the EMS.

4.1.6. Sizing of power conversion systems

Regarding the power converter systems, there will be two in the vehicle in this prototype: the inverter for the electric motor and the DC/DC boost converter for the FC. As far as the former is concerned, its power and voltage values will be defined once the electric motor is defined, in any case they will have to adapt to the voltage of the HV bus, i.e. 400 V, and to the currents available from the EM. The boost converter is a more complex matter, since it also represents a fundamental element for the powertrain of a hydrogen hybrid vehicle for FC control purposes. Such a converter will have to match the output voltage of the FC with that of the HV bus, and will probably have a rather high power, as the voltage conversion should be high. This is because the output voltage of a FC with low power is predictably low, in the range of 50 to 100 V. Additionally, the boost converter is not only needed to increase the tension: FC stacks are sensitive to load variance, it means that when the load increases, the fuel cell stacks voltage will drop steeply at first, which will affect the output voltage. Therefore DC/DC converter is mandatory also to stabilize the output voltage and reject the disturbance from transient behaviours. In any case, the precise selection of power and voltage ranges even for such a component can't be defined before sizing and selection of the final FC.

4.1.7. "Follow me" FCEV expected requirements summary

In conclusion, wanting to create a general summary of the FCEV expected requirements, obtained through the analysis of the powertrain data available from the "Follow me" vehicle, theoretical evaluation and market research, needed to recreate the expected performances with the new FC architecture, the following Table 9 is created.

Component	Requirement
High voltage battery	Li-ion battery with expected nominal 400 Vdc (in the range 250 – 500 Vdc) with an energy in the order of 30 – 50 kWh
High voltage DC bus	Expected nominal 400 Vdc (in the range 250 – 500 Vdc)
Electric motor	Synchronous with permanent magnets, expected peak power in the range 100 – 120 kW, maximum torque in the range 300 – 500 Nm, maximum rpm in the range 6000 - 10000
DC/AC power inverter	Possibility to deal with 400 Vdc of the HV bus line and with the peak power of the EM
DC/DC boost converter	Possibility to increase the output voltage of FC to the 400 Vdc of the DC bus
On-board charger	Expected voltage of 500 V
Fuel Cell system	Expected output power in the range 10 – 20 kW
Hydrogen tank	Non-refillable and theoretical capacity of at least 1 kg
Vehicle architecture	Very likely Range Extender, very unlikely Load Follower

Table 9: Summary of "Follow me" FCEV powertrain expected requirements

4.2. Electric motor final sizing

4.2.1. Longitudinal flange-model for vehicle testing

As mentioned in the previous chapter, not all requirements could be determined simply from the analysis of powertrain and driving missions' data. Specifically, the torque characteristic and speed range of the electric motor need further analysis. Their requirements depend on the characteristics of the Iveco Massif's driveline, rather than on the vehicle from which the data were taken, being respectively a front-wheel drive vehicle and an all-wheel drive vehicle, with different gearbox and differential ratios. Appropriate peak torque and speed values can be obtained through simulations with a suitable model, subjecting the vehicle architecture to tests to determine its capabilities. The FCEV prototype will be equipped with a single-speed transmission by selecting among one of the six possible gears, not by changing the gearbox. In fact, the current Innvextran features a ZF 6S400 overdrive 6-speed transmission, coupled to the remote-mounted Santana transfer box, able to provide either 4x2 or 4x4 traction. In this way the transmission, in combination with the transfer box, provides 12 forward gear ratios and 2 reverse gear ratios [52]. As far as transmission ratios are concerned, those of the ZF 6S400 and the transfer box are:

ZF 6S400	Gear 1	Gear 2	Gear 3	Gear 4	Gear 5	Gear 6	Reverse
Transmission ratios	5.373:1	3.154:1	2.041:1	1.365:1	1.000:1	0.791:1	4.838:1

Transfer box	High	Low
Transfer box ratios	1.003:1	2.300:1

Table 10: Transmission ratios for Innvextran gearbox and transfer box

To define torque and speed range values, the vehicle can be subjected to two tests: an acceleration test and a slope test. The first is necessary to find out what speed and torque the vehicle needs to complete a high acceleration, testing every gear that can possibly be used; the second is necessary to find out what gear and torque the vehicle needs to overcome a high gradient. When the vehicle has the ability to satisfactorily complete these two actions, it can be said to possess an engine with the appropriate characteristics to cover all its use, along with those discussed in the previous chapter. In order to subject the vehicle to such tests, AVL Cruise™ M software was used, enabling the longitudinal dynamics of the vehicle to be modelled as realistically as possible, but with a high simplified powertrain model, with all its characteristics in terms of masses, dimensions, and driveline (characteristics of the wheels, differentials and gearbox). In order to obtain an indication of the maximum torque required by the vehicle to perform a given driving cycle, a flange element was used instead of the electric motor, which returns angular velocity or torque values as a function of the cycle it is subjected to. The model used for these tests is presented below:

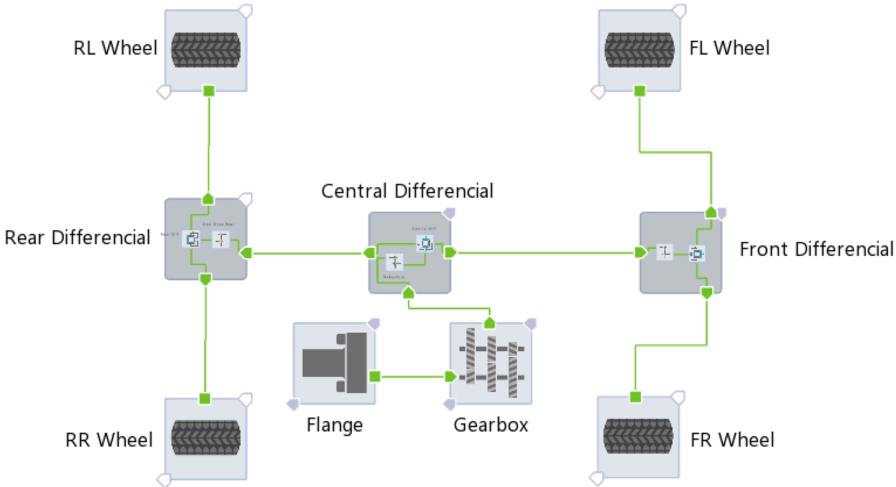

Figure 30: Simplified vehicle model with flange for acceleration and slope testing

4.2.2. Blocks used in AVL Cruise™ M flange-model

A brief explanation of the main blocks used in the longitudinal model, and which will also be used in future models, is presented below:

- *Differential*: the differential unit compensates for discrepancies in the respective rotation rates of the drive wheels. With rare exceptions for special applications, the differential is a bevel-gear drive unit. When the output bevel gears on the left and right sides are of equal dimensions, the differential gears act as a balance arm to equalize the distribution of the torque to the left and right wheels. The functioning of the differential takes reference on the following scheme:

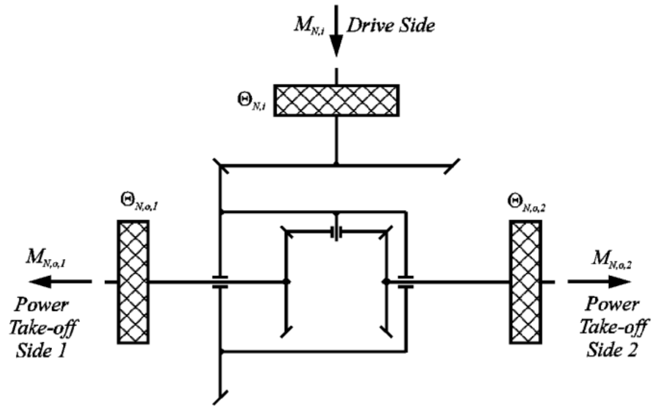

Figure 31: representation of the differential scheme used in AVL Cruise™ M

The equation used to compute the speed at the two take-off side is the following:

$$\dot{\varphi}_{N_{in}} \cdot (i_N + 1) = \dot{\varphi}_{N_{out,1}} + \dot{\varphi}_{N_{out,2}} \cdot i_N$$

Where $\dot{\varphi}_{N_{in}}$ is the angular velocity at the drive side, $\dot{\varphi}_{N_{out,1}}$ and $\dot{\varphi}_{N_{out,2}}$ at the take-off sides and i_N is the current gear ratio.

- *Gearbox*: gear transmissions featuring fixed ratios can maintain a correspondence between the respective performance curves for engine and vehicle. The component contains a model for a gearbox with different gear steps. For each of the six gears it is possible to define its transmission ratio, the mass moments of inertia, and the moment of loss. In the component for manual gearbox, the engine torque will be turned into a power take-off torque by considering the transmission, the mass moments of inertia, and the moment of loss. The efficiency is evaluated as follow:

$$\eta G = \frac{M_{G_{out}} \cdot \dot{\varphi}_{G_{out}}}{M_{G_{in}} \cdot \dot{\varphi}_{G_{in}}}$$

Where $M_{G_{out}}$ is the power at the take-off side, $M_{G_{in}}$ at the driver side, $\dot{\varphi}_{G_{out}}$ is the angular velocity at the take-off side and $\dot{\varphi}_{G_{in}}$ the one at the drive side.

- *Wheels*: the wheels and tires link the vehicle to the road. The component considers many influencing variables and their effect on the rolling state, like load, wheel pressure, velocity and temperature. The reference wheel load is computed as follow:

$$F_L = \mu_{road} \cdot \mu_{tire} \cdot C_F \cdot C_S \cdot F_W$$

Where μ_{road} and μ_{tire} are the friction coefficients of road and wheels, C_F and C_S are the slip correction coefficients and $F_{W,s}$ is the load on the wheel. The model asks for static and dynamic wheel radius. The latter is evaluated directly from the map of the actual wheel speed $\dot{\varphi}_{W_{out}}$:

$$r_{W,dyn} = r_{W,dyn}(v_{veh}) = r_{W,dyn}(\dot{\varphi}_{W_{out}})$$

- *Flange*: the equation implemented within the model to allow the flange block to work with the appropriate angular velocity, appropriately converted according to the vehicle kinematic chain, is as follows:

$$\frac{v_{cycle}(t)\ [m/s]}{R_{wheel}\ [m]} \cdot \tau_{diff}^{front} \cdot \tau_{diff}^{centr} \cdot \tau_{gearbox} = \omega_{flange}(t)\ [rad/s]$$

The equation represent the input for the flange: $v_{cycle}(t)$ is the value of velocity for each time instant for the implemented cycle, R_{wheel} it's the dynamic wheel radius, (equal to 390 mm), τ_{diff}^{front} is the front differential ratio, (equal to 3.909), τ_{diff}^{centr} is the central differential ratio, which is the transfer box ratio, and $\tau_{gearbox}$ is the transmission ratio of the selected gear, among the possible six listed before. The output of this equation is $\omega_{flange}(t)$, which is the value of angular velocity for each time instant, followed by the flange to produce the torque which would be requested by the electric motor.

4.2.3. Flange acceleration test

In order to determine an appropriate acceleration profile to be able to define the needs of the EM, the various driving missions were analyzed to find an intense and prolonged acceleration to high speeds in a short period of time. It was preferred to search for a real-life case, rather than defining a standard acceleration value, to try to trace the real needs of the vehicle as closely as possible. The driving mission number 255 has an acceleration from 0 to 115 km/h in 25 seconds, which was selected as the most representative direct and homogeneous acceleration at high speeds of all the various driving missions, even when looking at the demanded engine load data (which, for this case, was for the most part 100%). The maximum acceleration value for this selected part of the profile is 1.958 m/s^2, which is not the maximum measurable, but still high enough to be relevant to the requirements definition. The cycle that is converted to an acceleration test, inserted within the model to provide input to the flange block and thus obtain the graphs that will be shown later, is as follows (suitably made suave to obtain an acceleration profile that is as constant as possible):

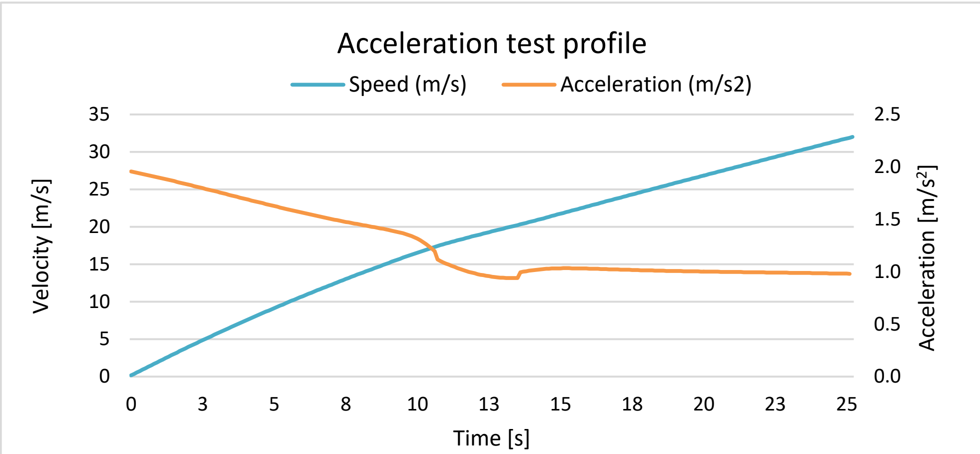

Figure 32: Acceleration profile selected for electric motor acceleration testing

The results obtained are shown in the next two Figure 33 and 34. Various simulations were carried out by varying the gear and load of the vehicle, between empty and full, and the values of maximum torque and speed were represented for these various conditions.

- *Torque*: as can be seen from Figure 33, the lower the gear selected, the greater the torque required to move the vehicle along the acceleration. For low gears, low torque values of less than 150 Nm, which can be obtained from practically any vehicle EM for automotive purposes in the market, are already sufficient. For higher gears, however, the need increases to values of more than 300 Nm, defining more stringent requirements. The peak torque values possessed by electric motors on the market with maximum powers in the range of 100 – 120 kW are between 250 and 500 Nm. Consequently, as far as low gears are concerned, maximum torque does not seem to be a problem, considering that very easily one of them would be selected for the final prototype, as they allow adequate acceleration, in contrast to high gears that would lead the vehicle to have a slow and unresponsive behavior.
- *Speed*: Figure 34, on the other hand, shows the maximum angular speeds required for the motor to complete this acceleration with a single gear ratio. The first gear has an excessive value that cannot be reached by automotive EM, so it can be

directly discarded. As far as the others are concerned, second gear exceeds 8000 rpm, a value that not all motors can achieve, while for the other gears, angular speed values are easier to obtain. Consequently, combining what we have seen for both maximum torque and maximum speed, the candidate gears to be the final one for the vehicle are the first three, where as far as the first is concerned, it is unlikely that it can really be used for reasons of excessive speed.

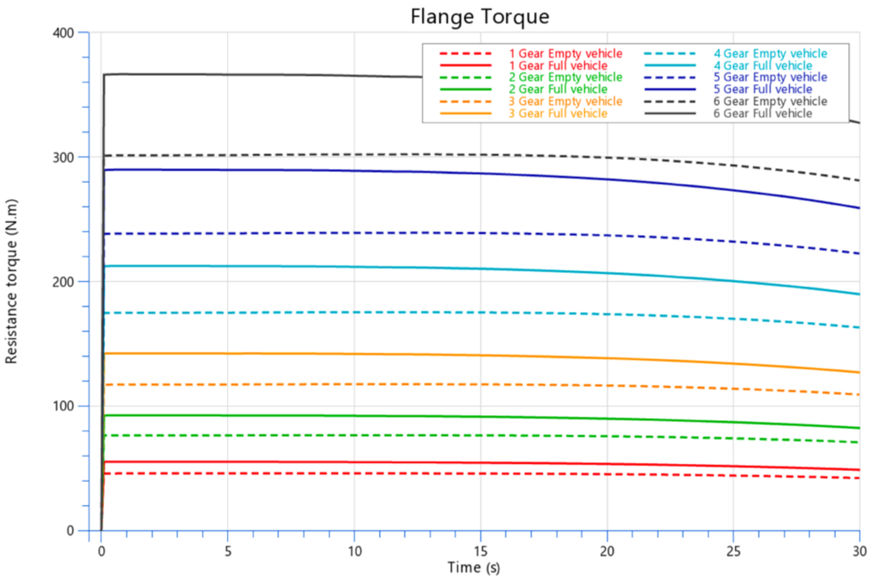

Figure 33: Peak torque needed for the vehicle to complete a 0-115 km/h acceleration in 25s for each gear, in empty and full condition

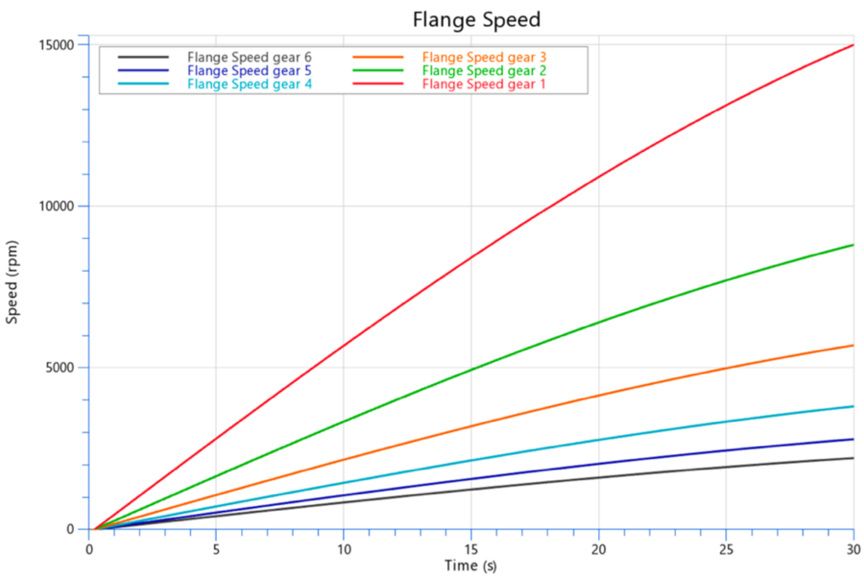

Figure 34: Maximum speed needed for the vehicle to complete a 0-115 km/h acceleration in 25s for each gear, in empty and full condition

4.2.4. Flange slope test

To define an acceleration profile that would allow the vehicle to be subjected to a grade test, considering that the vehicle is required to pass it even very slowly and with very low accelerations, the following profile was recreated:

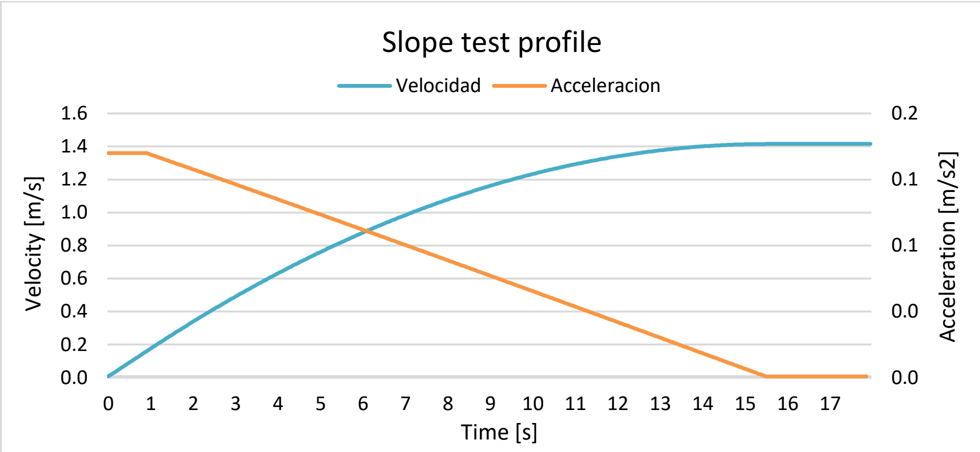

Figure 35: Acceleration profile selected for electric motor slope testing

It is an almost-zero acceleration, to go from 0 to 5 km/h in 18 seconds. The vehicle configuration was simulated in such a way as to recreate the worst case, i.e. full. As far as the transfer box is concerned, the architecture of the Innvextran, as shown above, allows the use of an additional ratio from the transfer box, precisely to help overcome higher gradients, since it is a 4x4 vehicle designed for off-road use. Consequently, the maximum torque required by the vehicle to overcome even a very steep gradient is not excessively high, when considering the first few gears. The Figure 36 in the following page shows the results of the test, with the maximum torque values for each gear, with a gradient value of 35%, selected as a reference because it is a standard value that vehicles should be able to overcome with their characteristics. Gears 4 to 6 require too much torque for an engine capable of delivering a maximum power of 100 to 120 kW, while the lower gears can be considered, reaching maximum values of 500 Nm. Without the additional gear ratio provided by the transfer box (equal to 2.3), the torque values obtained, all other things being equal, would have been twice as high. This would have meant that only the first two gears could have been considered, or that with the use of the others the maximum slopes would have been lower.

It is useful to see on the maximum gradient: in reality, as mentioned above, the maximum gradient that such a vehicle can face in an airport is almost zero. In fact, with a worst value of 6% in the airport layout, can be seen that a "Follow me" vehicle does not need to possess any particular torque capacity to overcome slopes. However, since the vehicle is also useful for emergency situations and is useful to possess the ability to cover unusual task, a higher torque value can always be useful, which is why it was decided to test it with higher slope.

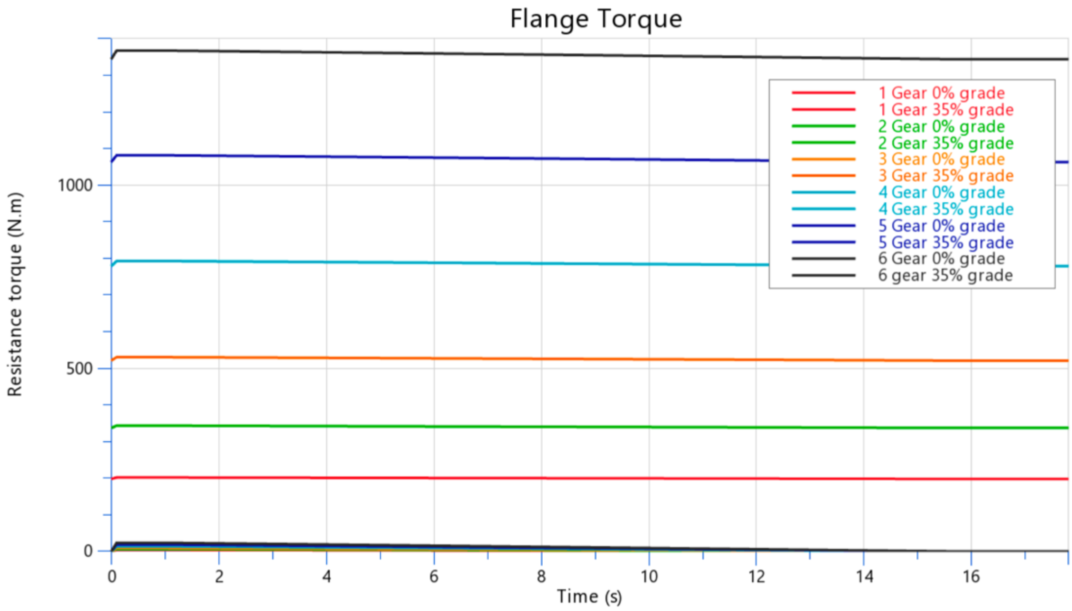

Figure 36: Peak torque needed for the vehicle to move in a 35% grade surface

4.3. Electric motor evaluation

4.3.1. Longitudinal eMotor-model for vehicle testing

Now that all the requirements of the electric motor have been defined, it is possible to evaluate concrete solutions on the market, in order to select the one which will be bought. Of the various solutions proposed by the various electric motor manufacturers, four were selected for in-depth analysis, meeting the necessary characteristics. In fact, knowing the characteristics of these electric motors, as well as their power and torque curves, it was possible to carry out a series of simulations on a simplified vehicle model in the AVL Cruise™ M programme. The simulations can be considered as a series of tests, as done for the definition of the EM requirements, to verify how the prototype-vehicle would behave with the given electric motor, under various operating conditions. These tests were, in addition to the acceleration and the grade ones, the completion of certain driving missions derived from the data of the real ones analysed in the data analysis part. Since these were related to power, angular velocity and torque features, it is not necessary to simulate the model on driving missions upon operative days, but it is sufficient to do so on individual driving cycles.

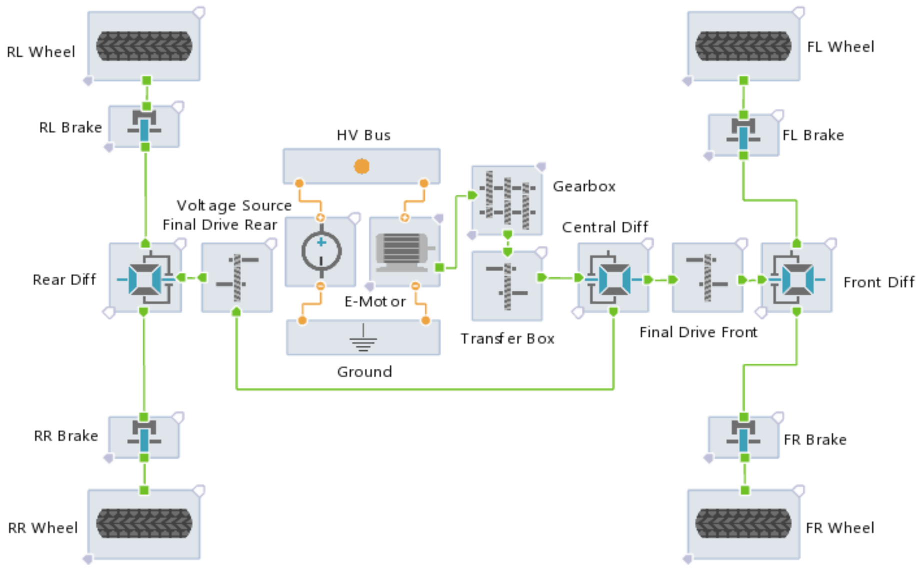

Figure 37: Simplified vehicle model with eMotor and voltage source for eMotor testing

The model used for these simulations is presented above in Figure 37, the blocks modelling brake dynamics have been added, as well as one simulating the behaviour of a standard driver. This time, the model is implemented with an electric motor and a battery in the form of a constant voltage source, since battery discharge and SOC do not vary significantly for driving missions lasting in the order of minutes. The specific performance in terms of delivery of battery and fuel cell powers is also not significant, the only requirement being that the electric motor receive a voltage input of approximately 400 V to function as it would in a real powertrain. The constant voltage source is therefore created in such a way that constantly sends the value determined as a requirement, i.e. the nominal 360 V. The four electric motors found on the market, which at least theoretically meet the necessary characteristics, are presented in the following Table 11:

Electric motor	Peak power	Cont. power	Peak torque	Cont. torque	Max rpm	Max operating voltage	Mass
Emrax 228	125 kW	65 kW	228 Nm	112 Nm	6.500	680 V	12 kg
Phi Power PHI301	150 kW	85 kW	320 Nm	190 Nm	9.000	800 V	29 kg
Borgwagner HVH250-115	100 kW	80 kW	425 Nm	300 Nm	10.500	700 V	57 kg
Cascadia iM-225W	120 kW	80 kW	500 Nm	325 Nm	11.800	800 V	60 kg

Table 11: Main features of the four proposal electric motors for the analysis and selection

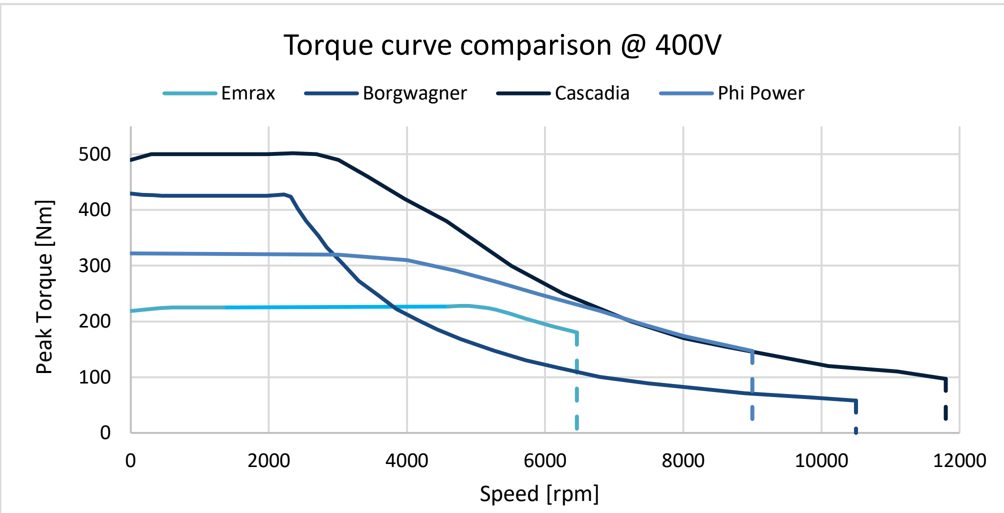

Figure 38: Graphical comparison between peak torque curves of all eMotors

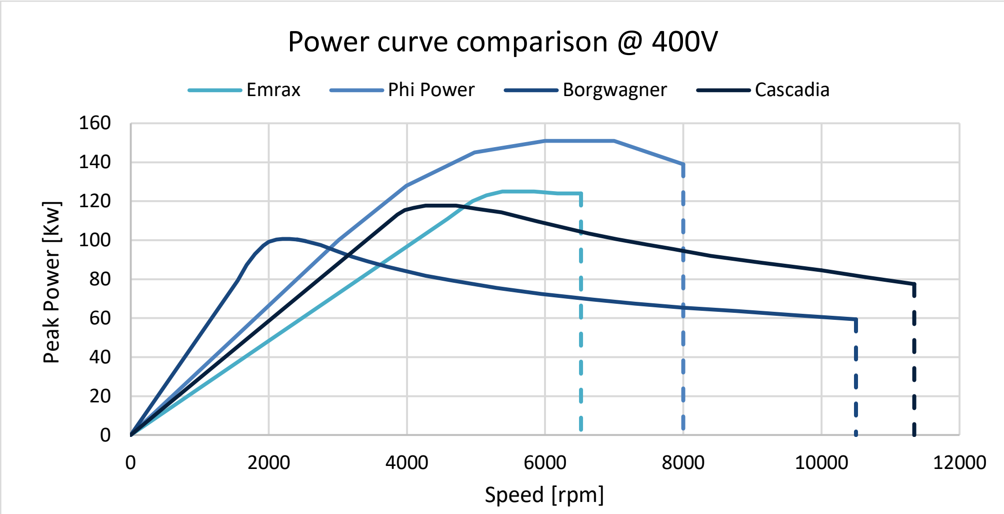

Figure 39: Graphical comparison between peak power curves of all eMotors

All of them are synchronous with permanent magnets electric motors, operating with a maximum power range between 100 and 150 kW, maximum torque between 230 and 500 Nm and maximum angular speed of not less than 6500 rpm. The two Figures 38 and 39 presented above show the peak power and peak torque curves for the first positive quadrant of the motors considered at a voltage value of 400 Vdc. These characteristics and how they combine will vary the performance considerably, as will be seen in the results proposed below. However, the results of the simulations will provide the final conclusions as to which engines will be suitable and which engine is the best, for what regards the considered powertrain characteristics and the driving missions to be completed.

4.3.2. Blocks used in AVL Cruise™ M eMotor-model

Compared to the previous flange-model, additions are present in this latter one. A brief explanation of the added blocks used in this longitudinal model is presented below:

- *Continuous voltage source*: an ideal voltage source that is able to output a user-defined voltage without regard to the current flow through the component.
- *Electric motor*: the electric machine component present in AVL Cruise™ M can be used to model electric motors using a simple map based approach. Losses maps are also present, depending on mechanical power, both for efficiency and heat. If desired, the inverter's power losses can also be specified separately. The EM tries to deliver the requested torque (or the equivalent torque based on the full load

characteristic and requested mechanical load), then the power losses are added to the delivered mechanical power to get the electrical one. For permanent magnet synchronous machines (PMS), a temperature correction is also applied, based on the following equation:

$$Torque_{eM,max}^{PMS} = \left(1 + \beta E_{eM_{rem}} \cdot \left(T_{eM} - T_{eM_{layout}}\right)\right) \cdot Torque_{eM,max}$$

Where $Torque_{eM,max}$ is the max deliverable torque, T_{eM} and $T_{eM_{layout}}$ are respectively the actual and layout temperature of the EM and $\beta E_{eM_{rem}}$ is a remanence induction coefficient. The layout temperature is the value at which the reference full load characteristics are specified, while the remanence coefficient is used to modify the full load characteristics with a linearly machine's temperature-dependent correction. In order to provide an example of the losses implemented in the model of EM, the following Figure 40, representing the first quadrant losses both for EM and power inverter for the Cascadia iM-225W for a 400 V line are shown:

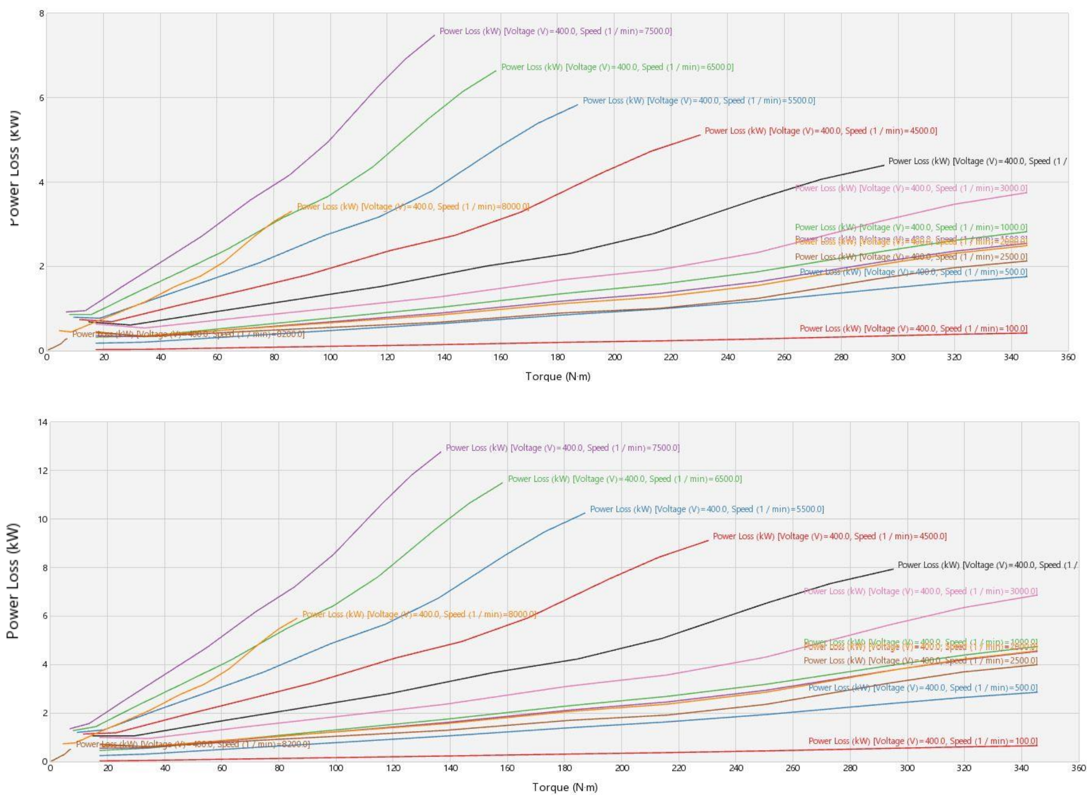

Figure 40: Losses curves for EM (above) and inverter (below) for the Cascadia iM-225W

- *Brakes*: the brake component is used to simulate the braking characteristics of each wheel and is described by brake data and dimensions. The braking torque is computed considering the braking dimensions and the input brake pressure. When the control variable is the pressure, the instantaneous braking torque will be computed as follows:

$$T_b = 2\, p_B\, A_B\, \eta_B\, \mu_B\, r_B\, c_B$$

  Where p_B is the braking pressure, A_B the braking piston surface, η_B the efficiency, μ_B the friction coefficient, r_B the effective friction radius and c_B the specific brake factor. Being the braking torque, a resistant torque which opposes the brake rotation, its value is zero when the brake rotational speed is zero. The specific brake factor is a factor that depends on the design of the brake. For disc brakes it is always one, for drum brakes it is usually bigger than 1.

4.3.3. eMotor acceleration test

For the acceleration test, the powertrain model is subjected to the cycle implemented for the same test seen before with the flange, so that it presents the most realistic high speed and acceleration values. This means an acceleration of 0 to 115 km/h in 25 seconds, reaching maximum values of 2 m/s^2. The electric motor must be able, according to its characteristics, to successfully complete the cycle, reaching maximum speed at the end of 25 seconds. The vehicle is tested empty and with the first three gears, as the other three will not be taken into consideration for the final selection. The results obtained are as follows:

- *Emrax*: indeed, as its characteristics would lead one to believe, it is the engine which with most difficult is possible to achieve such accelerations. Only in third gear it reaches 125 km/h, while in first gear it does not even reach half the target speed. In terms of acceleration, this engine can only be considered when using third gear.
- *Phi Power*: although it has a slightly higher torque than the previous engine, thanks to its high peak power values it can satisfactorily complete acceleration with the second and third gear.
- *Borgwagner*: in the same way as the previous engine, it appropriately achieves top speed values, excluding first gear.

- *Cascadia*: again, as the engine characteristics suggested, it is the one that achieves the best performance in terms of acceleration. Even in first gear, it manages to reach a speed of 100 km/h, remaining at maximum rpm for a short time.

In order to provide an example of what could be analysed in the simulations, the results obtained with the Borgwagner in first and second gear are presented below. The Figure 41 and 42 show the profile that should be followed by the vehicle (*'Desired Velocity'*) and what is actually obtained (*'Vehicle Velocity'*), also in terms of angular speed (*'eMotor Speed'*). The torque (*'eMotor Torque'*) and power (*'eMotor Power'*) values that are achieved during the test are also shown. When the EM, with the gear considered, cannot successfully meet the cycle, the vehicle velocity reaches a certain value and then continues with the same until the end of the 25 seconds. This obviously results in a sudden decrease in torque and consequently also in power. Conversely, as in the case of second gear, if the engine is able to complete the test, vehicle velocity follows the desired velocity curve very well, torque is maintained throughout the test and power increases as speed increases.

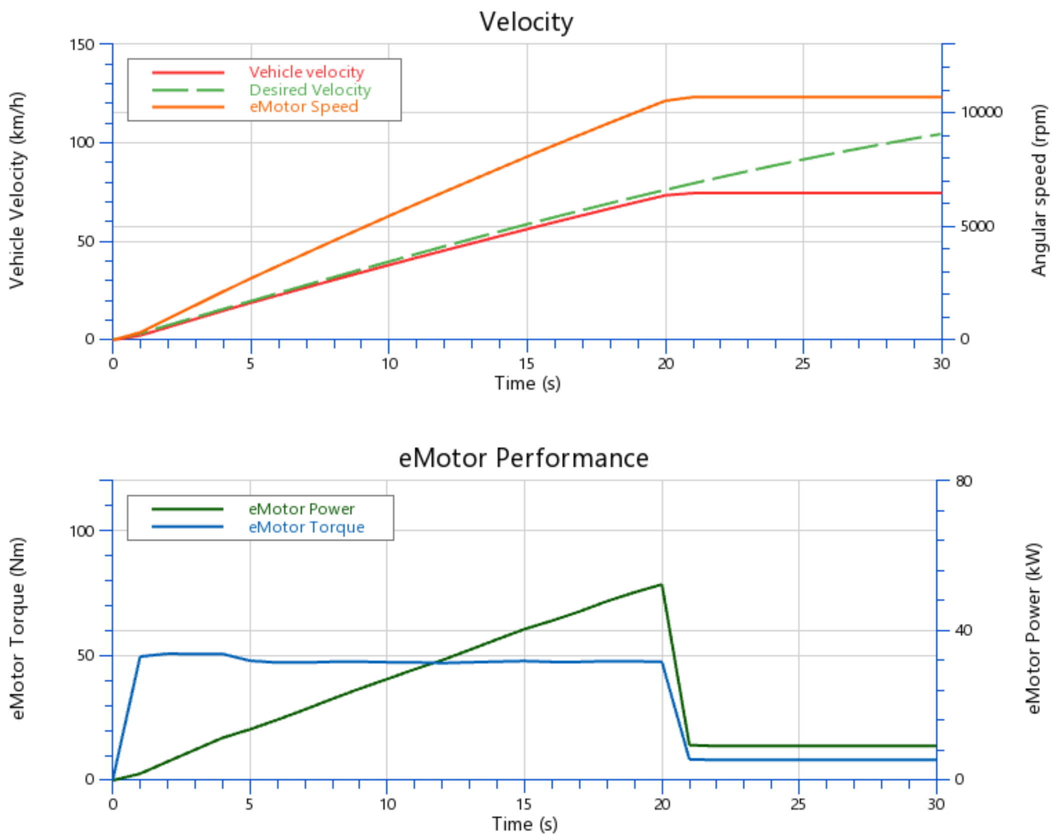

Figure 41: Speed and performance results for acceleration test with BW-1 gear eMotor

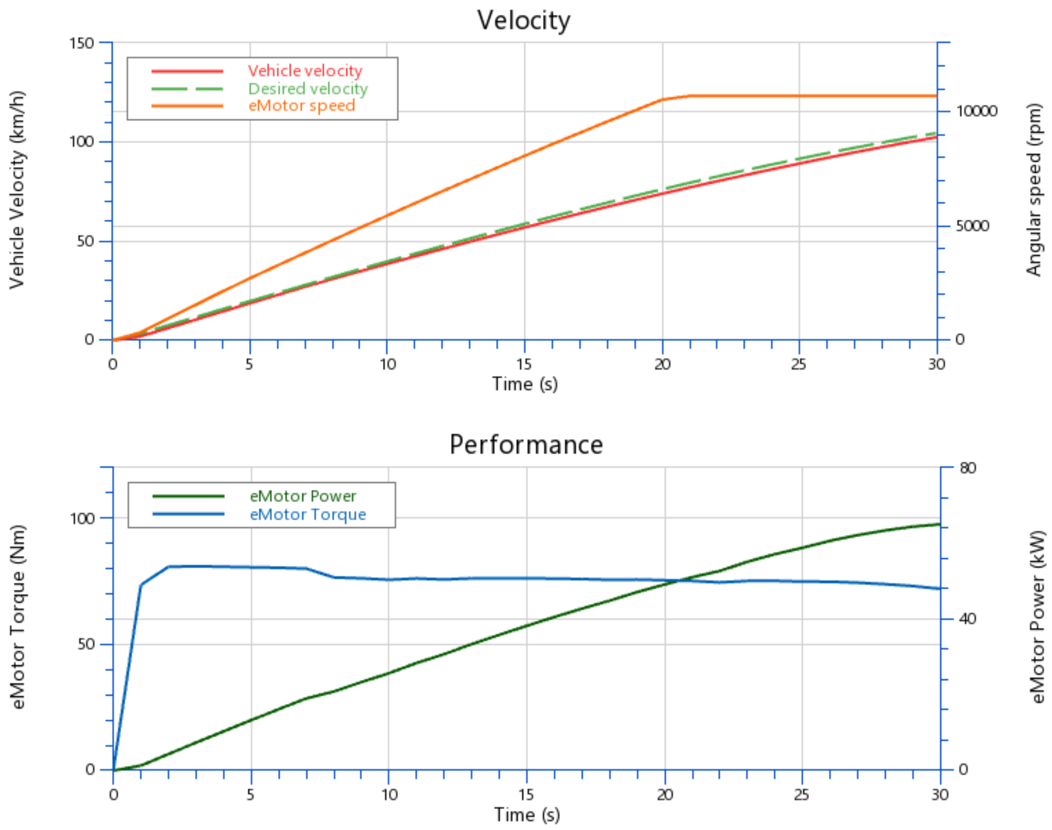

Figure 42: Speed and performance results for acceleration test with BW-2 gear eMotor

4.3.4. eMotor slope test

As before, the same cycle presented in the test part with the flange model is used again. The vehicle is required to go, even very slowly and with very low acceleration, from 0 to 5 km/h in 18 seconds. The configuration of the vehicle was simulated in such a way as to recreate the worst case, i.e. full vehicle. As far as the transfer box is concerned, the Innvextran architecture allows the use of an additional transmission ratio to help overcome higher gradients. Again, only the first three gears are tested, with a maximum slope of 35% (or less in case the EM is unable to successfully cycle at this slope value). In this case, again thanks to the central differential that allows a reduction in the gear ratio due to the off-road characteristics of this vehicle, the test is passed by all EMs and in any gear, with the only exception of the Emrax in 1st gear. In this case, the engine manages to overcome a gradient of up to 32%, which although not the value tested, is still a very high gradient, which would not preclude the performance of the vehicle. In fact, as mentioned above, having to operate on mostly flat routes, such a high gradient will never be reached by a "Follow me" vehicle.

In any case, this pattern gives an indication of how this EM is the only one that suffers most from high gradients, while the other three have no problems whatsoever.

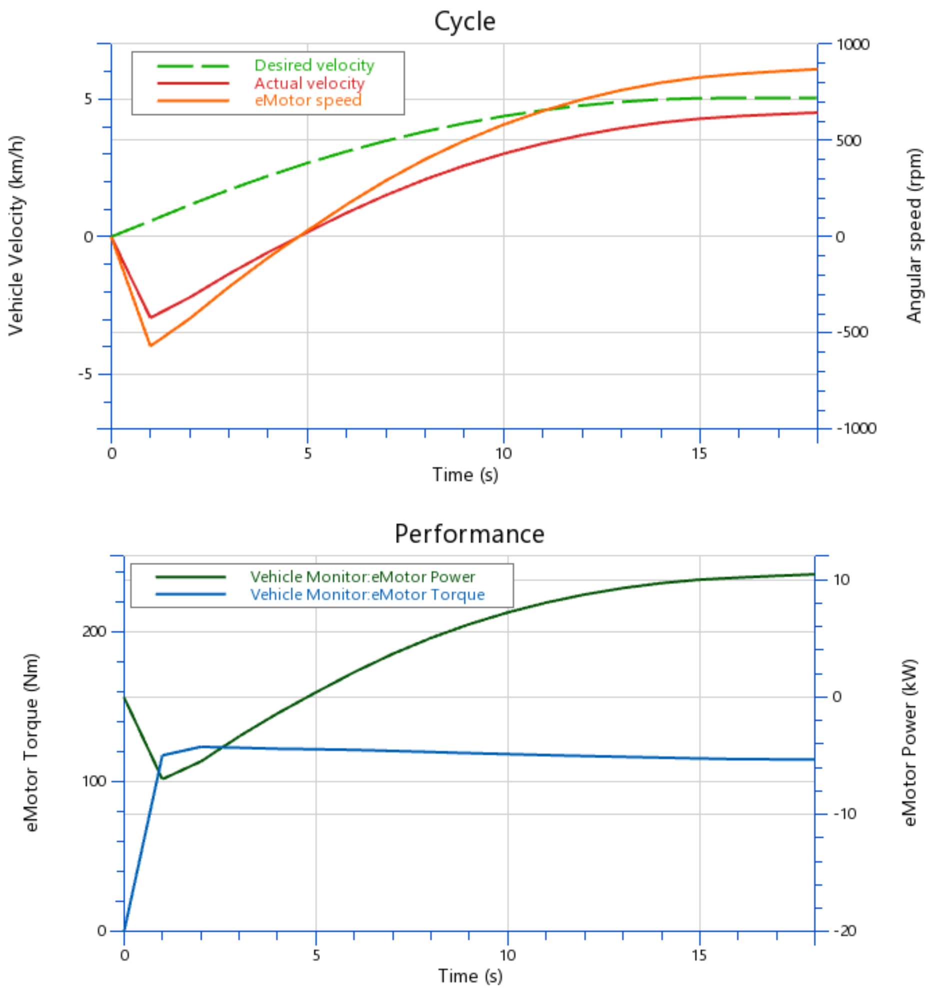

Figure 43: Speed and performance results for 35% slope test with EMRAX-2 gear eMotor

Again, with the aim of providing an example, the Figure 43 and 44 relating to the results obtained in the case of a completed or non-completed test are shown, therefore with the Emrax electric motor. In the first case (in Figure 43) 2nd gear, the figure on the top shows the profile that should be followed by the vehicle (*'Desired Velocity'*) and what is actually obtained (*'Vehicle Velocity'*), also in terms of angular speed (*'eMotor Speed'*). The torque (*'eMotor Torque'*) and power (*'eMotor Power'*) values that are achieved during the test are also shown, in the bottom figure. In a case of completed test, it can be seen that the trend in vehicle speed follows the desired one, albeit with a certain difference. This is due to the fact that in the simulations there is a time delay in which the driver's model applies maximum acceleration and the vehicle wins its inertia for movement, which does not happen instantaneously. As in the acceleration test, torque is maintained over the whole time, while power increases in proportion to vehicle speed.

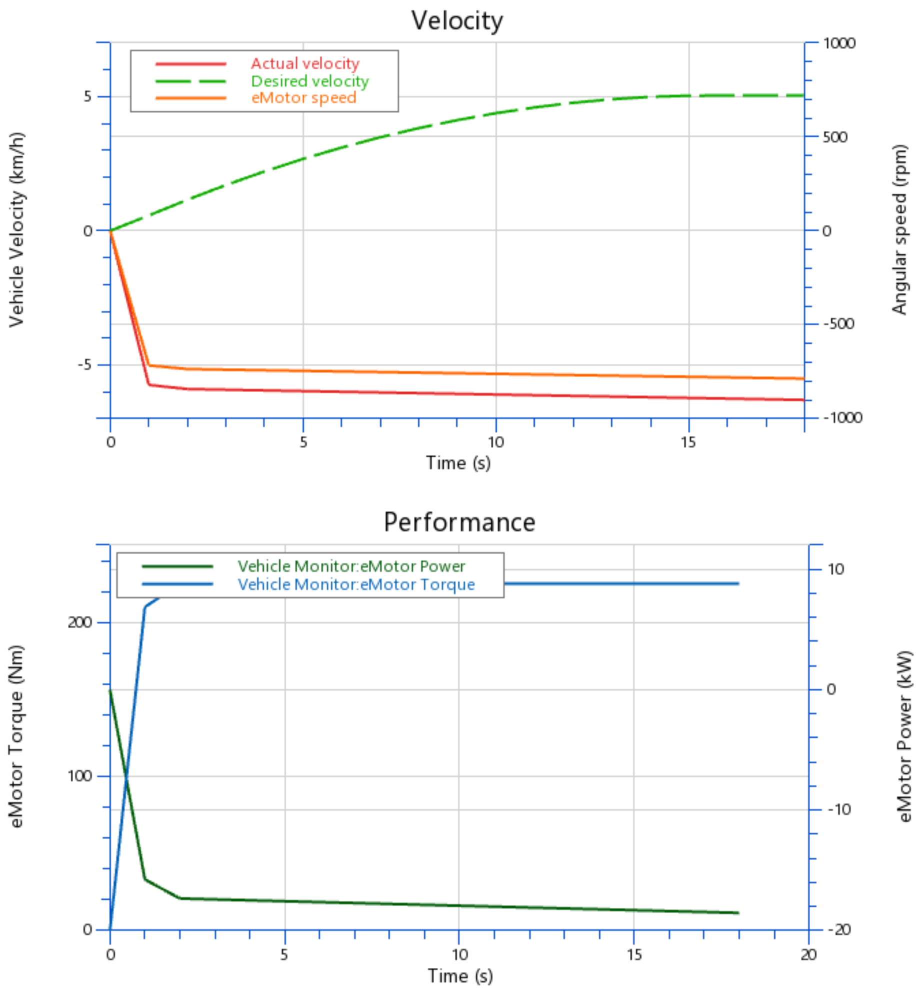

Figure 44: Speed and performance results for 35% slope test with EMRAX-3 gear eMotor

In the second figure, however (Figure 44 above), the EM is unable to complete the test: the vehicle's speed does not follow the desired profile and undergoes a continuous decrease, indicating that the vehicle is moving backwards in trying to climb an inclined path. Torque is higher, brought to maximum to try to overcome the slope, while power is very low, as there is not much movement.

4.3.5. eMotor driving mission tests

In order to test the longitudinal model of the vehicle with the various EM in different driving missions, profiles capable of recreating real-life conditions must be encountered from among those available from the data analysis. In fact, thanks to the data analysis carried out in the previous chapter, it is possible to know all the data of the various driving cycles, as well as all the profiles. For this purpose, four representative diving missions were identified and are shown below. In reality, the model has been tested in other cycles, with other features, but the most representative ones, meaning only whose results can actually help to give an indication of the final choice, are presented below.

- Driving mission n°32: it possesses most of the average values in Table 5, i.e. the average values among all the various driving missions analyzed. This is a cycle of 77 minutes, with a max speed of 109 km/h, maximum power of 120 kW, ratio between idle and movement time 55-45% and average fuel and energy consumption. The point is to test the vehicle in a cycle that is as standard as possible.

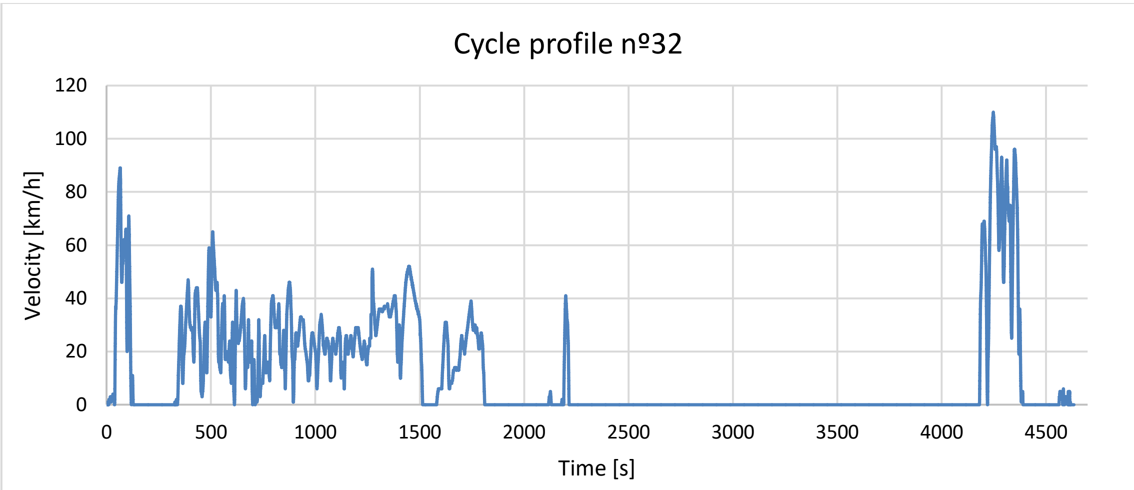

Figure 45: Four driving mission profile selected for eMotor testing

- Driving mission n°144: it is a cycle with fairly average characteristics but featured by a high movement time (88%). It therefore represents a cycle with a high energy demand, high average power and average energy (5.62 kWh). The point is to test the vehicle in a cycle with a high presence of movement.

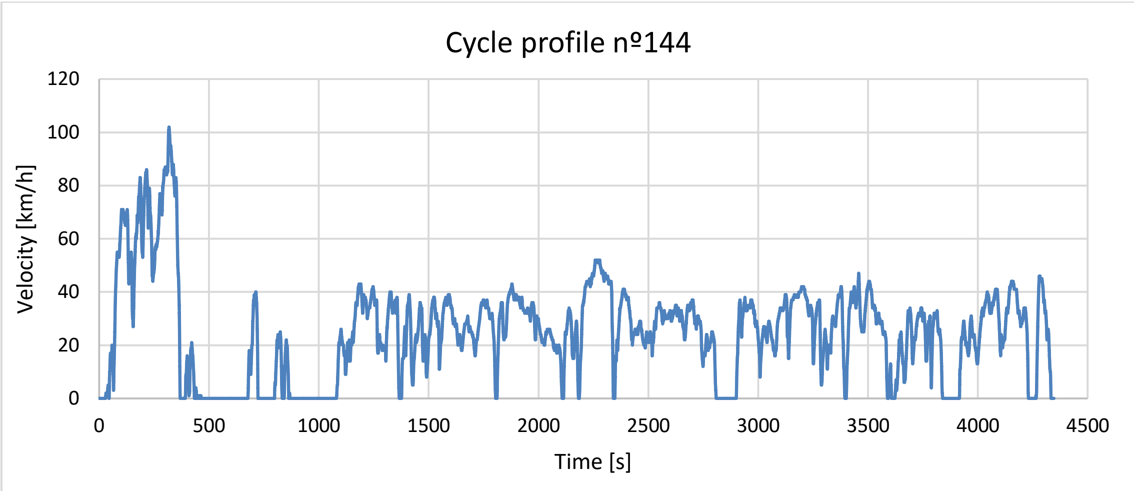

Figure 46: Four driving mission profile selected for eMotor testing

- Driving mission n°187: it represents the same pattern as n°32, but is longer, with a total time of 120 minutes, and with higher speeds, with a maximum of 120 km/h. Consequently, while maintaining a standard cycle, the energy and fuel consumptions required are higher. The point is to test the vehicle in a cycle that is standard but more challenging in terms of performance requirements.

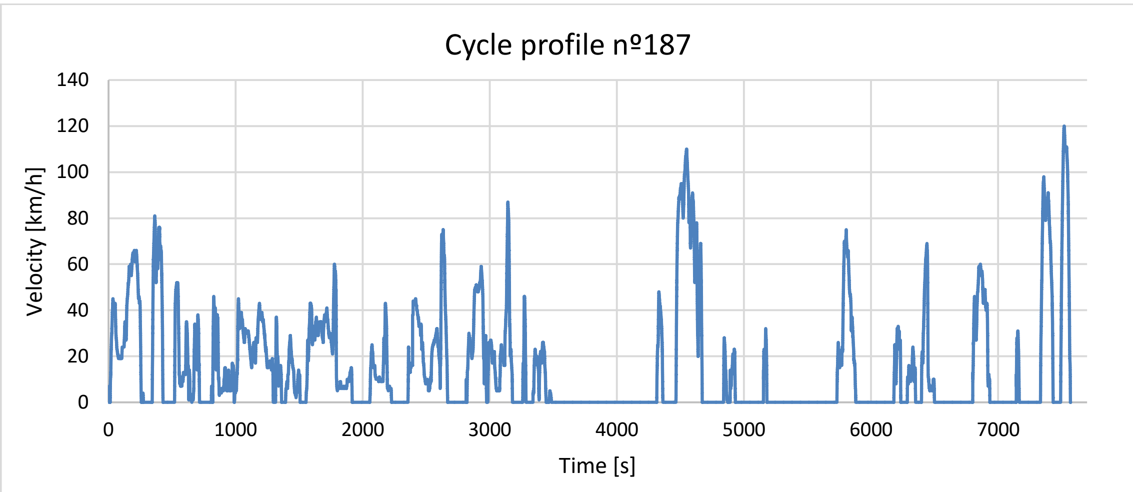

Figure 47: Four driving mission profile selected for eMotor testing

- Driving mission n°241: it is a very long cycle, one of the longest of those analyzed, with a total duration of 241 minutes, therefore with a high energy demand (8.58 kWh). As for the other characteristics, they are all more or less average, with maximum speed just under 100 km/h and peak power in the region of 120 kW. The point is to test the vehicle in a cycle which is long to complete.

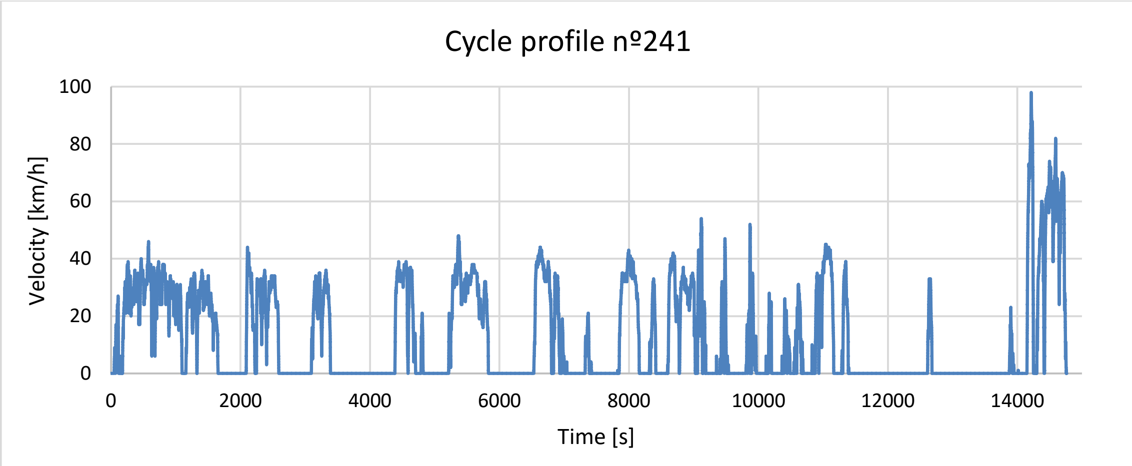

Figure 48: Four driving mission profile selected for eMotor testing

For all these driving missions, the EMs were tested in the first three gears, with full vehicle configuration to observe the results in the worst cases.

4.3.6. eMotor evaluation summary

The engines previously presented were therefore all tested within the longitudinal model in the various profiles presented so far, with the aim of evaluating their behaviour and their effectiveness. The following Figure 49 shows the various results obtained and at the same time, including results of acceleration and slope tests, attempts to provide a whole view of the possible performance with the four EM tested. For cycles nº32 and 187, the speed and torque values are primarily reported in order to observe whether the electric motor is able to achieve adequate performance and at what cost in terms of maximum torque. For cycles nº144 and 241, on the other hand, the energy values required for their completion are given, in order to observe the energy efficiency of the given EM under the specific conditions. For the acceleration test, it is noted whether the final speed reached is the maximum speed, while for the slope test, it is reported whether or not it was successfully completed. Having an adequate budget for all the electric motors evaluated, it was decided to opt for the Cascadia, as it produced the best results and would allow a utilization least limited as possible.

		EMRAX 228			PHI POWER PHI301			
		Gear			Gear			
Test ID	Data	1ª	2ª	3ª	1ª	2ª	3ª	Max reference value
32	Speed (%)	41	71	100	58	98	100	109 km/h
	Torque [Nm]	131	225	227	162	258	321	
187	Speed (%)	37	64	99	52	98	100	120 km/h
	Torque [Nm]	226	226	226	320	320	320	
Acceleration	Max speed (%)	43	73	100	60	99	100	105 km/h
144	Demanded energy (%)	80	87	85	90	94	87	5.62 kWh
	Max eMotor efficiency (%)		95			95		
241	Demanded energy (%)	85	87	81	95	90	82	8.58 kWh
	Max eMotor efficiency (%)		95			95		
Gradeability	Successful?	✓	✓	X (33%)	✓	✓	✓	Goal: 35%

		BORGWAGNER HVH250-115			CASCADIA IM-225W			
		Gear			Gear			
Test ID	Data	1ª	2ª	3ª	1ª	2ª	3ª	Max reference value
32	Speed (%)	68	100	100	75	100	100	109 km/h
	Torque [Nm]	145	259	326	149	229	326	
187	Speed (%)	62	98	100	82	100	100	120 km/h
	Torque [Nm]	426	427	428	500	500	493	
Acceleration	Max speed (%)	71	99	99	79	99	100	105 km/h
144	Demanded energy (%)	94	93	87	100	95	88	5.62 kWh
	Max eMotor efficiency (%)		96			96		
241	Demanded energy (%)	97	91	83	100	92	84	8.58 kWh
	Max eMotor efficiency (%)		96			97		
Gradeability	Successful?	✓	✓	✓	✓	✓	✓	Goal: 35%

Figure 49: Resume table for eMotor evaluation

4.4. Powertrain component selection

4.4.1. Definition of final vehicle architecture

This vehicle, given the requirements, the elements that will compose it and the limited power of the FC, will be a Plug-in Range-Extender Fuel Cell Electric Vehicle (P-ReFCEV). The installed power of the FC is not sufficient for a hybrid series LF architecture, as it cannot meet the continuous power demand in every foreseeable scenario. The vehicle therefore will be Plug-in since it is not possible to implement a control strategy that allows a CS utilisation profile of the battery, but instead a recharging profile that is typical of Plug-in hybrid vehicles, the CD-CS one. It is therefore necessary to install an OBC in the vehicle to allow battery charging from external charging stations, with benefits in terms of:

- *Lower fuel costs*: for what regards the fuel cost, the one for charging an electric vehicle depends on the price of electricity in the area and the battery capacity of the vehicle. In general, charging an EV can cost between 0.10€ and 0.20€ per kWh, depending on the area. On average, for an electric car with a standard battery capacity of 70kWh, the cost of a full charge (not considering fast recharging) could be 7€ to 15€ [60]. On the other side, the cost of filling up with hydrogen is higher by now. It depends on the availability of filling stations in the area and the current price of hydrogen. Currently, the price of hydrogen varies greatly depending on the area and can be between 10€ and 20€ per kg. On average, a FCEV with a standard tank can use between 4 and 6 kg of hydrogen, so the cost of refuelling can be 40€ to 60€, quite lesser or similar to what can be expected to a vehicle which uses conventional carbon fossil fuels. This is why recharging an electric vehicle is currently less expensive than refuelling with hydrogen, but this may change in the future as the availability of hydrogen refuelling stations increases and the price of hydrogen falls [61].
- *Fuel availability*: for what regards the fuel availability, the presence of charging stations for EV is growing rapidly worldwide. There are currently about 2 million charging points available worldwide, with a strong concentration in Europe and North America. There are also many options for charging at home, such as home chargers and charging stations for private car parks [62]. On the others side, the presence of hydrogen refuelling stations for FCEV is still limited. There are currently about 400 hydrogen refuelling stations worldwide, with a strong concentration in California and Germany [61]. However, despite the network of hydrogen refuelling stations is expected to grow

in the future as demand for fuel cell vehicles increases, by now this represents an important limit.

The "Follow me" FCEV is a RE series hybrid because, from a conceptual point of view, such a hybrid can be seen as an electrically driven vehicle that, thanks to the additional hybrid unit represented by the fuel cell system, manages to achieve what is an extension of the range and battery life compared to an ordinary BEV. The FC is therefore not used mainly to power the wheels of the vehicle directly but serves most of all as an energy generator for the battery. The idea of these vehicles is to use battery electric power most of the time, and then only use the hydrogen engine when the battery approaches a lower level of charge, to extend the range of the vehicle. The final P-ReFCEV architecture for this activity will therefore consist of the following components:

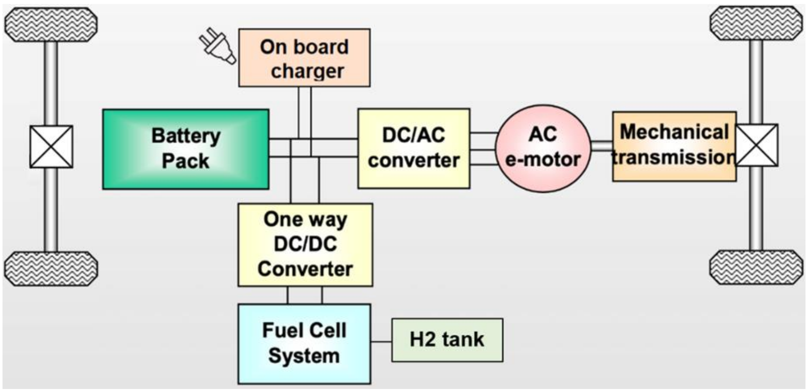

Figure 50: Representative diagram of the P-ReFCEV architecture with its main elements [61]

The Figure 50 shows the central electric propulsion line with the battery and EM, to whose HV bus is coupled the hybridization unit with its converter and the OBC for Plug-in functionality. The chosen components and their characteristics will be presented below.

4.4.2. Selection of final components

Based on the results obtained in the previous phases of the project, it was possible to conduct a market analysis and to establish contacts with supplier of the various components needed. Considering the availability, the timing of order shipping, the costs related to shipments and customs and above all the budget limits that had to be met for each component, several compromises were made. In the end, the components defined for the final purchase, which will be installed inside the new powertrain, will still be sufficient to achieve the performance defined in the earlier stages of the activity, at least theoretically. The commercial components useful for the creation of the fuel cell powertrain are presented below:

- *Electric motor*: the HVH250 electric motor included in the integrated module called iM-225W is a water-cooled, permanent magnet electric motor with a horizontal orientation and directly associated inverter. Its performance has been presented and analysed in the previous paragraphs.
- *DC/AC power inverter*: the CM200-DX inverter included in the integrated module called iM-225W, is a perfectly matched inverter for motor powers up to 225 kW and voltages up to 480 VDC.
- *High voltage battery*: Leclanché INT-39 Energy LV, Li-ion battery with a configuration of two 10-cell stacks in parallel (10s2p), providing a rated voltage of 330 VDC, a capacity of 120 Ah and maximum currents of 200 A. Considering the 2C C-rate which usually can withstand these suppliers, this battery should be able to provide peaks of 100 kW and an energy of 40 kWh.
- *Fuel Cell system*: complete BoP system from Horizon Group including radiator for heat dissipation, system with a nominal output of 15 kW (net, taking the BoP's demand into account) with current output up to a maximum of 222A and voltage up to 80 VDC.
- *DC/DC boost converter*: dedicated programmable converter manufactured ad hoc by Horizon Group, capable of boosting the FC voltage up to the nominal HV bus voltage. The converter is monodirectional, can be used with boost or buck function as required, and is liquid cooled.
- *On-board charger*: for the time being, this component has not yet been defined. It must certainly possess a minimum voltage equal to the highest voltage of the vehicle battery. In more advanced stages of the project, this element will be better defined.
- *Hydrogen tank*: the containers will be Air Liquide's Alphagaz 1, with a variable size yet to be defined depending on the volume and weight available inside the vehicle with the components installed and future experimental necessities. These tanks are type II, to store it at 200 bar, with a volume varying between 1.8 and 10 m^3, thus capable of holding between 0.163 and 0.9 kg of hydrogen per tank.

The following Table 12 summarises the components currently selected and defined for the realisation of the FCEV prototype, with their main characteristics:

Component	Selection	Technical features
High voltage battery	Leclanché INT-39 Energy LV	Module configuration: 10s2p Pack nominal voltage: 330 VDC Pack nominal capacity: 120 Ah Nominal energy: 40 kWh Maxi discharge/charge current: 250 A
Electric motor	Cascadia HVH250	Peak toque: 500 Nm Continuous torque: 275 Nm Peak power: 210 kW (@700 VDC) Continuous power: 75 kW Maximum speed: 12000 rpm Voltage operating range: 300 – 700 VDC
DC/AC power inverter	Cascadia CM200-DX	Operating voltage: 50-480 VDC Max EM current continuous: 300 A Output peak power: 225 kW DC overvoltage trip: 500 VDC
DC/DC boost converter	Horizon VL DC-DC converter	Input voltage: 35 – 120 V Output voltage: 200 – 400 V Rated power: 4 – 30 kW Efficiency: 98%
Fuel Cell system	Horizon VL15kW	Cells number: 115 Rated power: 15 kW Output voltage: 90 VDC Operating temperature: 60 – 70 °C Operating pressure: 1 bar
Hydrogen tank	Air Liquide Alphagaz 1	Operating pressure: 200 bar Volume size: 1.8 – 2.8 – 10 m^2 Mass of hydrogen: 0.163 – 0.901 kg

Table 12: Summary of "Follow me" FCEV powertrain final selected components

Chapter 5: Energy Management Strategy

In this chapter, the energy management strategy developed and refined to be implemented within the FCEV "Follow me" prototype will be presented, with the aim of enabling efficient interaction and energy management for the elements within the electric powertrain.

After a brief theoretical overview of EMSs, the one that will be used within the FCEV control unit will be explained in detail, considering its nature, composition and expected goals. Will be presented the methodology used for its creation, relying on the simultaneous simulation of vehicle longitudinal dynamics and powertrain control logic, as well its fine-tuning. All the elements composing the state-flow decisional structure of the EMA and the algorithms that make up its operation will be shown and explained in detail.

5.1. Introduction to EMS

5.1.1. Energy management strategies for FCEV

The energy management strategy (EMS) of the electronic part of Battery/FC/EM will be designed with the use of MATLAB® Simulink, having more in-depth language knowledge in this program. These control logics will then be imported and used within the AVL Cruise™ M program. To achieve an energy-efficient powertrain, several control objectives, often conflicting, must be addressed, such as drivability, fuel consumption, emission reduction and SoC conservation. The main objective of an EMS is to share power through the various powertrain components efficiently by selecting the appropriate mode of operation. The output data of the EMS can be the activation or non-activation of certain components, the increase or reduction of the power output or the modification of the operating ranges. This task makes EMS the most crucial aspect of powertrain design. These strategies can be focused on different optimization objectives in a FCEV, some of them focus on manage the system with fuel economy as the only optimization objective, trying to reach the lowest possible requirement of hydrogen for the driving task. However, the fuel cell has some features, such as a high production cost, limited lifetime or low operating temperature, which push many strategies to extend the dealing with other objective too. Nevertheless, since there are conflicts between different optimization objectives, a trade-off is required to make the best decision [53].

The most common goals are to satisfy driver's power demand, to keep the SoC inside threshold efficiently, to optimize the efficiency of the powertrain or, as said, and to reduce hydrogen consumption. In order to make an example: considering a FCEV, one of the objectives is to have a final SoC equal to the initial SOC. In order to do that, the technique used to deal with the charge of the battery is called Charge Sustaining (CS), where the level of charge of the battery is kept between a lower and higher level which can't be exceeded by the SOC. Consequently, a correct rule of utilization of battery energy and FC energy splitting between traction and charging requirements must be designed. In all the duty cycle, there will be phases where a certain amount of FC energy could have sufficient for traction, but the battery needs to be recharged and consequently additional energy must be directed to recharging it, maybe moving away from the maximum efficiency condition of the cell. Or again, there might be phases where the battery energy would have been sufficient for vehicle traction, without consuming hydrogen, but the too low SoC level dictates that the latter cannot be used, consequently increasing fuel consumption. According to basic principles, the classification of EMS is the following:

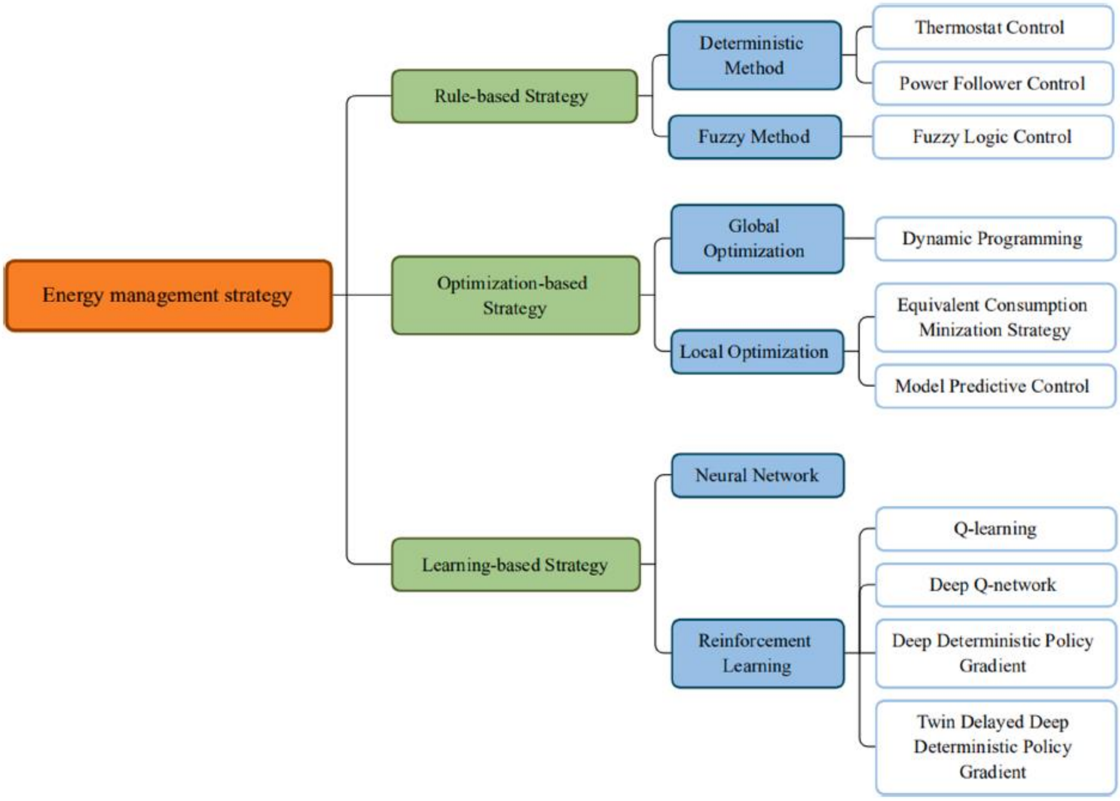

Figure 51: Diagram showing the composition of the main EMS [50]

5.1.2. Rule-based strategies

Rule-based (RB) strategies are sub-optimal control algorithm, quite flexibles, simple and implementable in real time, allowing an online installation inside the vehicle for energy management purposes. The rules, strategies and decisions inside these algorithms can rely on heuristic optimization, namely simple self-decided rules coming from experience, previous knowledge, mathematical models or on results and on what learned from the resolution of problems with optimization-based or learning-based strategies. The rule-based EMS generally requires the definitions of system state parameters and control rules of input/output variables organized in tables or schemes to determine and organize the power distribution in real time. In general, this type of EMS has advantages of low computational intensity, good real-time performance and no need for information about driving conditions. These advantages have made the rule-based EMS widely used in commercial FCEVs: Toyota and Hyundai rely on RB strategies, including deterministic and fuzzy logic, to manage their Mirai and Nexo. However, RB strategies have also some disadvantages. For example, the lack of optimality, since it would require information regarding the driving cycle in advance. Moreover, high calibration effort is required to guarantee a satisfactory performance and the rules or tables are usually not scalable or usable for different powertrain, component sizes or driving cycles [54]. Inside RB strategies, two approach can be followed: rely on a deterministic strategy, looking as much as possible for an exact and precise match between data, or on a probabilistic one, using statistics to define matches or non matches between data, dealing also with vagueness and uncertainties.

- Deterministic method (DM) is described by pre-defined modes of operation with distinct boundaries, always passing through the same sequence of states while paring inputs with consequential outputs. This strategy, being a RB one, generally do not require a priori knowledge of the driving cycle and perform power managing within the vehicle. Are developed based on efficiency maps, fuel and emissions data and driving experience and implemented via look-up tables and mathematical functions. [53]. Currently, the common DM strategies are Thermostat Control Strategy (TCS) and Power Follower Control (PFC).
- On the other hand, fuzzy method (FM) is based mainly on human experience and reasoning and rely on a set of If/Then rules and membership functions. Its statistical structure allows to deal with nonlinear relationships and uncertainties, which can be modelled without the need for precise mathematical models [55]. Therefore, FM has a language that is easy to understand and is expressed in a more natural form. Advantages are the possibility to deal with imprecise data, to incorporate insight of experts and to be implemented together with other control techniques, without any kind of incompatibility [54]. Since FM strategies cannot guarantee an optimal performance, several studies had been conducted in order to improve this type of control. Examples are optimized FM, where an optimization algorithm is used to adjust the performance of the fuzzy algorithm to achieve a minimization of the fuel consumption, of the emissions, SoC maintenance and enhance the driving performance [53]. Adaptive FM, integrated in a control strategy to improve the self-adaptation of the controller relying on neural network [53]. Predictive FM, working on the predicted future vehicle state, thanks to a real-time control of the vehicle [54].

5.1.3. Deterministic methods

As said before, the two DM are the thermostat control strategy (TCS) and the power follower control (PFC) strategy, similar in the structure but with important differences. In a TCS, known also as ON/OFF strategy, the FC can operate at its optimal efficiency power point, providing a constant torque and speed also to maintain the battery SOC between the predefined upper and lower limits. The upper and lower values of SOC usually are calculated based on battery resistance models. This can be achieved by turning the FC ON and OFF when required. The difference between the power produced by the cell and the required one for traction can be supplied in excess to charge the battery, otherwise used to support the battery, while it generates traction energy, for supplying the required power. As this strategy works mainly on trying to use the fuel cell only when needed and at its peak performance, TCS offers the best efficiency for the fuel cell system, at the expense of the overall system efficiency of the whole FCEV, and also an improved durability of the FC when compared to a power follower strategy. Usually, this strategy is found in vehicles where the battery power is low or modest and the majority of it is supplied by the FC [54][56]. In the power follower control (PFC) strategy, the FC system is treated as the main power source and the strategy adjusts the output power to follow the required power of the vehicle. Rules of PFC are based on heuristics reasoning, in order to give an example: the EM only works if the vehicle speed is below a certain minimum value which will lead to an inefficient utilization of the FC. On the other end, the EM supports the FC if the required power is greater than the maximum fuel cell power. Battery is normally charged through regenerative braking, but the FC charges the battery if the battery SoC turns lower than its predefined minimum value. Since this strategy works mainly to follow the power request of the vehicle, the PFC strategy offers a higher overall system efficiency, at the expense of FC efficiency, and also an improved durability of the batteries when compared to a thermostat strategy [54]. The two strategies, being of the same deterministic character, can easily be mixed together to improve the performance.

5.1.4. Optimization-based strategies

Optimization-based (OB) strategies are optimal control algorithm used to minimize a (multi) objective function, by breaking down the whole problem into simpler sub-problems, while dealing with dynamic state constraints. These constraints can have two different natures: global constraints, like the battery SoC, or local constraints, such as speed limits, power limits, torque limits or temperature limits. The objective functions can be different, such as the fuel consumption, the hybridization costs, and the payload weight of the vehicle or the exhaustive gases emissions. OB strategies can usually be grouped into two categories: offline-global and online-local strategies, in relation of their dependency on a priori knowledge and information of the driving mission and possibility of real time implementation inside a vehicle.

5.1.5. Global and local OB strategies

The main example of the global OB strategies is the dynamic programming (DP), a global optimization method to define the optimal control strategy of the whole driving mission, through the whole timeframe. DP optimizations rely on the fact that the optimal solution for the whole multi-stage problem depends on the optimal solutions of its sub-problems. In fact, the optimal solution can be found by an iteratively optimization of the same bigger sub-problem in a recursive way. DP is an offline optimization strategy, it requires the knowing in advance of the driving profile, giving the optimal trajectory or component design over a predetermined mission with fixed features. Therefore, is not implementable in real time and applicable, can't be used inside the ECU of the vehicle for energy management purposes. What is useful from DP is the possibility to have a reference on which is the way to maximize components efficiencies or what is the best strategy to adopt and to extract rules used to build and/or recalibrate effective real time control algorithms, like RB ones [57].

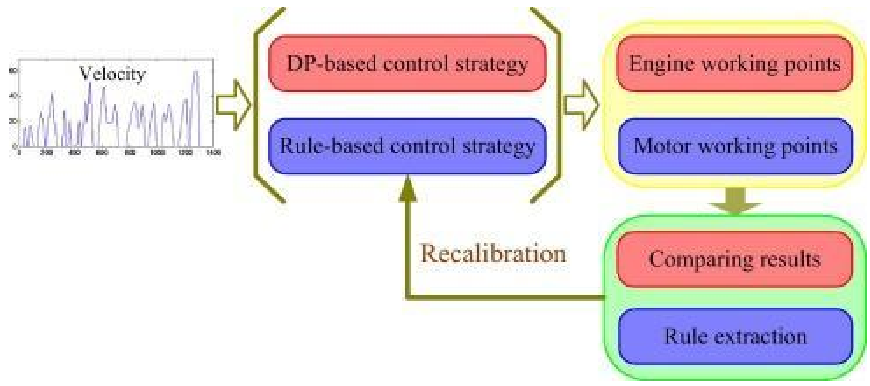

Figure 52: Example of an optimization-based recalibration of rule-based strategies [57]

For what regards local OB strategies, equivalent consumption minimization strategy (ECMS) is a local optimization algorithm, time instant by time instant, without knowing in advance the mission, of the objective function, which is an equivalent fuel consumption, subjected to a charge sustainability constraint. The ECMS calculates the equivalent fuel factor, which accounts for the actual fuel consumption required to recharge the batteries and to recuperate the regenerating braking energy [54]. The goal of the ECMS is to find a near optimal control strategy or trajectory which is as much as possible close to the one reachable with a global optimization. Even if ECMS is not limited from the knowledge in advance of the driving mission, can't be implemented inside the vehicle for energy management purposes since is strictly related to the features and characteristics of the driving profile over which the strategy have been calibrated. Therefore, changing it, the strategy may not lead to an optimal solution or to a CS profile [53]. Another OB local strategy is the model predictive control (MPC) based strategy, again based on the local optimization in a receding-horizon control strategy, using a predictive scheme composed by three main steps: define the optimal inputs over a prediction horizon to minimize an objective function subject to the constraints; implement the elements of the optimal inputs into the physical plant; move the prediction horizon forward and repeating from the beginning. The goal of the MPC is the same, namely to find a near optimal control strategy as much as possible close to the global one. However, the performance of the MPC is affected by the model quality, considering the differences the represented models with respect of the wheel, weather, road conditions, and sensor models. To adjust this differences, the horizon length has to be calibrated, or GPS data can be used [53].

5.1.6. Learning-based strategies

Learning-based (LB) strategies employs data-driven and self-learning for massive historical and real-time information to derive optimal control laws, which can reach the optimal control results through interactions between system, environment and trial-and-error learning. In these controllers, the precise model information is no longer required to make the control decision, even if are also able to present a good adaptability to different driving conditions [58]. LB algorithms can be incorporated into model-based approaches to tune the control parameters optimized for different driving cycle types (e.g. urban or highway), derive the thresholds for rule-based EMSs, or recognize the driver's driving style (e.g. calm or aggressive), since data-driven methods and machine learning are adaptive and are able to manage large datasets efficiently under different external driving conditions and drivers [54]. By grouping the algorithms based on their learning type, the learning-based EMS is mainly divided into neural network (NN) and reinforcement learning (RL). The NN-based needs to select the characteristic parameters under different working conditions as the model's inputs, and the optimal power distribution as the model's outputs to train the NN. Such EMS needs large amounts of data, so the NN is usually used for working condition classification and speed prediction rather than direct energy management. The RL-based can learn the optimal EMS directly from the data even when the amount of data is small. The core idea is that the controller exchanges current state and action information with feedbacks, through continuous interaction with the environment. Then, the controller learns control rules through exchanged information until reaching the optimal control strategy [53]. Among all of them, is quite complicated which accounts the best overall performance of the RL-based EMS, since is evaluable depending on several features, related to the vehicle, environment, driver and driving mission, because these controller can account a large amount of data [58].

5.2. Proposed energy management strategy

5.2.1. Longitudinal FCEV-model for EMS

Given the greater possibilities, the versatility offered and the greater personal expertise possessed on the MATLAB® Simulink software, it was decided to develop the energy management strategy for this vehicle FCEV on this program. Although various blocks for creating such strategies are present in the AVL Cruise™ M software, using the C language, the versatility offered by Simulink's state flow allows an EMS of greater extension and versatility to be recreated. Various variables calculated iteratively within the simplified vehicle model in AVL Cruise™ M will be exported for use within MATLAB® Simulink as input. The output produced by the latter will be fed back into the former software for its iterative calculations, all in real time. In order to develop a suitable EMS for the study's vehicle, a simplified longitudinal dynamics model of the target FCEV must be created before moving on to its actual programming. Up to this point, what can be considered a simplified model of a battery electric vehicle with a constant and unlimited current supply has been used. Consequently, it is necessary to add blocks capable of simulating the dynamics of the FC, the boost converter to raise its voltage to that possessed by the HV bus and to control its operation via current control, as well as blocks that can include the dynamics of the LV auxiliaries and the compressor possessed by the fuel cell BoP. Thus, the model used for the simulations intended for the formulation, control and fine-tuning of the EMS is as follows:

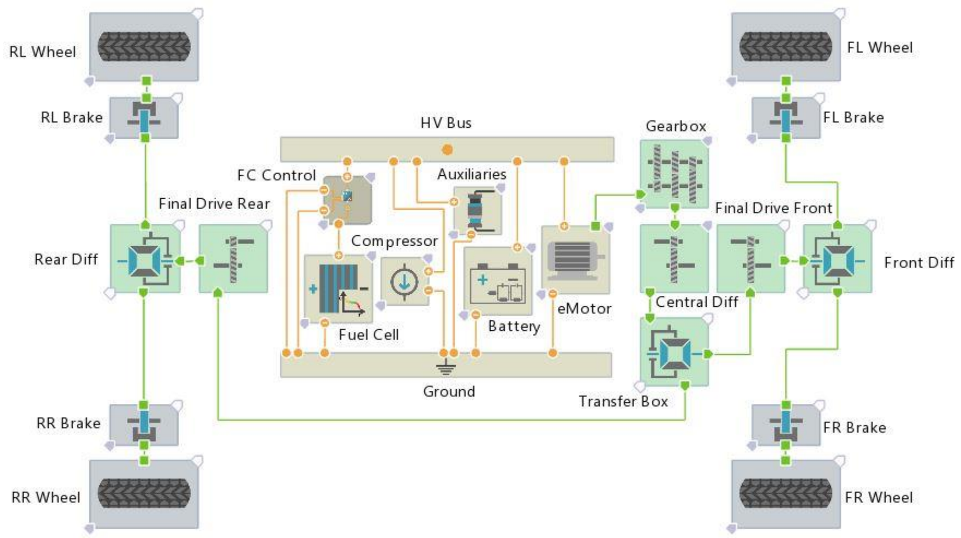

Figure 53: Vehicle model with Fuel Cell, Battery and eMotor for EMS tuning

From now on, the name "Follow me" EMS, abbreviated to FEMS, will be used to refer to the control strategy for the "Follow me" FCEV prototype of this activity.

4.4.3. Blocks used in AVL Cruise™ M FCEV-model

Compared to the previous eMotor-model, additions are present in this latter one. A brief explanation of the added blocks used in this longitudinal model is presented below:

- *Fuel Cell*: The electrical fuel cell model is based on analytical electro-chemical equations derived from the polarization curve of the PEMFC cathode side. The approximate solution of the equations takes into account the oxygen and proton transport losses in the cathode catalyst layer, and the oxygen transport losses in the gas diffusion layer for different temperature, relative humidity and gas pressure on the cathode side. The model can be utilized to evaluate the electrical properties such as voltage, power, power loss and efficiency of the fuel cell, as well as the gas properties such as the total amount of consumed oxygen and hydrogen. In the electrical fuel cell component, in addition to the fuel cell, a simple compressor model can be activated so that the power consumption of the compressor, which significantly influences the operating efficiency of the fuel cell system, can be taken into consideration. The voltage of the electrical fuel cell model is calculated as:

  $$U_{cell} = U_{OC} - \eta_0 - j_0 R$$

  Where the three terms on the right-hand side of the equation are the ideal open circuit voltage, the cathode voltage loss and ohmic voltage loss of the fuel cell. The mass flow of the reacted hydrogen and oxygen can be calculated by:

  $$m_{reactedH2} = \frac{I_{stack} \cdot n_{cells}}{2F} \cdot M_{H2}$$

  Where M_{H2} is the molar mass of the hydrogen. The power consumption of the compressor is expressed as:

  $$P_{compressor} = m_{flow\,in} \cdot \frac{1}{n_s} c_p \cdot T_{in} \cdot [\Pi^{\frac{k-1}{k}} - 1]$$

  Where $m_{flow\,in}$ is the inlet mass flow of the compressor inlet, n_s is the isentropic efficiency of the compressor, c_p the specific heat at constant pressure between the compressor inlet and outlet and the term Π represent the pressure ratio power the heat capacity k. The power of the fuel cell is defined as:

$$P_{cell} = U_{cell} \cdot I_{stack}$$

And the power loss of the fuel cell is:

$$P_{loss} = (U_{OC} - U_{cell}) \cdot I_{stack}$$

- *Battery*: The battery model is based on an equivalent electrical circuit, and it can predict the voltage response to a current at a particular SOC and temperature. The basic model consists of a controlled voltage source and an Ohmic resistance used to describe the instantaneous voltage response to a current input. In addition, besides the electrical model, a thermal model, i.e. a solid wall is embedded in the model to predict the transient thermal behavior of the battery.

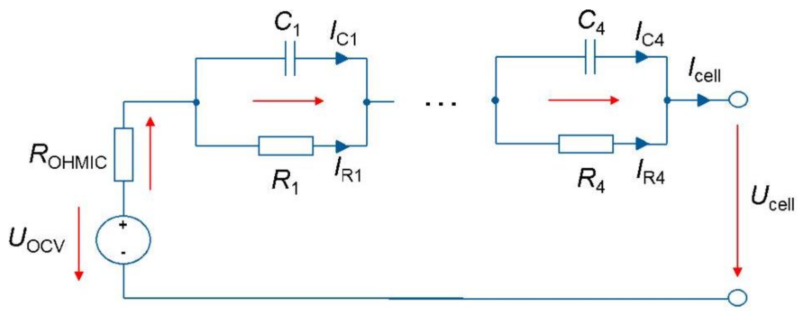

Figure 54: Equivalent circuit of the battery model used in AVL Cruise™ M

The state of charge during discharge is evaluated by the following equation:

$$SOC = \int eff_{Coulomb} \cdot I_{cell}\, dt$$

The cell voltage can be calculated as:

$$U_{cell} = U_{OVC} - I_{cell} \cdot R - \sum_{i=1}^{n} \frac{Q_i}{C_i}$$

The battery pack or module voltage is calculated by:

$$U_{batt} = U_{cell} \cdot n_{series}$$

And the battery current is calculated as:

$$I_{batt} = I_{cell} \cdot n_{parallel}$$

In addition, the charge of the battery is equal to:

$$Q_{batt} = Q_{cell} \cdot n_{parallel} = Q_{max} \cdot SOC \cdot n_{parallel}$$

- *Power consumers (LV)*: represents an electrical resistor, which consumes a user-defined power quantity. It can be connected to the thermal network via its thermal pin. he powers consumer model is described by the following equation:

$$P = U \cdot I$$

Where P, U and I are power, voltage and current of the power consumer, respectively.

- *Continuous current source (Compressor):* represents an ideal current source that can output a user-defined current without regard to the voltage drop across the component.
- *DC/DC converter*: represents a behavioral model of a power converter. It regulates either the voltage or the current imposed on the load side. It also draws the demanded power from the supply side to the load side to keep the balance of input power, output power and power loss. The converter can support bidirectional power flow between supply side and load side.

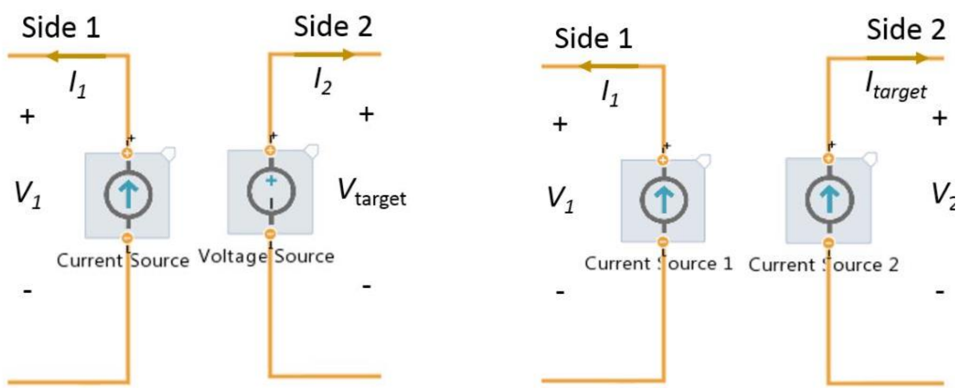

Figure 55: Equivalent circuit of the DC/DC converter used in AVL Cruise™ M with the target voltage control setting (left) and target current control setting (right)

When in target voltage control setting:

$$V_1.I_1 \cdot eff = V_{target} \cdot I_2$$

On the other hand, when in target current control setting, such as the one used for the DC/DC boost converter for a FC:

$$V_1.I_1 \cdot eff = V_{2t} \cdot I_{target}$$

5.2.2. FEMS typology

The objectives of the EMS of this "Follow me" FCEV are different:

- Synergy between power sources: it must be able to create a perfect interaction between the two energy sources prevailing in the vehicle, the FC and the battery, to meet the energy needs at all times and conditions.
- Efficient use of fuel cell: the FC must only be used under certain conditions, to favour high efficiency and low fuel consumption operation, for continuous operation and for regeneration when necessary.
- Satisfy transients: the battery must be able to meet the high energy demands during acceleration, when the power of the FC cannot cover the total demand, as well as cover the continuous demand when the FC is not active.
- Implement regeneration dynamic: in addition, the battery must be able to store the excess energy produced by the FC during decelerations and braking, as well as accommodate directly the electricity produced directed for regeneration from the wasted kinetic energy.
- Improve powertrain safety: controls for system operating temperature, battery charging and discharging current management, state of charge management, and HV bus safety must also be implemented within the EMS.

The FEMS that will be used in this prototype FCEV, given the premises and characteristics of its operation, will be included within the RB family, more specifically a DM strategy. This is because RB strategies are flexibles, simple and implementable in real time, allowing an online installation inside the vehicle for energy management purposes. In fact, since is needed a strategy that guarantees the fulfilment of driving missions' requirements with rather defined characteristics, while presenting a wide internal variety, and that can function without a priori knowledge of the driving cycle, a DM is a solution that can achieves excellent results, in short times and with the software available. Between the DM family, two options were possible, but the final choice was the PFC strategy. If a simple TSC is used, there are different decision which can be made to operate it, depending on the power level at which the fuel cell is to be operated. The power of the range extender unit can be set to a constant value, for example:

- The maximum output power of the FC. However, if the fuel cell is always running at the maximum output power, its efficiency be low, the life of the FC will be shortened, and a high consumption of hydrogen will be generated.
- The power which corresponds to the maximum efficiency. However, if the FC output power works at the highest efficiency, the FC can provide quite low power.
- A variation between these two values, or more values of FC power. However, the issue will be the same since each of these power values will be related to the same concerns.

Therefore, the other type of DM strategy, the Power Follower Control (PFC), is selected for the FEMS, as proved to be more adjustable based on the current needs of the vehicle, more capable of follow the real power request of the driving cycle without significant losses in efficiency.

5.2.3. FEMS formulation

In this PFC strategy, an attempt is made to recreate the typical CD-CS profile of a Plug-in EV. Specifically, the hydrogen hybrid unit will not be used (OFF-state) until a certain $SOC_{FC\text{-}ON}$ value is reached, after which the FC will be used (ON-state) to help in traction and mainly recharge the battery in an alternating manner, trying to keep the SOC within a window between SOC_{high} and SOC_{low}, always inside its maximum and minimum limits SOC_{max} and SOC_{min}. Before reaching the threshold for FC activation, the battery will provide 100% of the power for vehicle traction, as well as after exhaustion of the hydrogen for FC operation. During ON-state, the FC will provide a certain level of power P_{FC} depending on the vehicle's power demand P_d, either to aid traction or by recharging the battery whenever the power demand is below a certain threshold P_{reg}.

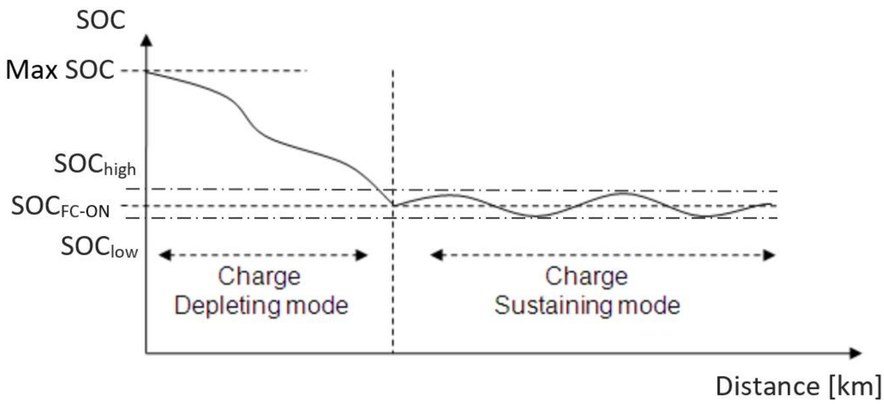

Figure 56: Charge depleting – Charge sustaining profile typical of a Plug-in Hybrid Vehicle

Without considering the various special conditions for switching from one mode to another, the four modes in which the vehicle's energy management strategy moves are as follows. They are a function of the state of charge of the battery and the torque command to the electric motor.

- *Battery traction mode* (BTM): in this modality, the only source of traction energy is the battery, which deplete its charge while providing the torque needed to satisfy the demand of the vehicle. In this sense, the vehicle acts as BEV, without any hybridization unit. This mode is possible only when the SOC is higher than the level for which the FC is activated ($SOC_{FC\ ON}$) and below this value if the tank of hydrogen is empty.

$$\begin{cases} SOC_{max} \leq SOC > SOC_{FC\ ON} \\ T_{trac} > 0 \\ P_{FC} = 0 \\ P_{batt} = P_d \end{cases}$$

- *Battery charging mode* (BCM): when requested by the EM, in braking or when the vehicle is still, the electric machine becomes a generator and recharge the battery. This occurs along all the utilization of the vehicle, no matter if the FC is ON or OFF, if the SOC is between the maximum and minimum allowable levels.

$$\begin{cases} SOC_{min} \leq SOC \leq SOC_{max} \\ T_{trac} < 0 \\ P_{FC} = 0 \\ P_{batt} = P_{reg} \end{cases}$$

- *Hybrid traction mode* (HTM): when the FC is turned on, reached the target $SOC_{FC\,ON}$, the vehicle starts to act as a hybrid vehicle, the profile changed to a CS mode, where the FC supply power in order to satisfy the demand of the vehicle, always higher than the minimum power to keep the FC ON and till the maximum power which it can deliver. When the demanded power is higher than the one available from the FC, the battery satisfies the rest of the part.

$$\begin{cases} SOC_{min} \leq SOC \leq SOC_{FC\,ON} \\ T_{trac} > 0 \\ P_{FC} = P_{FC_{min}} \leq P_d \leq P_{FC_{max}} \\ P_{batt} = P_d - P_{FC} \end{cases}$$

- *Hybrid regeneration mode* (HRM): can be seen as a sub-modality of the BCM, if the FC is ON. When the requested torque of the EM is negative, in braking or when the vehicles is still, the regeneration dynamic is activated, and the battery receive the current coming from the FC to be recharged. When the FC is used to such purpose, its level of power is set to the minimum one, to allow a utilization with fuel saving with an acceptable level of efficiency. The hybrid regeneration modality is available as far as there is hydrogen to fuel the FC or the SOC is lower than $SOC_{FC\,ON}$. In fact, if it goes above it, the FC is turned OFF and the strategy goes back to BTM.

$$\begin{cases} SOC_{min} \leq SOC \leq SOC_{FC\,ON} \\ T_{trac} < 0 \\ P_{FC} = P_{FC_{min}} \\ P_{batt} = P_{reg} - P_{FC} \end{cases}$$

5.2.4. FEMS stateflow

The presented control logic must be translated in a graphical language that includes state transition diagrams, flowcharts truth tables to obtain the same results. In order to do that, Stateflow functionality of MATLAB® can be used, to relate input signals, events, and time-based conditions to determined objective to be reach. Stateflow enables the design and tuning of energy management strategies in a simple, understandable and direct manner. AVL Cruise™ M allows the possibility of associating a functional mockup unit (FMU) generated by external software, such as MATLAB®, for exchanging real-time dynamic simulation with the control system developed in both software, in a standardized and comparable format. Variables in AVL Cruise™ M can be used as inputs to Stateflow, which in turn generates outputs that can be other inputs to AVL Cruise™ M, generating a dynamic system that allows simulation over time. In the image below, the complete structure of the FEMS implemented in MATLAB® can be seen: on the left are listed the inputs (coming from AVL Cruise™ M) and on the right the outputs, which are intended to control various elements in the longitudinal dynamics model of the hybrid vehicle. There are three main blocks, the Stateflow called "Energy Management Strategy", one to calculate the hydrogen consumed and one to simulate the presence of the hydrogen tank. The latter two will be described in section 5.3.7 respectively, and the Stateflow below. In the Table 13 and 14 below, the inputs and outputs that are interchanged between the two software to execute the control strategy are listed.

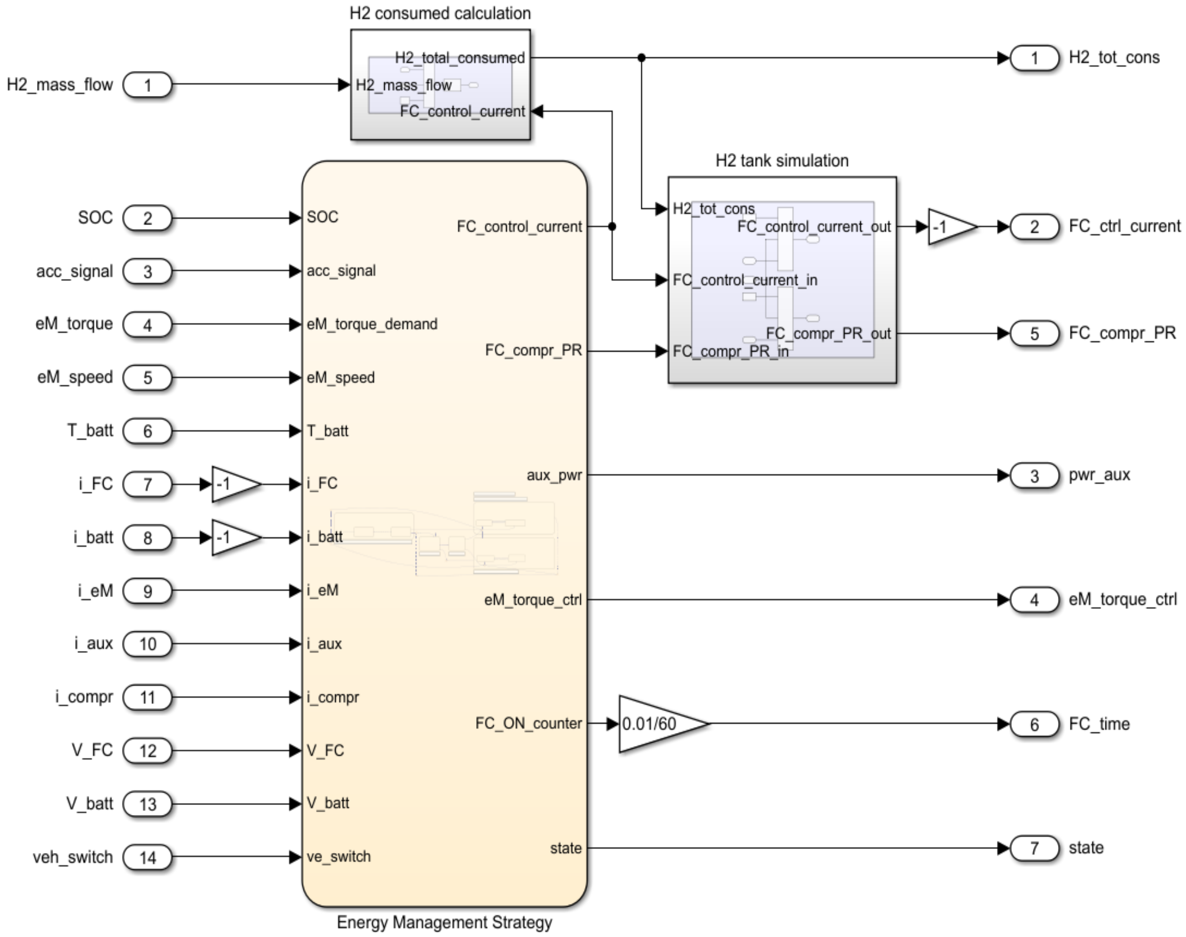

Figure 57: Complete Simulink structure of the FEMS

Input name	U.M.	Variable
H2_mass_flow	kg/s	Hydrogen flow mass output of the fuel cell stack
SOC	%	State of charge of the battery
acc_signal	[-]	Accelerator signal coming from the pressure of the accelerator pedal
eM_torque	Nm	Torque of the electric motor
eM_speed	rpm	Angular speed of the electric motor
T_batt	°C	Temperature of the battery
i_FC	A	Current produced from the fuel cell
i_batt	A	Current produced from the battery
i_eM	A	Current produced from the electric motor
i_aux	A	Current produced from the auxiliaries
i_compr	A	Current produced from the fuel cell compressor
V_FC	V	Voltage produced from the fuel cell
V_batt	V	Voltage produced from the battery
veh_switch	[-]	ON/OFF signal for vehicle switch

Table 13: Summary of input of the Stateflow coming from AVL Cruise™ M elements

Output name	U.M.	Variable	Function
H2_tot_cons	kg	Total consumption of hydrogen	To simulate the fuel tank and for evaluations
FC_ctrl_current	A	Control current for the DC/DC boost converter	To control the functioning of the fuel cell block
FC_compr_PR	[-]	Pressure ratio for the fuel cell compressor	To compute the power losses of the FC compressor
pwr_aux	W	Auxiliaries power losses	To compute the power losses of the LV auxiliaries

eM_torque_ctrl	Nm	Torque control for the electric motor	To control the EM
FC_time	min	Time spent with fuel cell ON	To evaluate time spent with hybridization unit activated
state	[-]	Current state of the FEMS	To control the state of the strategy for evaluations

Table 14: Summary of output of the Stateflow going into AVL Cruise™ M elements

The calculation of these outputs will be analyzed in the following paragraphs, where all the algorithms will be presented in more detail. As far as the variable "State" is concerned, it takes on a value varying between 0 and 6 depending on the logical state in which the Stateflow is, as follows:

State	Relative logical state
0	Vehicle Switch ON/OFF
1	Battery Traction Mode
2	Battery Charging Mode
3	Hybrid Traction Mode
4	Battery Regeneration Mode
5	Background Battery Charging – FC ON
6	Background Battery Charging – FC OFF

Table 15: "State" Stateflow variable association

This variable is useful since it allows one to see directly in AVL Cruise™ M what state one is in as a simulation is running, so that is possible to recognize results and/or errors more easily. Within the Stateflow, the structure is too complex not to propose the following simplifying diagram. The original structure is shown as a continuation, but the following Figure 58 is useful for understanding it.

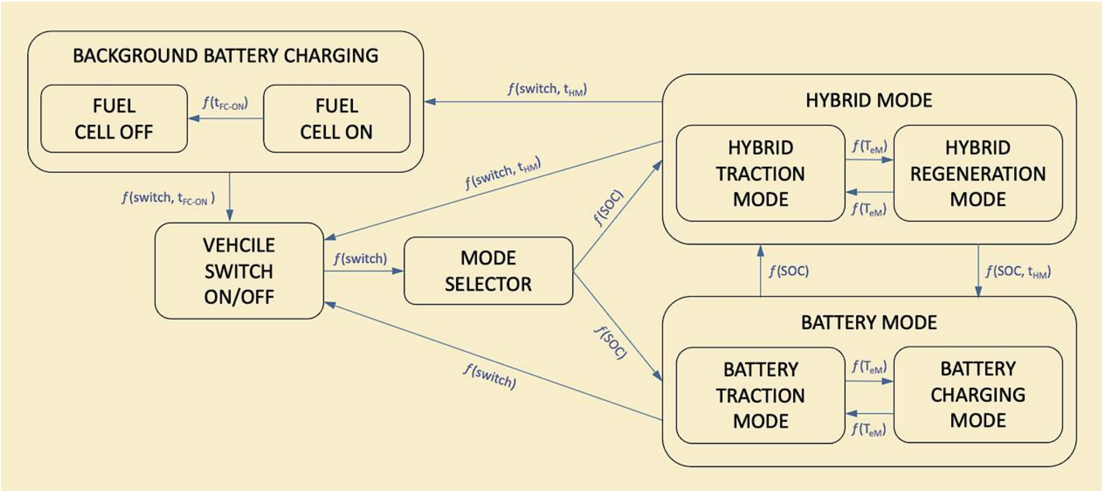

Figure 58: Simplified state-flow structure inside the Energy Management Strategy FEMS block

The "Vehicle Switch ON/OFF" block is the initial one and is useful as a reference point whenever the vehicle switches between ON/OFF states. When the vehicle is switched ON, the flow is directed to the "Mode Selector" block, where the control logic decides, depending on the SOC, whether to operate in HM or BM. Within these two are the four modes described in the previous paragraph (HTM, HRM, BTM and BCM), which are alternated by the control logic according to the torque command sent to the EM: if this command is positive or null, we speak of traction (or coasting), while if it is negative, we speak of braking and regeneration. The transition between BM and HM is a function of the change in battery SOC, as is that between HM and BM, where the operating time of the FC also matters. When the vehicle is switched OFF, both HM and BM can be switched back to the former block, waiting for the following vehicle ignition. For the HM, on the other hand, the control logic also makes it possible to switch to the special mode called "Background Battery Charging". In fact, depending on the operating time of the FC, it is possible to decide whether it is switched OFF together with the vehicle or kept ON charging the battery. Within this special block, after a predetermined time interval, the FC is in any case switched OFF, and then the flow goes back to the initial state of the process, until the next switch-ON. In the Stateflow, logical operations can be performed by means of direct links between states, or by means of functions, which are nothing more than MATLAB® Simulink subsystems that allow certain inputs and outputs within the Stateflow to be linked according to the selected state. These functions are the white blocks next to the logical states shown in the following Figure 59, which is the actual structure used within the FEMS in the longitudinal model developed in AVL Cruise™ M.

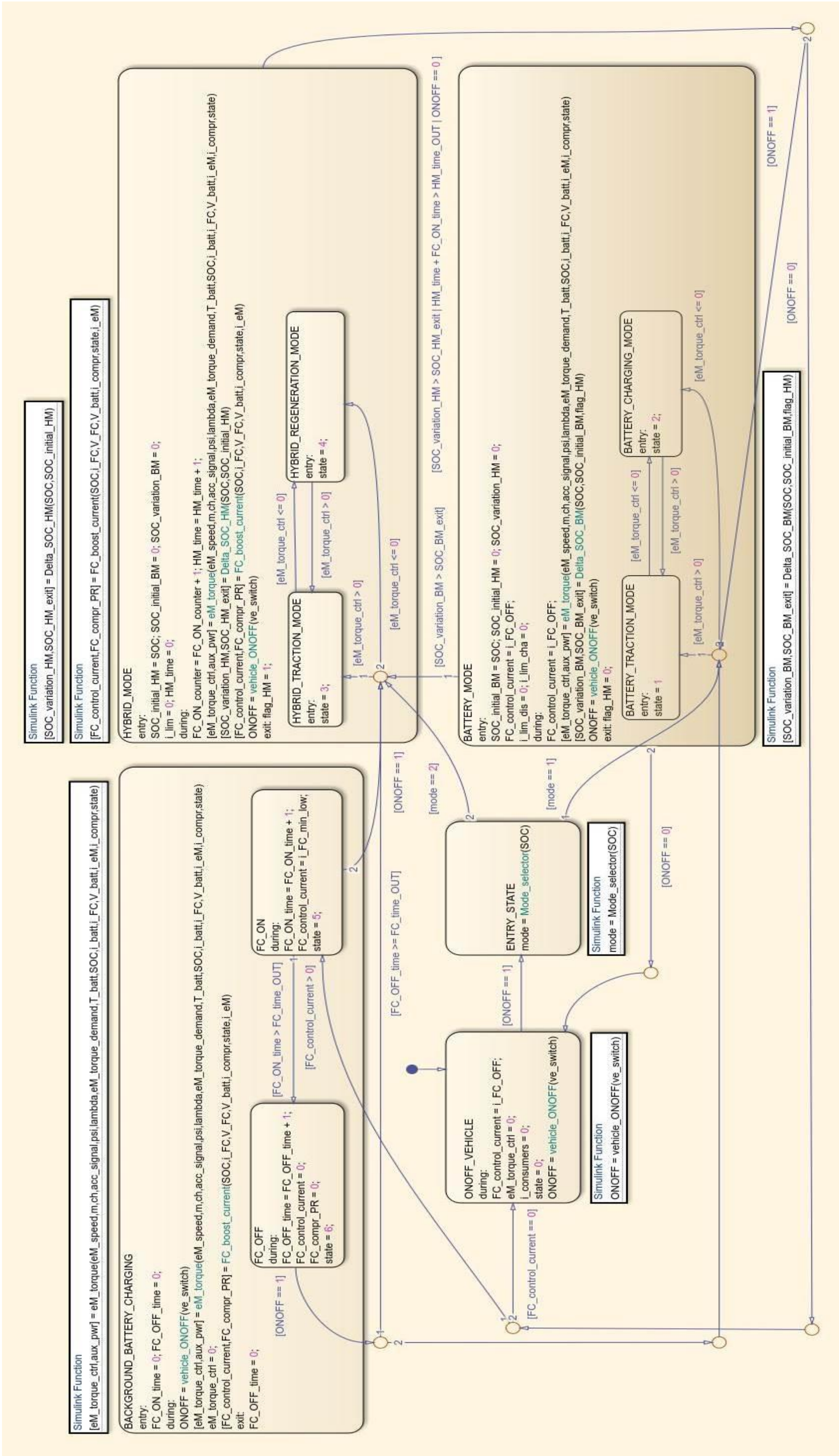

Figure 59: Original state-flow structure inside the Energy Management Strategy FEMS block

Among these functions, two in particular are the most important in terms of complexity and usage: these are the "eM_torque" function located above the "Background Battery Charging" block and the "FC_boost_current" function located above the HM block.

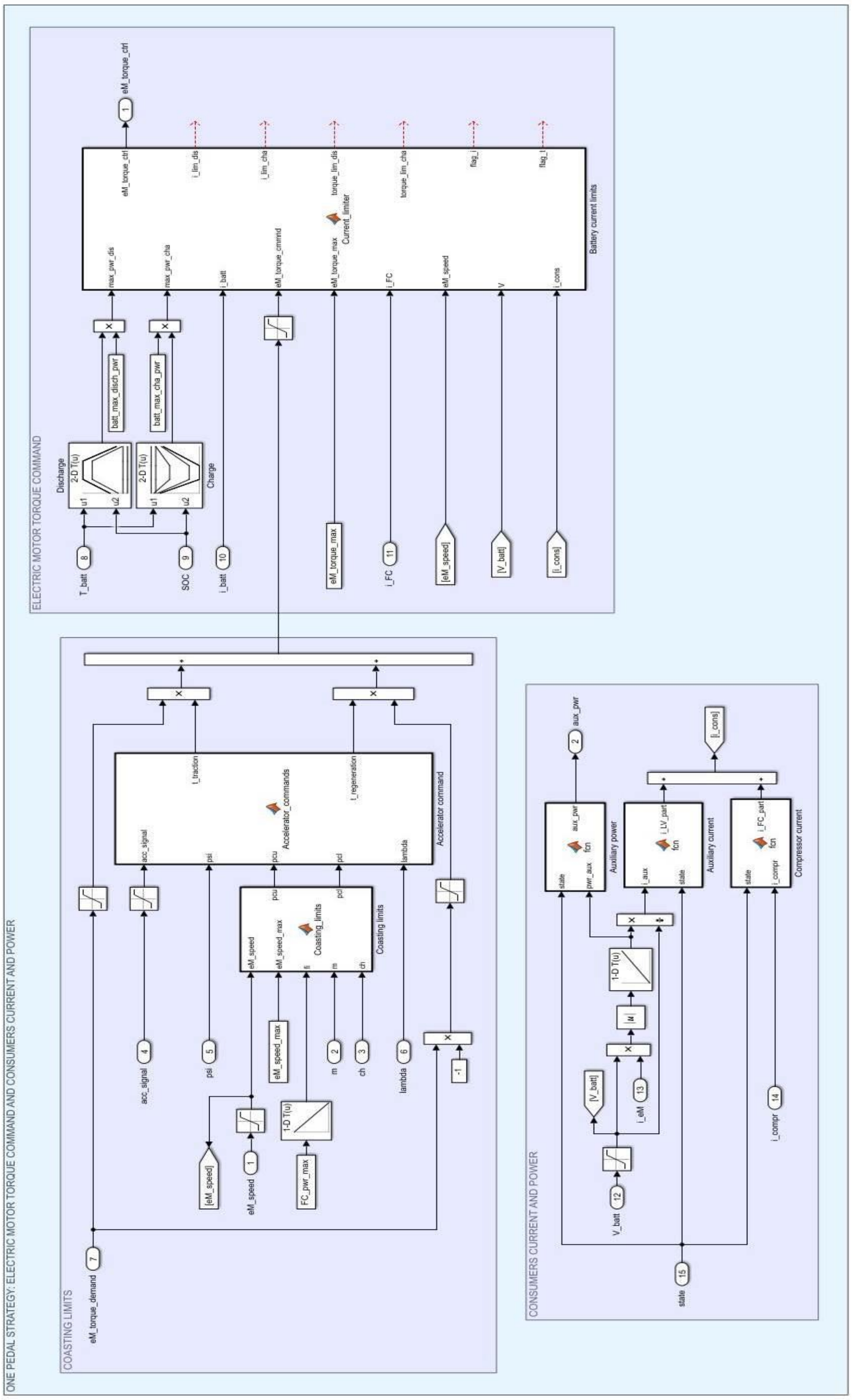

Figure 60: OPD function internal structure of the FEMS

The one presented on the previous Figure 60 is the internal structure of the "eM_torque" function, while the one presented in this page is the "FC_boost_current" one.

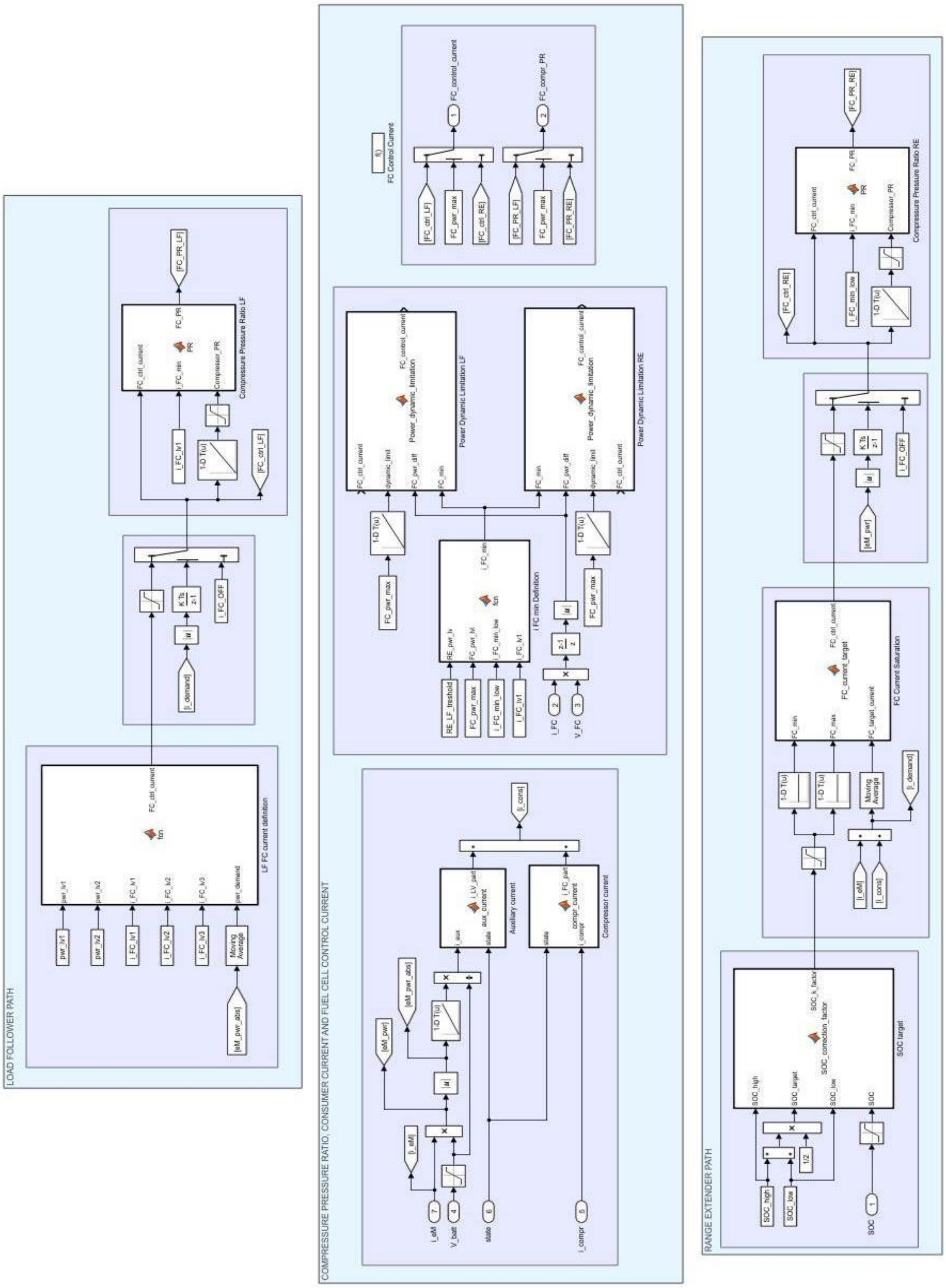

Figure 61: Internal structure of the FC control current function of the FEMS

The others will be presented in subsequent chapters. Regarding the "eM_torque", it is primarily used to calculate the torque command to control the electric motor of the longitudinal dynamics model, in its coasting, acceleration, deceleration and regeneration phases. In addition, the power of the vehicle's LV auxiliaries can also be derived with this function. As far as the "FC_boost_current" function is concerned, it has three sections: one for calculating the current for an RE hybrid (top), one for calculating it for an LF hybrid (bottom) and the middle one for applying two controls on these currents. Although FEMS is in fact used in this project referring to an RE, the control strategy has been implemented so that it also works with LF hybrids. The substructures in the two functions will be explained in more detail in the following paragraphs.

5.2.5. Behavior in traction

When the vehicle is turned on, it can find itself and vary as needed in two different modes, characterized by the active or non-active presence of the FC. When the fuel cell is OFF, we can be on BTM, while when it is ON, in HTM. Below the behaviour in traction is described, without going into full detail of its algorithms, which will be reported in the following sections.

- *In BTM*, the only energy source capable of supplying traction power to the vehicle is the battery, which can cover LV auxiliaries demand, traction continuous demand and transients. The vehicle is in BM when the FC is OFF: this occurs when the vehicle is turned ON and the SOC is greater than 50% and the fuel cell is not activated, or when the FC, after having been used, has completed one of its operating cycles and is placed in OFF again. The FC ends one of its operating cycles, once it is set to ON, when the SOC of the battery is increased by a defined threshold or automatically after a time window, to avoid too prolonged use. This mode is therefore entered either at start-up or while the vehicle is in use, always depending on the state of charge of the battery. During BM, the electric motor is controlled by the One Pedal Strategy described in Chapter 5.2.5, i.e. by the EM positive or negative torque characteristic, depending on acceleration/deceleration commands. The SOC is progressively consumed, in a Charge Depleting dynamic, even if a quantity of regenerative braking is present. To keep the FC in OFF, the associated boost converter is commanded to maintain a zero current.
- *In HTM*, the battery is also joined by the FC operation, in a hybrid configuration in which the two energy sources work together to meet the different demands of the vehicle. The vehicle is in HM when the FC is ON: this occurs when the vehicle, under

other secondary conditions, is turned on and its SOC is lower than 50%, or when it decreases by a certain threshold after entering in BM. Therefore, this mode is also entered either at start-up or while the vehicle is in use, always depending on the state of charge of the battery. Even during HM, the electric motor is controlled by the One Pedal Strategy. The regeneration dynamic present in the HM is stronger, thanks to the presence of the FC, the SOC is progressively recharged using the energy coming from hybrid unit, until a positive variation of a defined quantity is reached, the condition that allows the exit from the mode, the entry into the BM and the consequent switching OFF of the FC. To vary the level of power generated by the fuel cell while it is ON, in the PFC dynamic, the boost converter requires a certain value of current from it.

5.2.6. Behavior in braking

As far as the recharging part is concerned, a good strategy must be developed to store electric energy efficiently. In fact, as mentioned in the introduction, FC is not bidirectional and does not allow electricity to be stored in a reversible manner; within the vehicle, the only ESS capable of handling this flow is the battery. This energy to be stored will be directed to the ESS on two occasions: during braking and during periods of FC activation. When regeneration dynamic is activated, the vehicle will find itself in BCM or HRM, depending on the activation of the FC. As far as the latter is concerned, keeping the fuel cell ON for longer periods of time, to avoid a too frequent ON/OFF dynamic, will certainly present occasions where it will be used only as an electricity generator for the battery. For example, situations where the FC is switched ON and after a short time and the vehicle goes through a long period of its driving mission in idle: at this time the FC power is never used for traction, but being in ON it is advantageous that it is not turned OFF, but rather used for recharging. The FC has a lower limit power level, kept to supply electrical energy to the battery continuously and in between its acceptable efficiency range. The advantages of regenerative braking dynamics, on the other hand, are well known, as it makes it possible for the kinetic energy of braking to be recovered by the electric motor, used as a generator, increasing the overall efficiency of the vehicle, lengthening the range of the battery and its state of charge, and also the useful life of the braking system, decreasing the wear and tear on its mechanical parts.

Of the various regenerative braking strategies in the literature, the results and effectiveness of the concept of One Pedal Driving (OPD), produced by the Dynamics and Control

Group of the Department of Mechanical Engineering of Eindhoven University of Technology, led to the decision for its implementation within the EMS for this vehicle [59]. In this type of regeneration, the accelerator pedal is used for traction and to perform braking, depending on its position. An interesting part of the OPD is that it includes the presence of coasting, a situation where the vehicle is not given power for either traction or braking, but is efficiently allowed to flow freely, without consuming energy. As well as being efficient, this strategy has also been highly rated by drivers, as it allows the vehicle to be controlled almost usually with just one pedal in a simple and satisfying manner. The vehicle can be brought to stop using only the accelerator pedal, managing its deceleration with it while regenerating energy. The brake pedal continues to be present but used in emergency situations, therefore with less need and frequency, with advantages in terms of increasing the useful life of the traditional mechanical braking system.

5.3. Algorithms composing the EMS

5.3.1. OPD functioning

In this section, the operation of the OPD and the equations governing its algorithm will be briefly presented. The basic concept of such a model is to generate, as a function of the level of accelerator pedal pressure, a numerical coefficient called τ which, when multiplied by the torque curve of the electric motor, is able to give to the motor a command to apply proportionally to the wheels the torque required at each instant (positive, null or negative). It can be conceptually seen as an algorithm capable of modifying and correct the acceleration input from the driver, in the form of pedal pressure, to acceleration input for the electric motor, weighted for the motor speed. The pedal position is indicated by the variable p, which is expressed as a percentage of the maximum accelerator pedal position, where 0% is no pressure and 100% is fully pressed. The EM acceleration request is expressed with the variable τ, where 100% would indicate maximum acceleration, while -100% means maximum regenerative braking. As for coasting, when $\tau = 0\%$ no torque is applied, and the vehicle can roll freely. The value of this term, as mentioned above, depends on p, which together with speed defines instant by instant the type of torque required for electric motor, between regeneration, traction and coasting. Using numerical coefficients and depending on the two variables mentioned above, the motor's operation can be placed within the graph on the next page. The lower (p_{cl}) and upper (p_{cu}) limits which defines the coasting range are obtained from the following expressions:

$$p_{cu} = \emptyset \left(\frac{v}{v_{max}}\right)^{\frac{1}{m}}$$

$$p_{cl} = \emptyset \left(\frac{v}{v_{max}}\right)^{\frac{1}{m}} - c_h \left(\frac{v}{v_{max}}\right)$$

Where v is the vehicle velocity, v_{max} is the maximum speed of the vehicle, ϕ determines the pedal stroke at v_{max} when traction torque is applied, c_h is the size of the coasting range at v_{max} and variable m can be used to shape the characteristics. An example of how these variables change the patterns is shown in following Figure 62:

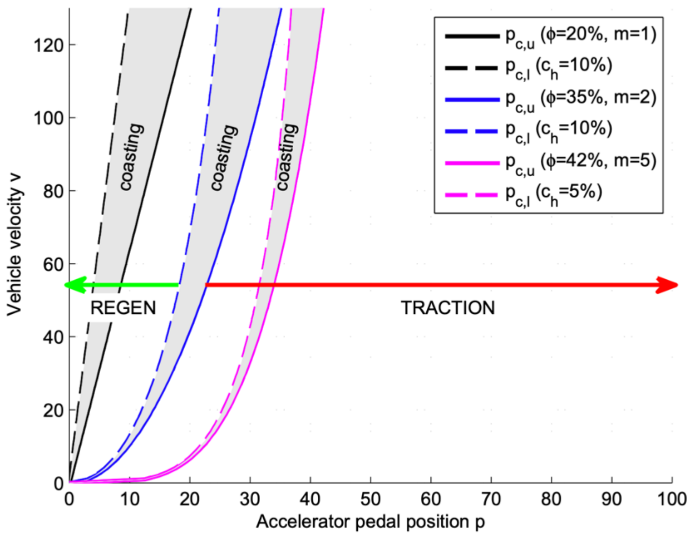

Figure 62: Definition of coasting, regeneration and traction ranges with different coefficients

Within the coasting zone, command τ to the electric motor is equal to 0, while those for the regeneration (τ_r) and traction (τ_a) case are presented below:

$$\tau_r = a_r p^{\psi} + b_r p + c_r \quad ; \quad \tau_a = \left(\frac{p - p_{cu}}{p_m - p_{cu}}\right)^{\gamma} \tau_{am}$$

Coefficients a_r, b_r and c_r are empirical and obtained by means of the following three conditions:

$$\begin{cases} \tau_r = \tau_{rm} & when\ p = 0 \\ \tau_r = 0 & when\ p = p_{cl} \\ \dfrac{d\tau_{rm}}{dp} = 0 & when\ p = p_{cl} \end{cases}$$

Where τ_{rm} is the value of the maximum regenerative braking command, τ_{am} is the value of the maximum traction command, defined when the position of the pedal is in p_m. Moreover, coefficients ψ and γ are also empirical and necessary to shape the characteristic of regeneration and traction. As shown in the Figure 63 on the next page, the higher the value of the former, the more linear the trend of τ, while for the second the trend is the opposite. Compared to the algorithm implemented by J.J.P. van Boekel, I.J.M Besselink and H. Nijmeijer, in the case of the prototype of this project, it was decided to use the angular velocity of the motor, rather than the speed of the vehicle, while still obtaining the same results. This choice stemmed from the fact that, in terms of actual implementation, measuring the EM rpm is simpler within the powertrain and can be used directly.

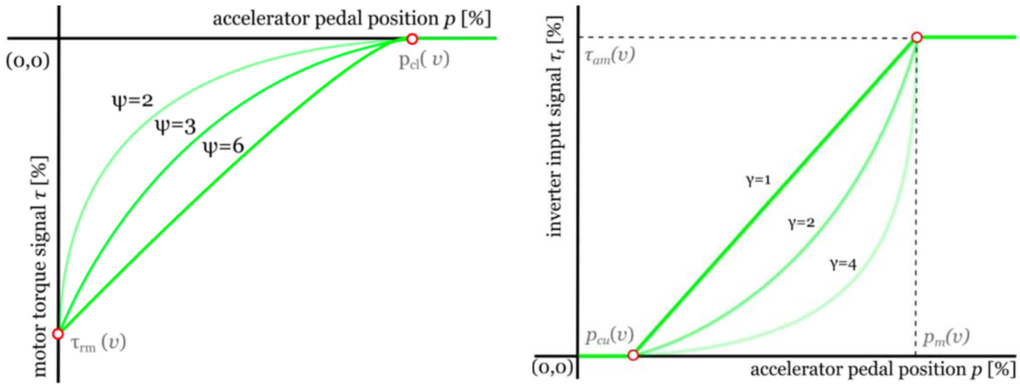

Figure 63: Graphical representation of ψ and γ coefficients

The implementation of OPD inside of the MATLAB® Simulink Stateflow is shown below:

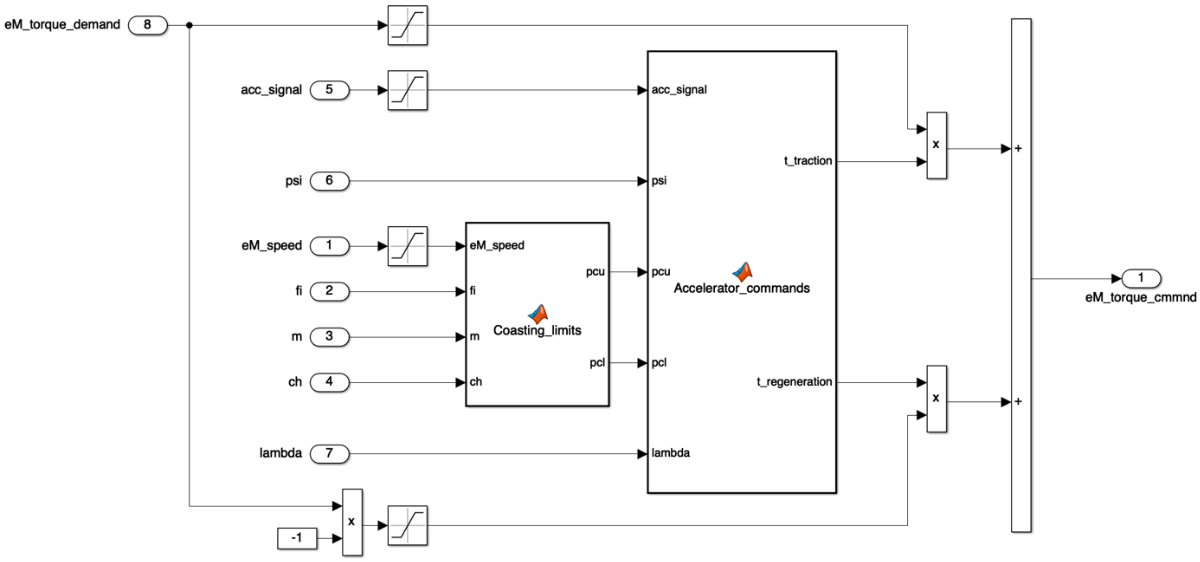

Figure 64: Simulink block scheme for the definition of the torque command for the EM

The input number 8 (i.e., the EM torque demand) represents the torque curve of the electric motor, which is then multiplied for the coefficient τ to obtain the corrected EM torque command, function of the EM speed and accelerator pedal signal (coming from the model in AVL Cruise™ M), used as input in the AVL Cruise™ M to control the electric motor block. This calculation is iterated continuously within the logical state representing the HM, when the fuel cell is ON and operates in conjunction with the battery. The block "Coasting limits" is needed to compute p_{cu} and p_{cl}, while the block "Accelerator commands" is the part in which the command τ is generated. For this specific case, the dimensionless coefficients used were as follows (in any case, they probably will be changed in future parts of the projects in order to adjust the behaviour of the vehicle):

$$\begin{cases} \psi = 6 \\ \varphi = 35\% \\ m = 3 \\ c_h = 7\% \\ \gamma = 1 \end{cases}$$

Thanks to the variable τ and knowing the characteristics of the EM, thus the level of torque τ_{eM} for the current speed, is possible to generate the torque command to control the EM, simply multiplying the two variables. With this torque command is possible to define the quantity of torque generated from the EM at each instant, depending on the driver accelerator pedal request:

$$\tau_{command}\ [Nm] = \tau_{eM} \cdot \tau$$

5.3.2. Over-charge and -discharge current and temperature limitations

In a control strategy for a vehicle using batteries as energy sources, it is imperative to provide control logic to avoid charging and discharging currents beyond the limits that the battery can withstand. This dynamic is present in what is the BMS of a battery, but since the battery model present in the longitudinal model does not include BMS, such an integration was necessary. Limiting the battery charging or discharging current is mandatory to prevent the relay from opening for safety reasons, regulating the charging and discharging current in such a way that the battery is not subjected to excessively high currents that could cause safety problems, with an increase of internal resistance and the risk of short circuits. The relay is a protective device used to interrupt the current flow in the event of excessively high currents, in order to protect the battery and other vehicle components from minor issues like reductions in battery life and capacity, till irreversible damage of components, exposition to unsafe currents and generation of fire. Obviously, such a situation must be avoided, since although it allows protection from dangerous situations, causes the vehicle to lose the possibility to use the battery and all the systems connected to it and to the HV line. The current limits that a battery can withstand, often expressed as maximum charge and discharge current or using the capacity C, are always specified by the battery manufacturers. The charging and discharging capacity is usually expressed in terms of the magnitude C [Ah], which represents the ratio between the maximum permitted charge or discharge current and the nominal capacity of the battery. The allowed C capacity depends on the type of battery and its manufacturer, usually a Li-ion battery may have a maximum permitted charge capacity between 1.5 and 3 C. To limit the current, can be used several techniques, including a direct limiting, adjusting the battery voltage or adjusting the battery temperatures. In this specific case, a simple algorithm has been introduced to adapt the torque required from the EM according to the battery's allowed charge and discharge current limits, i_{lim}^{disch} and i_{lim}^{charge}. These are a function of the SOC of the battery and its T, so that moving away from the ideal ranges of SOC (between 20 and 80 %) and T_{batt} (between 15 and 30 ºC), where the maximum permissible power is actually the maximum power, they are reduced. This power reduction dynamic is introduced by means of a two-variable function, which provides the following Figure 65:

$$P_{lim}^{disch/charge} = f(SOC, T_{batt})$$

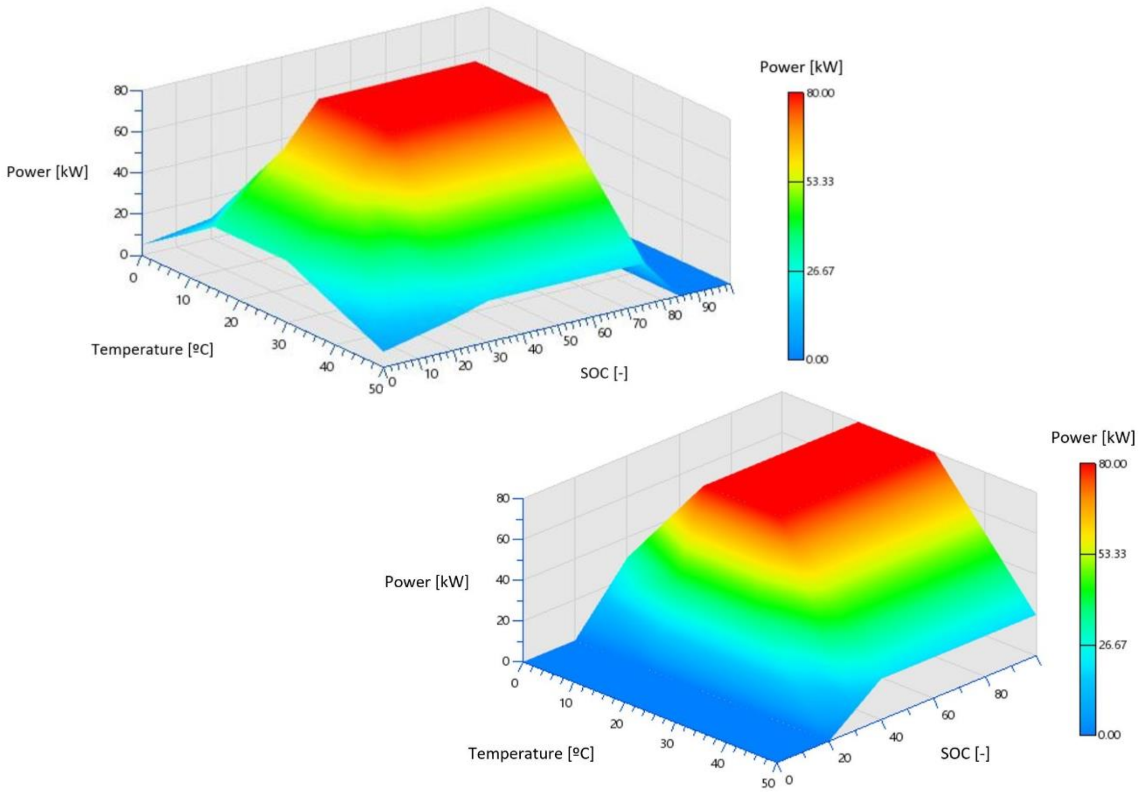

Figure 65: Battery power operating limits under discharge (above) and charge (below) conditions

The maximum power values used here were taken from the data sheet of the INT-39 10S2P battery, that will be used in the prototype powertrain, with a maximum power output in both charge and discharge of 80 kW under reference conditions. These relationships were derived from the models implemented within the programme AVL Cruise™ M, in the future for more advanced stages of the project they could be revised, without considering that for the actual implementation within the vehicle ECU this control will be carried out directly by the BMS. With this appropriately limited power, it is possible to define the maximum charging and discharging current at each instant for the battery, in order to obtain the appropriate torque for EM at all times. To do this, it is necessary to consider the current coming from the vehicle's low-voltage consumers I_{cons}, the one generated in the battery I_{batt} and the current made available by the FC I_{FC}. The torque limit command that is sent to the electric motor, in the event that this command is actually generating a current than the battery can't withstand, is formulated as follows:

$$\tau_{lim}^{discharge}\ [Nm] = \frac{\left[i_{lim}^{discharge} + max(0, I_{FC})\right] V_{HV}}{EM_{rpm} \cdot (60/2\pi)}$$

$$\tau_{lim}^{charge}\ [Nm] = \frac{\left[i_{lim}^{charge} - min(0, I_{FC})\right] V_{HV}}{EM_{rpm} \cdot (60/2\pi)}$$

$$i_{lim}^{discharge} = \frac{P_{lim}^{discharge}}{V_{HV}} - I_{cons} \quad ; \quad i_{lim}^{charge} = \frac{P_{lim}^{charge}}{V_{HV}} + I_{cons}$$

Where I_{cons} is the sum between the current from the LV auxiliaries and the FC compressor, V_{HV} is the value of the HV bus line tension, and EM_{rpm} is the rotational speed of the EM. The logic in this case is that:

- In traction: if $I_{batt} > i_{lim}^{discharge}$ then $\tau_{command} = min\left(\tau_{lim}^{discharge}, \tau_{eM}\right)$
- In braking: if $I_{batt} < i_{lim}^{charge}$ then $\tau_{command} = max\left(\tau_{lim}^{charge}, \tau_{eM}\right)$

Where $\tau_{command}$ is the generated torque command is used to control the EM and τ_{eM} is the torque output which would come out from the EM torque curve at a defined speed. This means that the torque is adapted in such a way that the battery is never required to generate a current that is above its physical limits. The following Figure 66 shows the Simulink block scheme of the current battery control.

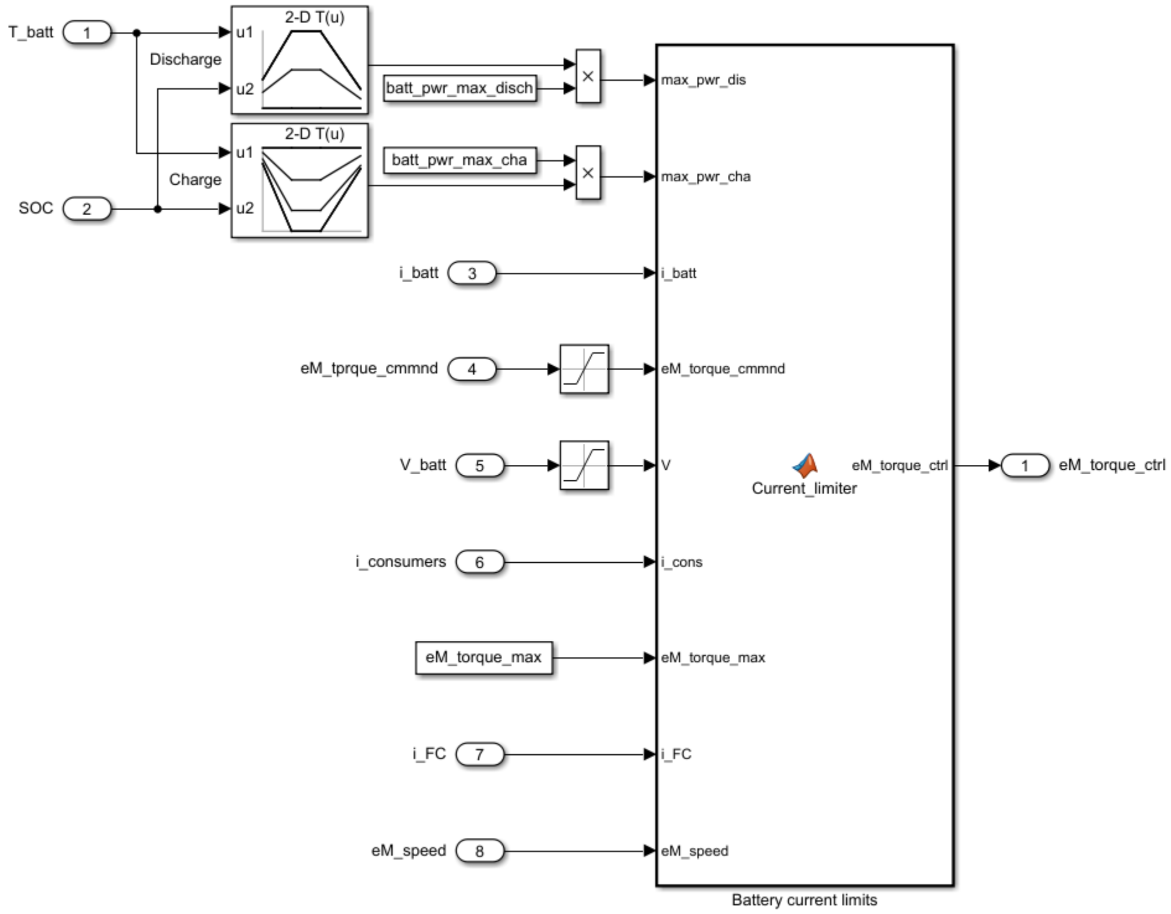

Figure 66: Simulink block scheme for the definition of the torque command for the EM considering also the current limits of the battery

In order to give an example of how this algorithm works, some graphs obtained by using the longitudinal FCEV model along the S&S average driving cycle profile are presented below. In the Figure 67, the current developed by the battery along the cycle is shown, together with the limit currents in charge and discharge calculated by the algorithm. It can be seen that there are times when the battery exceeds its limits, in the sections of the cycle with the highest power demand. These limiting currents result in a maximum torque limitation, both during charging and discharging, which are shown below, that can be seen in Figure 68. Within these, the torque without control of the EM is also shown, where it can be seen that in some instances where the battery current is very high, the torque of the electric motor also exceeds the limits generated by the limited currents. In these cases, the torque is corrected to assume the safe limit value it can assume, depending on the currents calculated earlier.

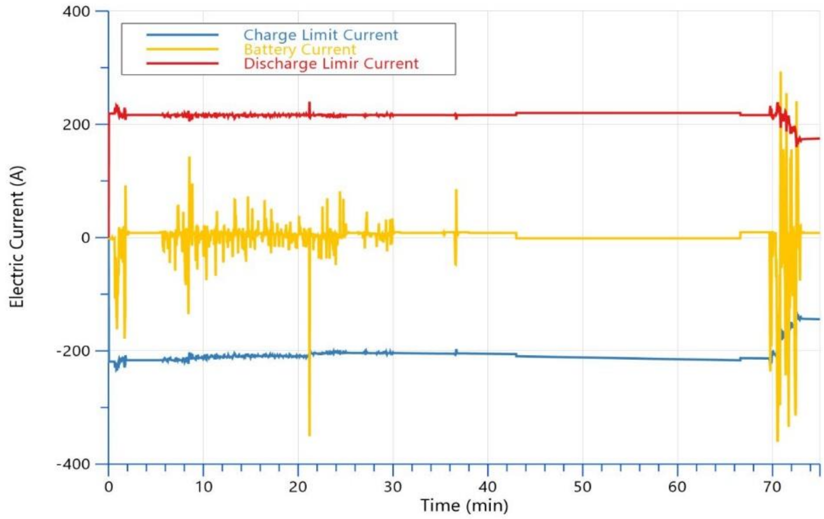

Figure 67: Comparison between battery current and its charging and discharging limits

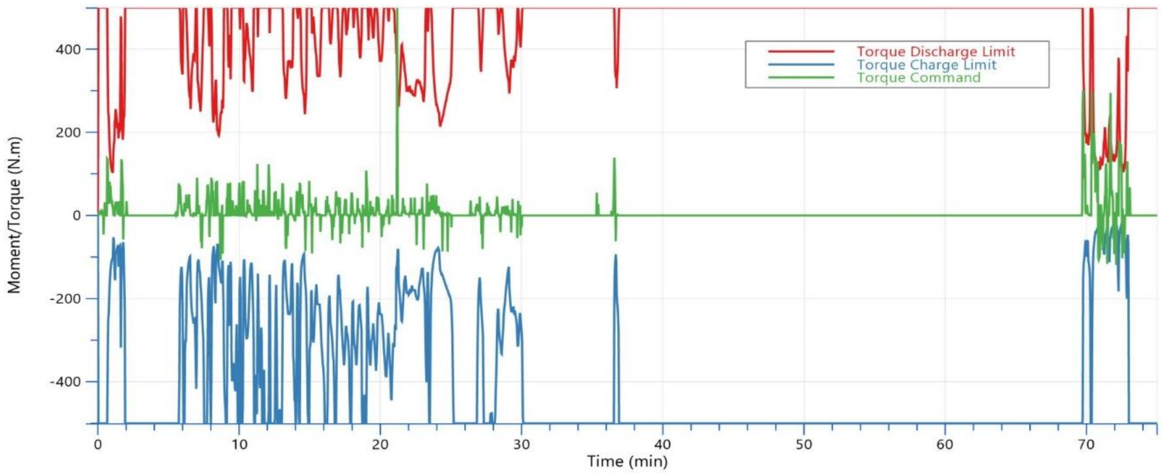

Figure 68: Comparison between torque command and its charging and discharging limits

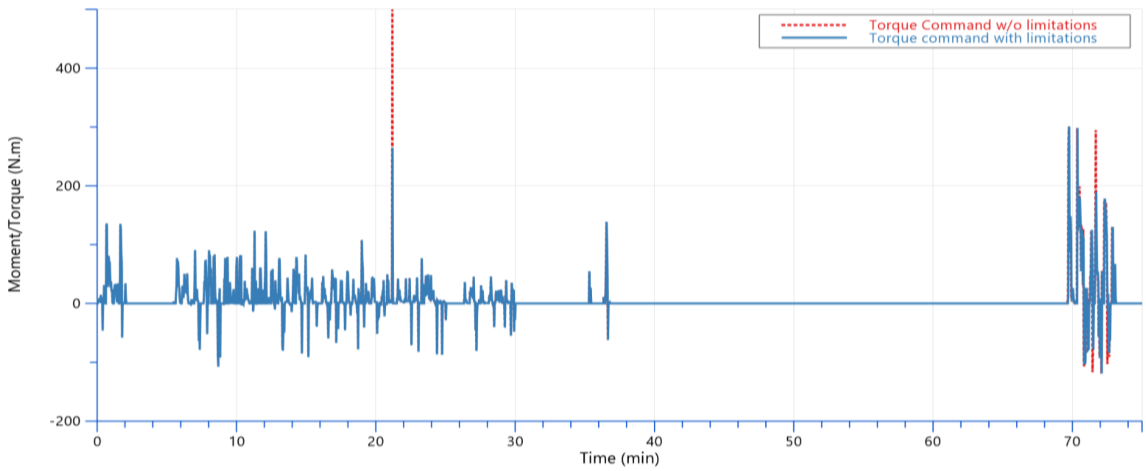

Figure 69: Comparison between command with and without limitations for battery currents

In this last Figure 69, the comparison between the torque command for the electric motor with and without the correction for current limitation is shown. In red, is possible to see how the torque command would have been if no limitation were applied, demanding to the EM a performance which have been asked to the battery an exaggerated current.

5.3.3. Consumer`s current and power

In the FCEV model used for the simulation of this vehicle's powertrain, consumer's power consumptions, i.e. those not directly related to electric and hybrid drive, must also be taken into account. To do this, two power-consuming elements are considered in the FEMS: these are the LV auxiliaries and the BoP of the FC (in this case modelled in the form of a compressor, which is the element that consumes the most power among the various FC systems). Therefore, is possible to speak accordingly of an LV part and a FC part of current produced from vehicle consumers, which generates power losses, according to the following image:

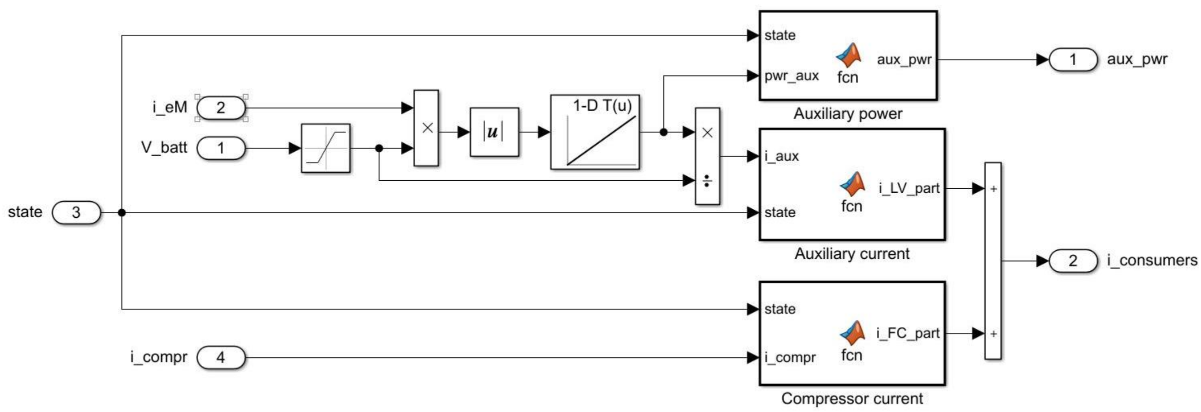

Figure 70: Simulink block for the computation of consumers' current and power

For the LV part, the power generated by the electric motor is associated to the power lost by the vehicle's LV auxiliaries, in a semi-proportional manner:

$$P_{LVaux} = P_{LVaux}^{const} + P_{LVaux}(P_{eM})$$

The part P_{LVaux}^{const} is a constant portion of consumption (equivalent to 500 W) that is present whenever the vehicle is ON, while the $P_{LVaux}(P_{eM})$ varies in function of P_{eM}, reaching 3 kW under the most severe conditions. For the FC part, as mentioned, it is the compressor that plays the most interesting part as far as consumption is concerned, therefore what is varied is the pressure ratio of the compressor PR_{compr}, proportionally according to the output power of the FC:

$$P_{BoP} = f(P_{FC}) = f(PR_{compr})$$

The more power is demanded from the FC, the higher the compressor's operation, the greater its compression and thus the more power it needs (and loses). This FC part is present whenever the FC state is ON. Again, power values that can be achieved in situations where the FC is required to perform is between 500 W and 2 kW. This means that the power lost between the various power consumers is between 1 and 5 kW, depending on the power required from the vehicle. In the next Figure 71, it is shown how consumption develops using an S&S average driving cycle with an initial SOC of less than 50%.

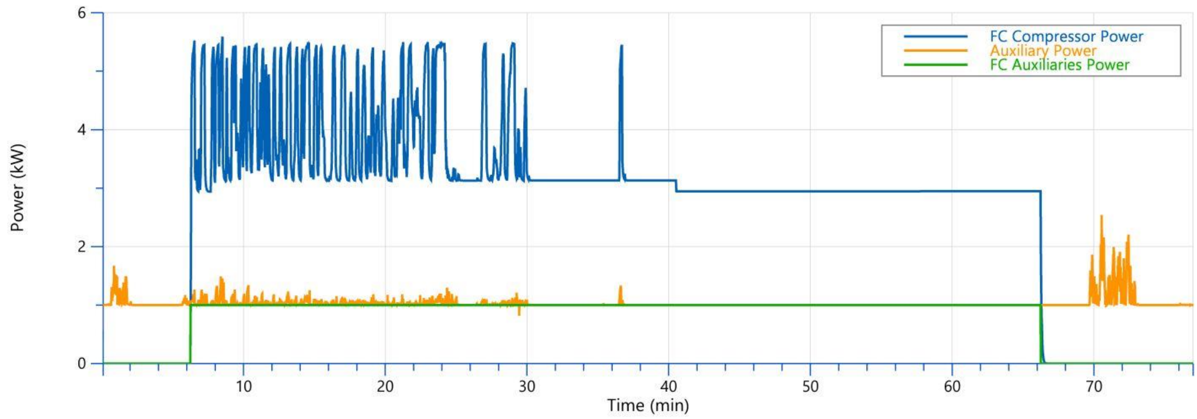

Figure 71: Consumers' power along a S&S average driving cycle

In addition to the consumer current output, the power directly consumed by the LV auxiliaries is also calculated, as it becomes a direct input in AVL Cruise™ M since this function is not present in this latter program.

5.3.4. FC control current of the boost converter

As said previously, the DC/DC boost converter is the element which takes care of the control of the power supply of the FC, together with its switch ON/OFF dynamic. To regulate the output of the fuel cell is mandatory since the unregulated output voltage cannot be directly interfaced to the DC bus, since the value is lower, in the order of less than 100 V. Moreover, with the boost converter is possible to provide a variable current or voltage reference to the FC which can follow to provide the required power, depending on how the EMS is implemented. In this way is also possible to operate the FC in its linear region (Ohmic region), since outside it the FC cannot be operated, as the electrolyte membrane of the cell may get damaged, or the efficiency will be too low. To be more specifically, is important to operate the FC outside the regions of polarization and concentration losses, defining a lower and upper limit of power. In the following Figure 72, is shown how the efficiency and output power changes in a FC depending on the demanded current (in this specific case, as example, on the DC/DC boost current) [64].

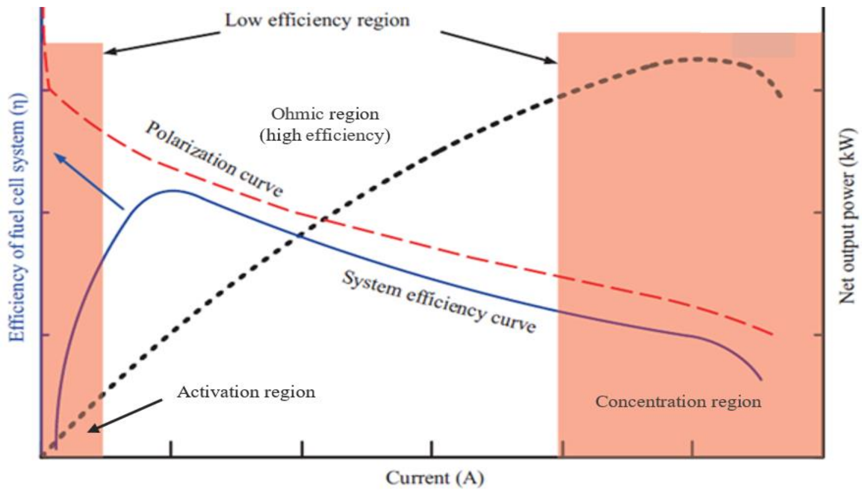

Figure 72: Efficiency and net output power as functions of load current in a Fuel Cell system

Switching devices, such as power MOSFETs are used in this end. For a given input voltage, the average output voltage is regulated by controlling the duty cycle of the semiconductor. A typical circuit diagram of a DC boost converter includes a power MOSFET, an inductance L, a capacitance C and a diode, as shown in the Figure 73 below [65].

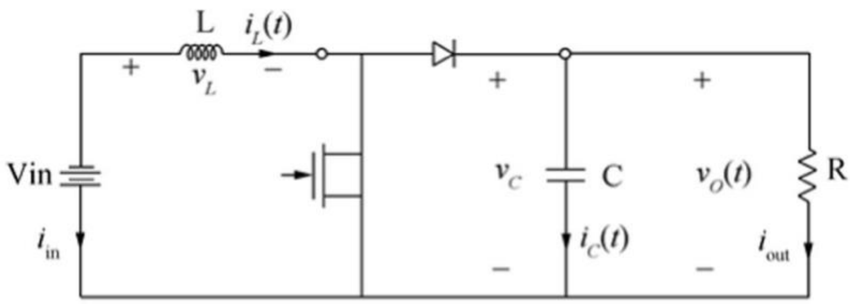

Figure 73: DC/DC boost converter topology

In this case, a reference current is sent to the block simulating a DC/DC boost converter within AVL Cruise™ M, so that the desired power is obtained. This reference current is a function of the current required at the HV line, i.e. the current required by the EM for movement and that required for the operation of the low voltage auxiliaries. The FC current in the FEMS, being a PFC control strategy, follows the demand of the vehicle in real time, so this reference current will also do the same. This current is modified and tuned with several sub-controls which considers various factor, in order to make the functioning of the FC as much optimal as possible:

- The *control current is saturated*, both in minimum and maximum, to adjust to the acceptable output power (and efficiency) window. In order to do it, the selected criteria is the utilization of a target SOC, as will be explained better in the next subsection. The basic dynamic is that if the SOC is above the SOC target, the power of the FC is decreased, while maintaining the same trend. This reduction is both in the lower and upper limits, in order to use less hydrogen while offering the advantages of the RE hybrid. On the other hand, if the SOC is lower than the SOC target, the power is increased, in order to charge more the battery, while consuming a higher rate of hydrogen. This variation is proportional, using the coefficient k coming out from the target SOC calculation.
- In order to avoid excessively fast current generation variations for what the FC can withstand, being a device that can be damaged if operated too much dynamically, the *demanded current is treated as mobile average*, within a time window of determined length. In this way, the current variation dynamics of the FC is decreased, allowing a slower power variation while still following the cycle variation over time. Being an RE, it is not necessary for the FC to precisely follow the power demand of the vehicle, as the battery allows 100% of the demand to be met.

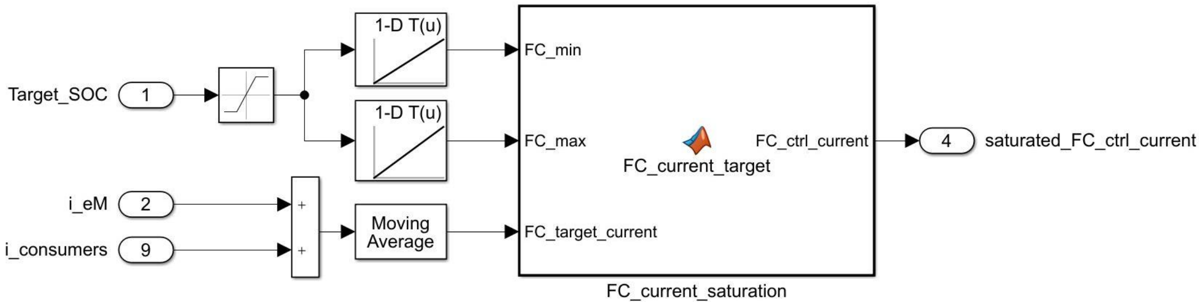

Figure 74: Simulink block scheme for the definition of the FC control current in function of the demanded one and limitation in function of the SOC target.

In the following Figure 75 is possible to see the difference between applying this control and simply following the cycle demand. The following graphs were derived from the simulation of an average cycle and showing 11 example seconds. By using the control, the FC has smoother dynamics, while still following the original request.

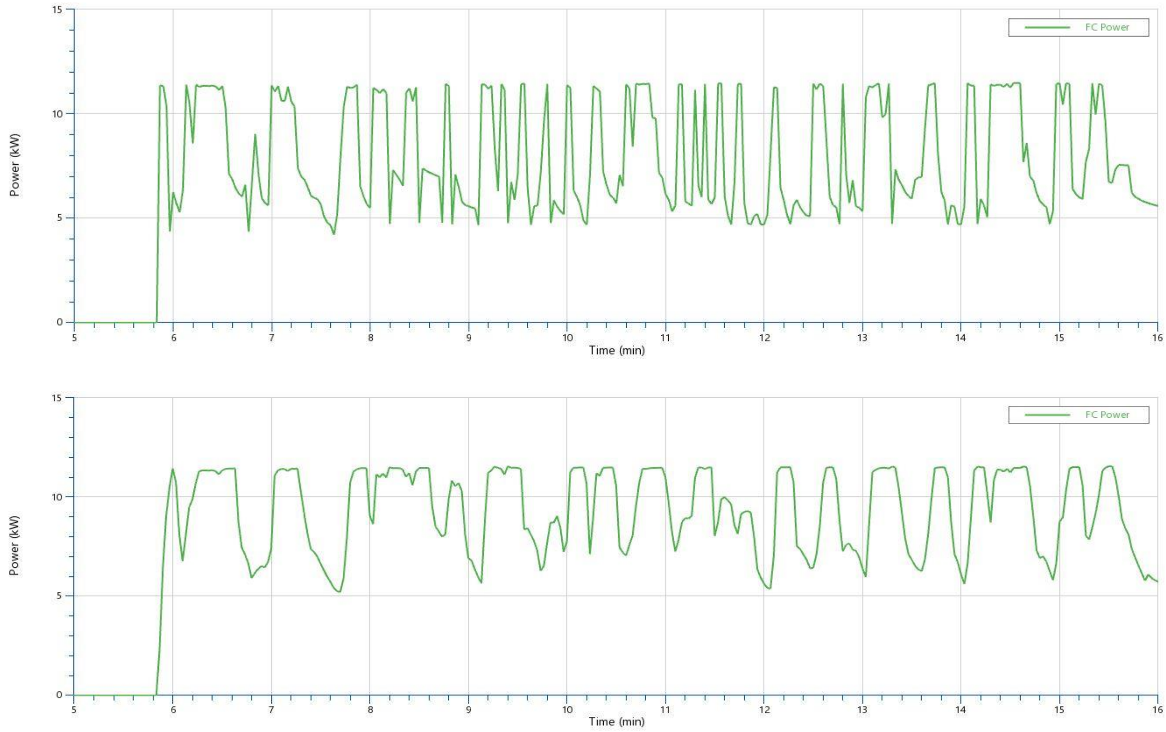

Figure 75: Comparison of FC power generation in with and without moving average demanded power control

- If the FC would be used for a very short timeframe, is will be inconvenient, since a frequent dynamic of ON/OFF could damage the FC itself. In order to avoid that dynamic and that the hybrid unit is turned ON in operations where the vehicle is used at a very low velocity or for a very short period of time, like parking manoeuvres or controls, a minimum quantity of generated demanded power to switch ON the FC is computed, called *FC activation power threshold*. It allows to start using the FC only after a period of time after the vehicle is turned ON, in function of the functioning: higher is the produced demanded power, faster will be turned ON the FC. Therefore, when the vehicle is turned ON, the demanded power is stored and accumulated, since a target is reached and, if the other conditions of FC ON are satisfied, is truly switched ON and start to operate.

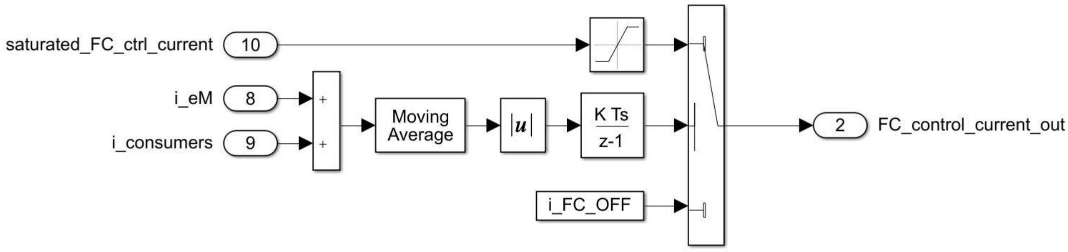

Figure 76: Simulink block scheme for the introduction of the FC activation power threshold

In the following Figure 77, taken from the simulation example of a standard cycle over 11 seconds, it can be seen that with this control, the FC does not start operating immediately, but does so after about half a minute, when a certain energy threshold is reached.

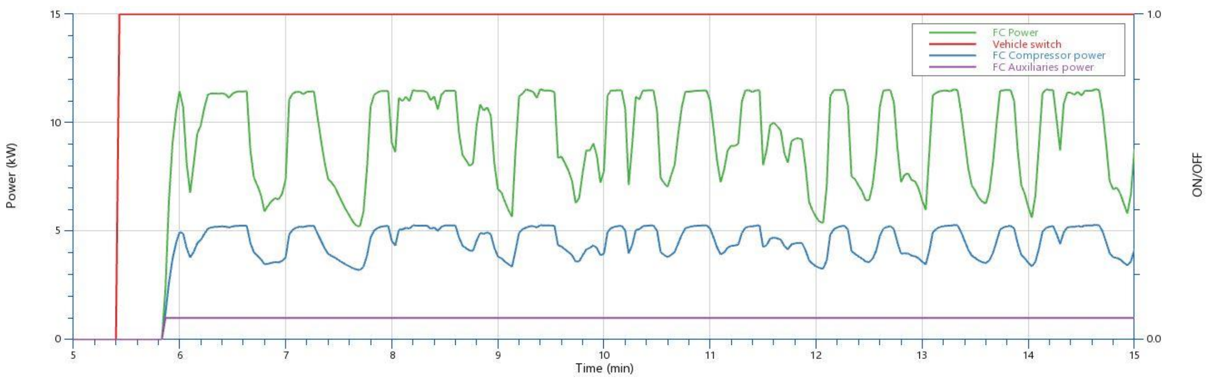

Figure 77: Example of the activation of the FC delay generation control

5.3.5. Target SOC

A target SOC control strategy works by constantly monitoring the state of charge of the electric vehicle battery and adjusting the output power of the battery to maintain a desired level of charge, known as the target SOC. Control of the target SOC can be performed using several techniques, including limiting the charge and discharge current, adjusting the power output of the electric motor and programming the battery life cycle. In general, a target SOC control system will use a combination of these techniques to ensure that the battery remains within a desired charge range. In general, over-charge and over-discharge, namely charge or discharge the battery above or below the upper and lower limit, are two situations to be avoided as they can cause irreversible damage to the electric vehicle battery by reducing its life and capacity. Using a control strategy with an objective SOC (state of charge) can offer several advantages for battery management in an electric vehicle:

- *Battery life*: by using a control strategy with an objective SOC, it is possible to avoid over-discharging the battery, which can reduce battery life over time.
- *Safety*: avoid over-discharging the battery can also decreased increase the risk of fire or other safety problems.
- *Energy efficiency*: by using a control strategy with a target SOC, the battery can be used more efficiently, which can reduce operating costs and increase vehicle range.
- R*eliability*: vehicle reliability can be increased, as the battery is used in a more controlled and predictable manner.

The control strategy for the prototype vehicle in this activity includes the use of an objective SOC. Many control strategies in the bibliography use a target SOC, the one below uses a similar function in the one that can be found, for example, in the Journal of Transportation Technologies, in a scientific article produced by West Virginia University, cited in the bibliography. Thanks to SOC_{target}, it is possible to generate a coefficient (called K, in this case) that can be seen as an adjustment factor for various control parameters, depending on how far the state of charge of the battery is from the target state. The formulation of the coefficient K to account for the target SOC is as follows:

$$SOC_{target} = 0.5\,(SOC_{high} - SOC_{low})$$

$$K = 1 - \left(\frac{SOC - SOC_{target}}{\frac{SOC_{high} - SOC_{low}}{2}} \right)^{a}$$

Where SOC_{high} and SOC_{low} are respectively the upper and lower limits for the battery state of charge defined heuristically. Formulated in this way, the coefficient behaves like this:

- When $SOC > SOC_{target}$ the K coefficient will be < 1: it means that the SOC is approaching SOC_{high}, therefore the factor is decreased to promote battery discharge.
- When $SOC < SOC_{target}$ the K coefficient will be > 1: it means that the SOC is approaching SOC_{low}, therefore the factor is increased to promote battery charging.

Non dimensional coefficient *a* is useful to vary the shape of the target SOC function, as shown in the Figure 78 below. To convert the coefficient K to a value between 0 and 1, it is halved so as to obtain the coefficient k.

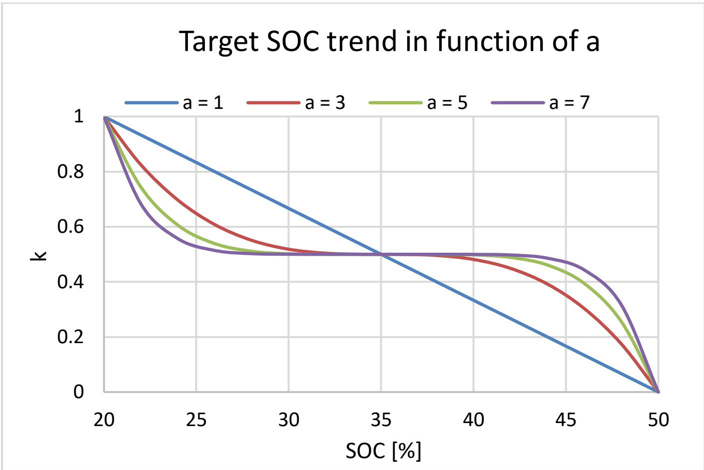

Figure 78: Trend of the SOC target as function of the coefficient *a*

In the case of the FEMS, the target SOC is used in defining the control current of the FC, as shown in the Figure 79 below. The coefficient calculated as above, oscillating between 0 and 1, is able to give a weight to the target current of the boost converter and thus to the power required and proportioned by the FC.

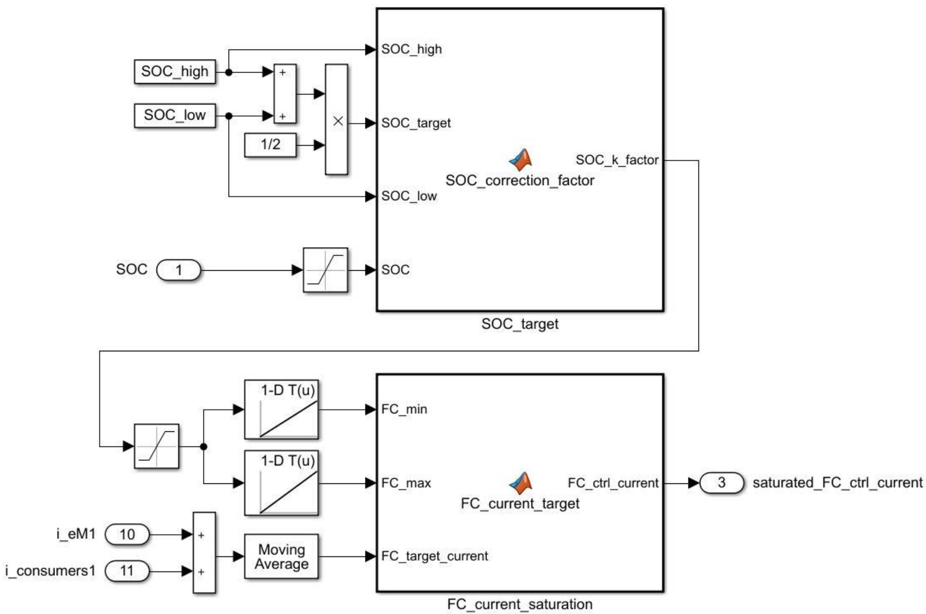

Figure 79: Simulink block for the computation of the target SOC for the definition of the FC control current

This coefficient is multiplied by the min and max target current of the FC, so that depending on how far the battery state of charge is from the target SOC, the power of the FC is adjusted accordingly: the lower the SOC, the more FC power will be generated, thus allowing the battery to recharge faster. Obviously, this will result in higher hydrogen consumption as one moves away from the target SOC, but the main objective is to try to keep the state of charge around that value, so consumption takes a back seat. In order to provide an example of the correction made by the target SOC, a simulation of the longitudinal FCEV model over a representative 13h cycle was carried out and the trend in HR power is shown below in Figure 80. This length was supposed in order to deplete the complete tank of H_2 and also to show the variation of the FC power along a wide SOC decrease. As can be seen, both min and max values of the FC power increase along with the decrease of SOC, namely by moving away from the target SOC. The variation is around 1 kW, both in minimum and maximum values. Moreover, is possible to see that not only between different ON/OFF cycles the values changes, but also inside them.

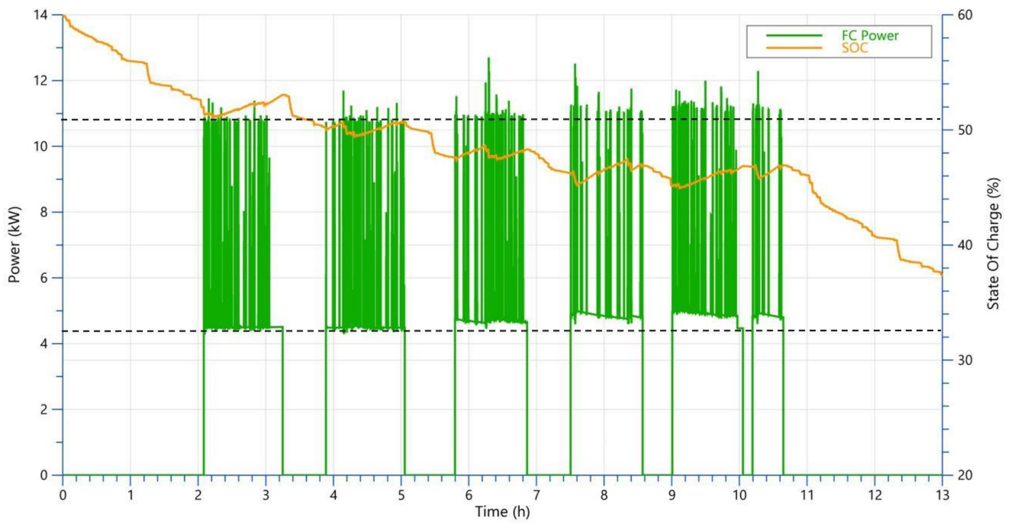

Figure 80: FC power trend with SOC target correction along a demonstrative cycle

5.3.6. Background FC battery charging

When the vehicle is switched OFF, a situation may arise where the FC had started its operation a few moments before having to be switched OFF again. Such a dynamic, as far as possible, should be avoided, since the activation of the FC should always be accompanied by minimal use, to avoid damaging of BoP components, decrease of FC lifetime and as well as the investment of initial energy for starting at low efficiencies that would only constitute a loss without the production of useful power. Without any special additional techniques allowing fast warm-up of the FC, such as preheating of air or ohmic heating with chemical reactions, the literature speaks of FC start-up time reaching optimum efficiencies in the order of a few minutes, depending on the power level of the FC and operative conditions [67]. Normally, slow start-up dynamics occurs with low temperatures, because the efficiency of the FC is related also to its working temperature. To try to avoid this issue, an algorithm for background battery charging is introduced, which allows the FC to be kept ON even when the vehicle is switched OFF, acting as an electricity generator to recharge the battery at a satisfactory efficiency. In this way, if the FC should be switched OFF when the vehicle is switched OFF but too little time has elapsed since it was switched ON, it is kept ON for a further short period at the minimum efficient power generation so that its start-up can provide some kind of benefit to the system despite the vehicle no longer being in motion. At the end of this additional period of operation, the FC will shut down and cannot be used for a further timeframe, even if the vehicle is started immediately afterwards and the SOC is low, in order to avoid this deleterious switching ON and OFF.

In order to simulate vehicle shutdown, it is possible in AVL Cruise™ M to introduce conduction cycles that consider the vehicle's switch-on and switch-off status, by means of a variable called *switch*, which takes the value of 0 when the vehicle is OFF and 1 when it is ON. With this in mind, it has been possible to recreate driving missions that include the switching ON/OFF of the vehicle along the cycle. Two profiles comprising this dynamic are shown as examples below (Figure 81 and 82), an average standard one lasting 77 minutes with 5 switch ON/OFF, and a long one lasting 9 hours with 5 switch ON/OFF, again characterised by the average values of the driving cycles seen in the data analysis.

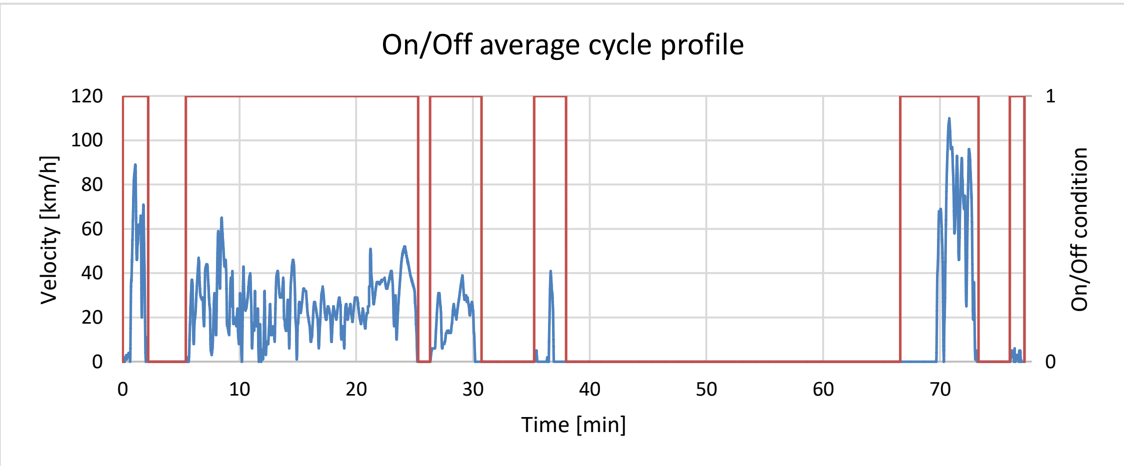

Figure 81: S&S average driving cycle profile with On/Off vehicle sequence

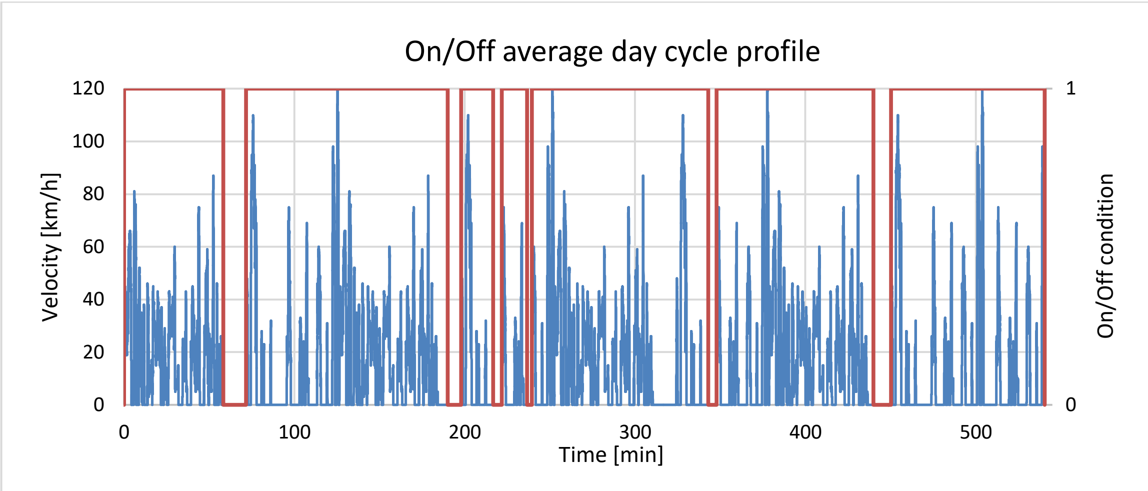

Figure 82: S&S average operative day driving cycle profile with On/Off vehicle sequence

The following Figure 83 shows an example of background charging operation, taken from a time window in the graph in Figure 81: at times when the vehicle is OFF, but less than 5 minutes have elapsed, the FC is not switched OFF, but continues to operate at minimum power generation. It is then restored to standard generation when the vehicle is switched back ON, while when the vehicle is OFF and this time threshold has passed, it is simply switched OFF.

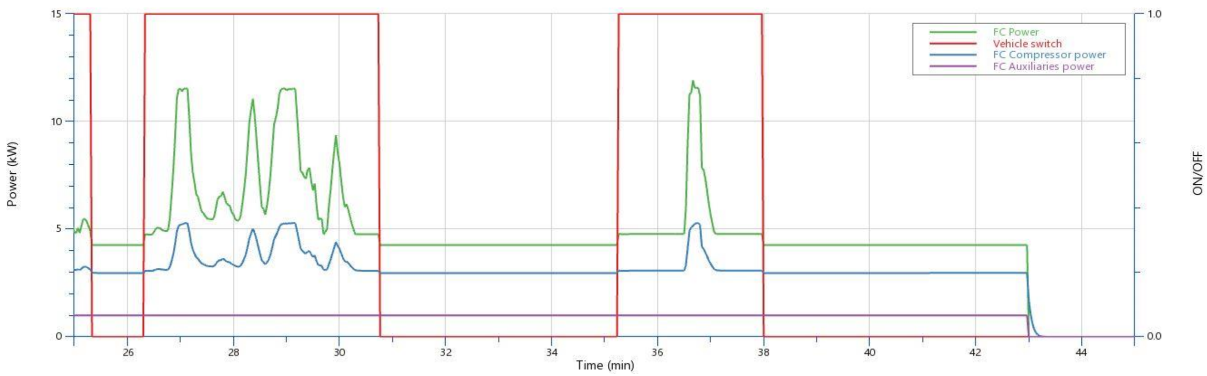

Figure 83: S&S average operative day driving cycle profile with On/Off vehicle sequence

5.3.7. Implemented algorithm for system safeguard

In addition to the operation just described, further algorithms have been added within the FEMS, following the fine-tuning process. These are blocks representing special cases that alter the normal behaviour of the strategy, in order to safeguard the health or proper functioning of the vehicle:

- *Depletion of the hydrogen fuel tank*: in order to simulate the presence of the hydrogen fuel tank, a limitation in this sense is implemented. Without this part, one could run simulations with unlimited capacity of the hybrid part, whereas the purpose is to take into account the limited availability of CF power. When the capability to produce power of the hybrid unit ends, the vehicle goes back to be a pure electric one, with a CD profile.

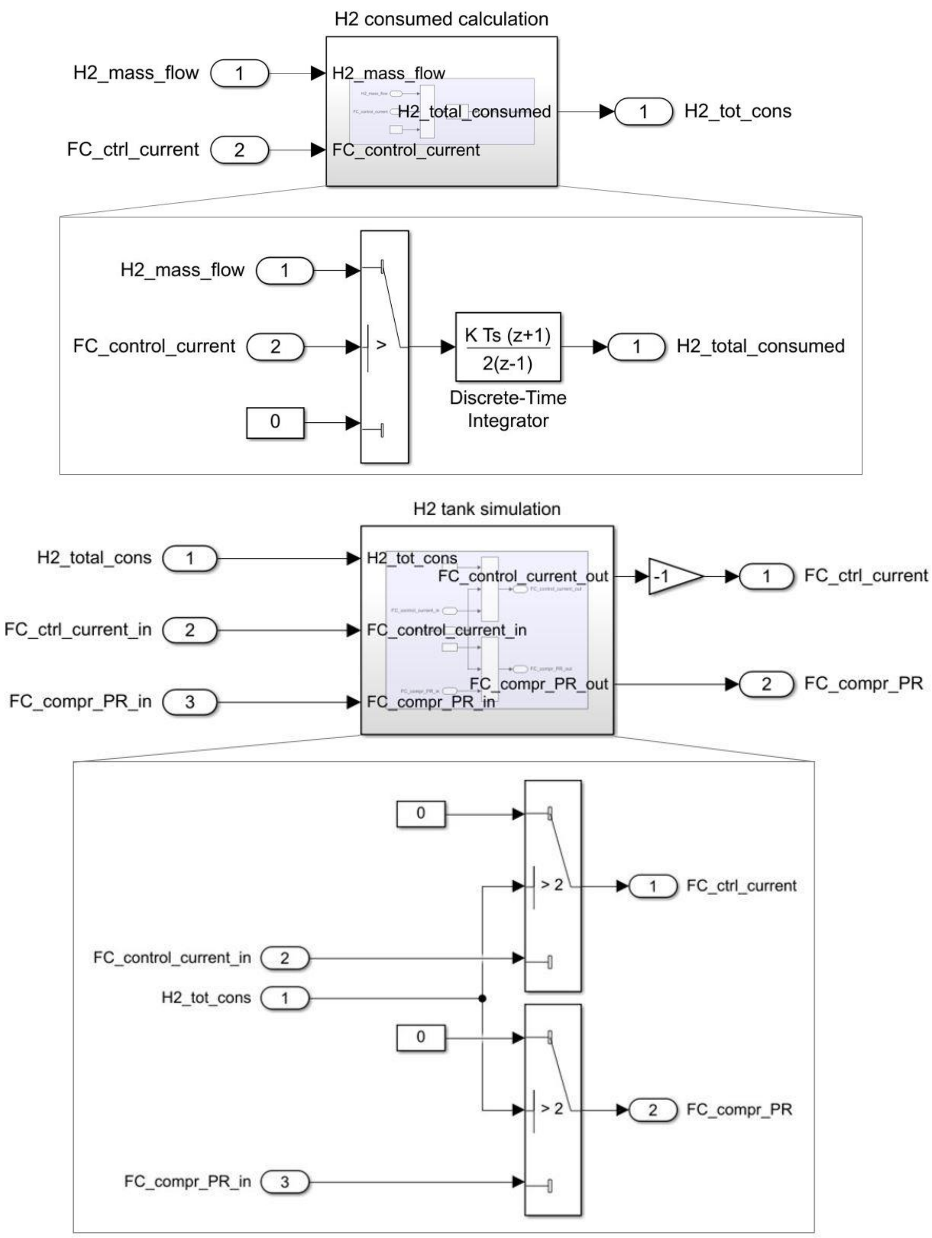

Figure 84: Simulink blocks for the computation of the consumed hydrogen (above) and for the creation of a hydrogen tank (below)

- *Limiting the power rate of the FC*: literature suggest that the maximum power variation is required to be lower than 4 kW/s in order to allow FC to have a safe fast dynamic. [68][69]. The reason of that is related to the phenomenon of reactant (hydrogen and air) starvation, which leads to a series of severe consequences such as carbon support corrosion, cell reversal, output performance degradation and reduction of FC lifetime. In the case of fuel starvation, hydrogen is no longer enough to be oxidized to maintain the current generation, and anode potential will increase high enough to make alter oxidized in anode with oxygen produced. At the same time, oxygen is reduced in cathode, so the net effect is pumping of oxygen from cathode to anode while water from anode to cathode simultaneously. On the other hand, oxidant starvation usually occurring under severe operating conditions such as start-up, rapid load change and water accumulation during long operation, transients, or if reactants are consumed in the fuel cell faster than they can be supplied [70]. In order to avoid that phenomenon, the dynamic of power generation of the FC can be limited. The current control for the DC/DC converter boost is subjected to a lockout where, depending on the power variation of the FC over time, calculated as the difference between successive values, it is corrected if this variation exceeds the above-mentioned limit, recalculating the control current of the FC in such a way that it generates a maximum current in the FC always corresponding to a variation within the limit.

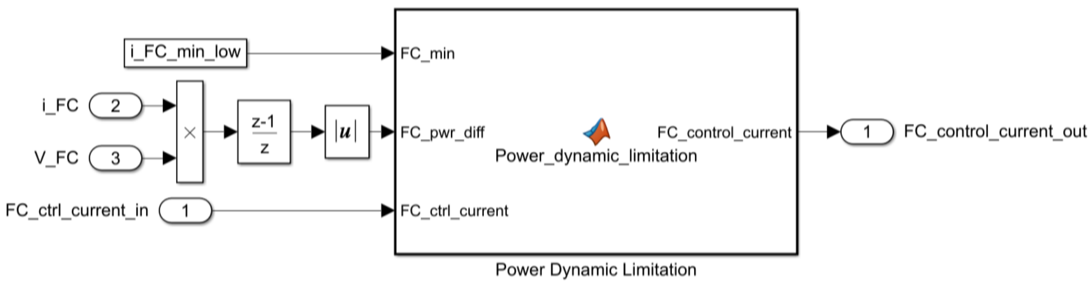

Figure 85: Simulink block for the power dynamic limitation to 4kW/s

- *Idle Fuel Cell power*: put the FC at minimum power to sustain the consumption of its BoP (compressor and auxiliaries' systems), in order to avoid its shutdown but consume as little fuel as possible. To do this, a moving average of current demand is taken into account; when this variable goes below a certain threshold, corresponding to the vehicle being idle for a long time, a current is commanded to the DC/DC converter boost that allows the FC to keep its system active but with the lower level of power as possible. In such operation, the FC is not really making a large contribution to recharging the battery, but is consuming minimal fuel to keep itself ON, even if with a lower efficiency.

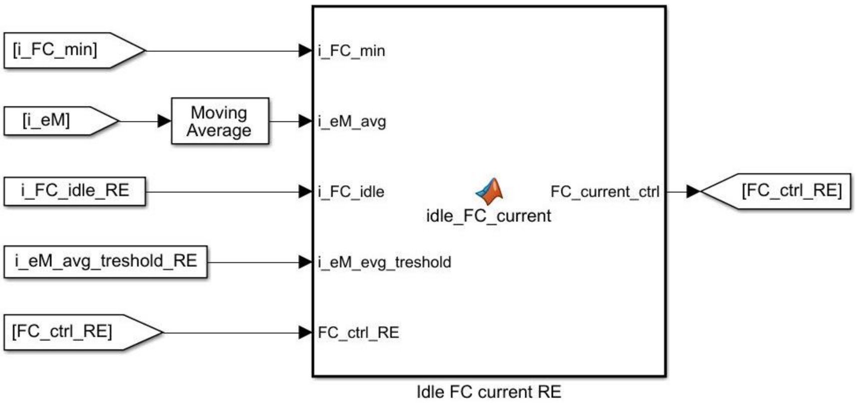

Figure 86: Simulink blocks for the application of the idle FC control current

The following Figure 87 shows a cycle where the FC is activated between minute 7 and minute 66. The power of the FC is always superior to that of the compressor, an element that consumes most of the power (between 3 and 5 kW), and from minute 41 the idle current is activated. In fact, from minute 39 the vehicle begins to idle (it will continue to idle until the end of the cycle), consequently the moving average power demand of the vehicle drops below a threshold which sets the FC control current at its idle value. With this power value, the FC is exactly able to support the power consumed by the compressor and BoP auxiliaries.

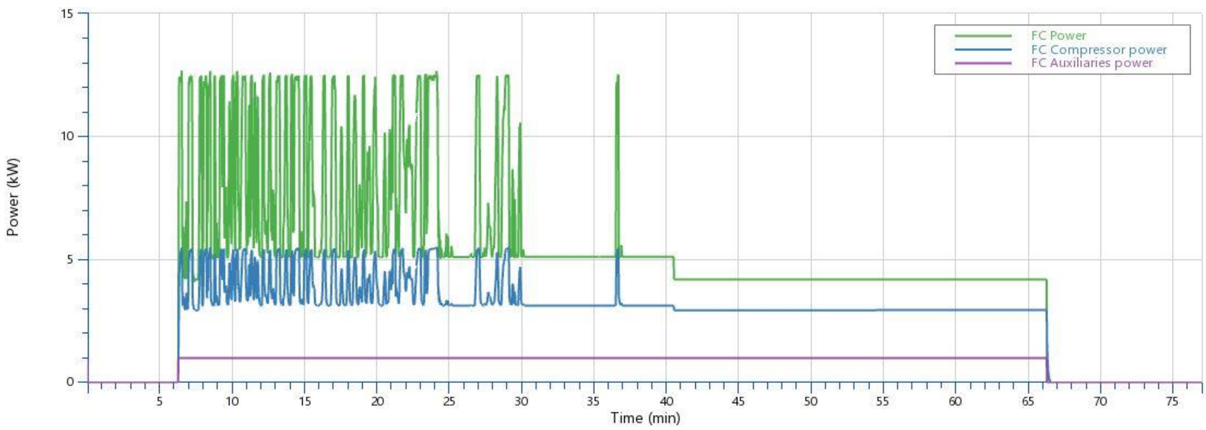

Figure 87: Operation of the idle FC power current in a cycle with extended idle time

- *Switching OFF the FC after a long operating time*: in order to prevent an excessive continuous utilization of the FC, considering that some driving cycles of the "Follow me" could last hours, a switch OFF dynamic for the hybrid unit is implemented. With this algorithm, is possible to cut the functioning of the FC in situation where it would continue working for an excessive time, trying to recharge the battery to a determined SOC level. This issue could be expected, for example, in the cases of SOC near to the $SOC_{FC\ ON}$ target in large idle portions of time, where the FC produced power to charge the battery would produce a small rate of charging, resulting in a continuous functioning even till the complete depleting of the fuel tank. These blocks are function of the SOC, considering the SOC value while entering the mode and evaluating the difference, when a threshold is reached, the command to change modality is executed.

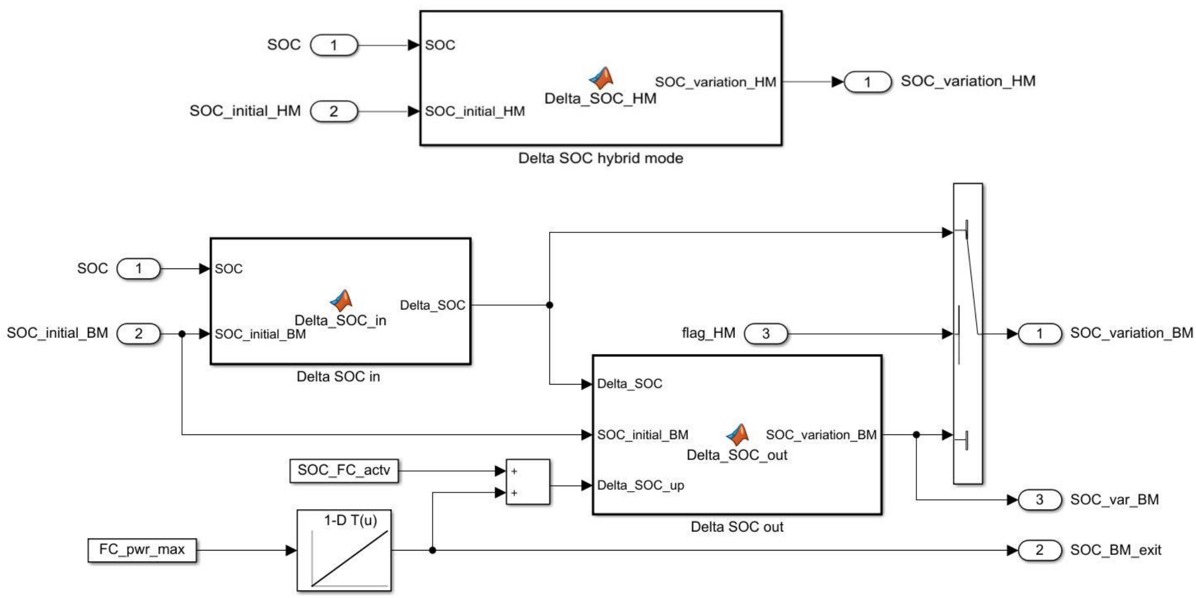

Figure 88: Simulink blocks for the computation of exit dynamic for HM (above) and BM (below)

Chapter 6: Results and Conclusions

In this chapter is done a summing up of what has been achieved so far in the previous chapter, as well as showing what will be done in future phases of the project.

The final presentation of the results obtained so far from simulations with the longitudinal dynamics model designed in the activity of the FCEV "Follow me" with the EMS tailor-made for its control is shown. A comparison with the results obtained with the same simulations carried out with a "Follow me" BEV is done in order to show the differences between the two architectures. Finally, a summary of the results achieved so far during the course of the activity is presented, as well as an analysis of the objectives achieved and the next steps of the project.

6.1. Longitudinal dynamic simulation results

6.1.1. "Follow me" FCEV results

By using the FEMS developed in MATLAB® Simulink with the longitudinal dynamics model of the P-ReFCEV implemented in AVL Cruise™ M, it was possible to obtain a series of results that iteratively made possible to understand whether or not what had been realised so far was appropriate. Based on the simulation results, in fact, it was possible to know whether the actual selected components, modelled by software, and the modifications to the FEMS were correct and adequate. All in all, what was realised at both the modelling and EMS level was satisfactory to enable the new hybrid "Follow me" to replicate the target performance defined on the basis of the actual driving cycles. Certainly, in the subsequent phases of the activity, especially in the real component test phase, parts of the FEMS will be modified according to the real features of the powertrain elements, but if will they comply with the theoretical data of the same, modifications should be minimal.

In order to provide an idea of what can be obtained through simulations, i.e. what can be obtained with longitudinal dynamics models combined with a purpose-built EMS in a FC hybrid vehicle, the graphs on the following pages are shown. They are related to the realisation of the cycle in Figure 81, in Chapter 5, which represents the average conduction cycle of 77 minutes with included the ON/OFF vehicle dynamic, with which is possible to obtain real indications of the possibility of the powertrain modelled up to now to recreate the starting "Follow me" performance in an average cycle of utilization. The initial SOC was supposed as 52%, thus around the threshold of FC activation, which is equal to 50%.

- Velocity profile with SOC trend and switch ON/OFF reference: it can be seen that the vehicle follows the reference speed profile very well, with some slight differences at high speeds or high accelerations, which are not relevant for still a satisfactory performance. The state of charge of the battery decreases over the cycle, with greater intensity during acceleration and higher speeds, remains constant at times when the vehicle and FC are OFF, while recharging at times of background battery charging.
- Power trend of powertrain, battery and FC: the overall powertrain demanded power is shown as a reference (is the sum of EM, LV auxiliaries and FC system power request) and is satisfied along the cycle by the battery and FC contributions, depending on the current modality. As far as the battery is concerned, the power for discharging and for recharging can be appreciated positively and negatively,

respectively. FC, being irreversible, only provides positive power, allowing the battery to provide less contribution on these parts and consequently discharge more slowly.

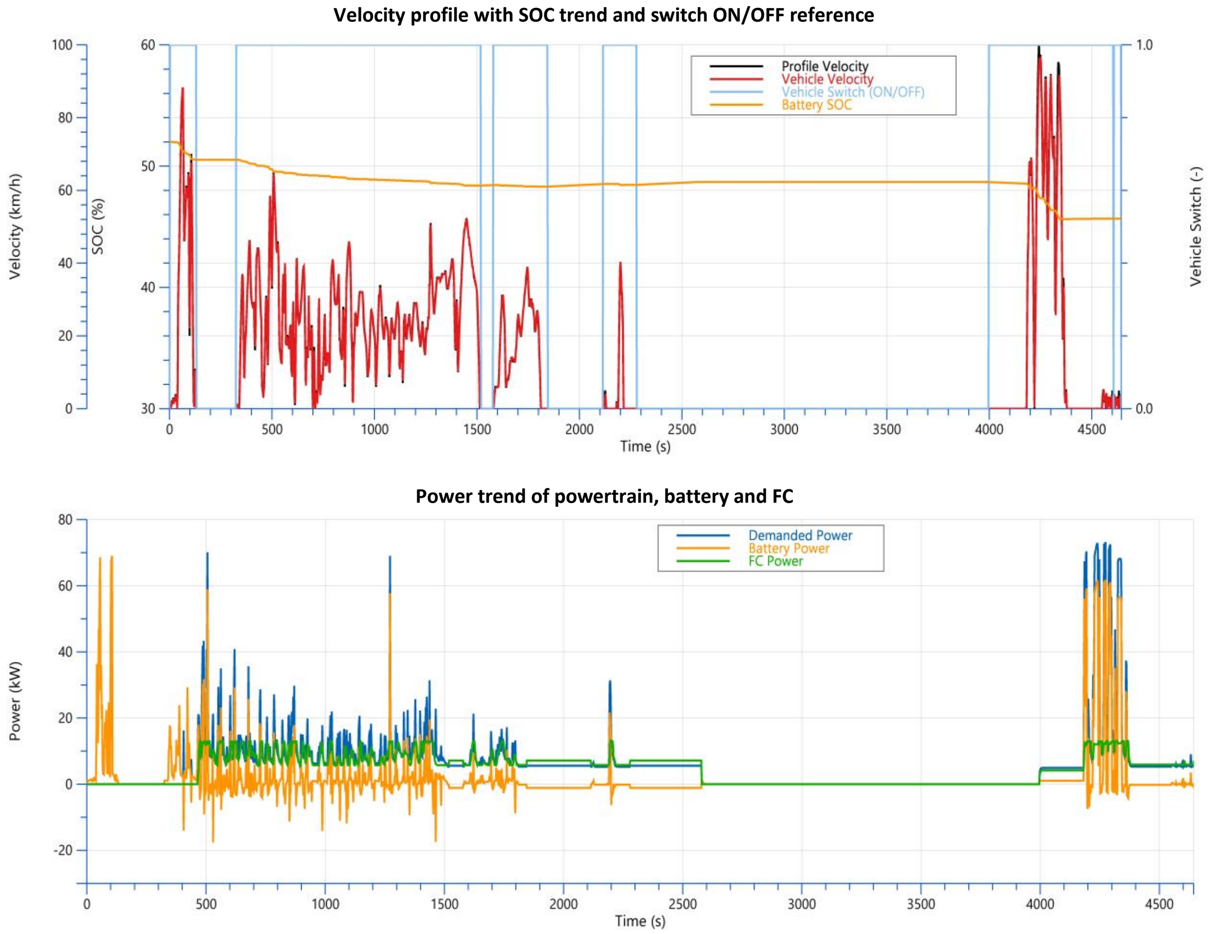

Figure 89: Charts 1 and 2 showing results obtained from the P-ReFCEV simulations model along an average real driving cycle with initial SOC of 52%

- Power trend of powertrain, battery and FC: the overall powertrain demanded power is shown as a reference (is the sum of EM, LV auxiliaries and FC system power request) and is satisfied along the cycle by the battery and FC contributions, depending on the current modality. As far as the battery is concerned, the power for discharging and for recharging can be appreciated positively and negatively, respectively. FC, being irreversible, only provides positive power, allowing the battery to provide less contribution on these parts and consequently discharge more slowly.
- Fuel Cell System components power trend: the PFC power trend of the FC can be observed, oscillating between minimum and maximum power values, as well as in the background battery charging phases. The same trend can be observed for the

compressor and BoP auxiliaries. The FC is always able to meet the power demand to keep the system active.

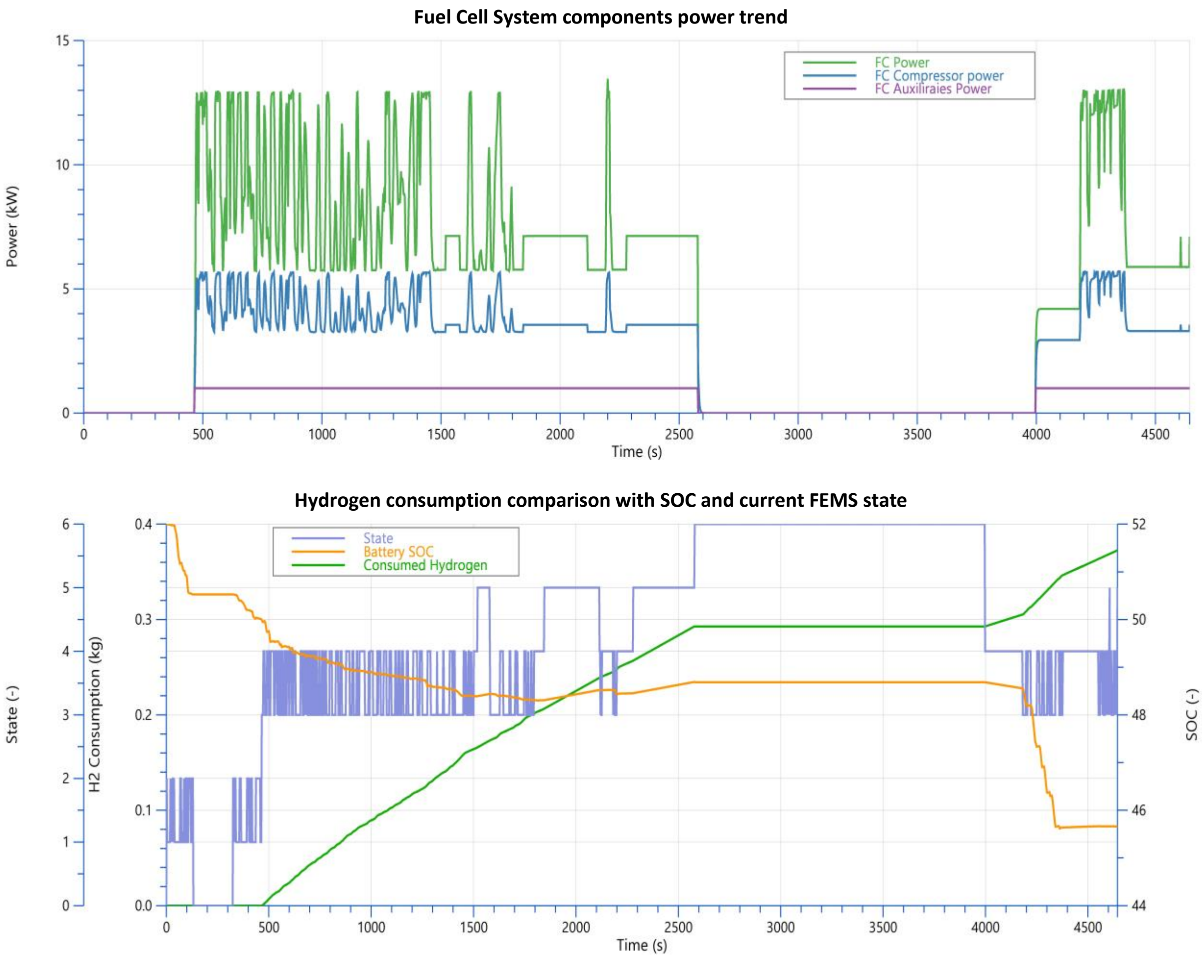

Figure 90: Charts 3 and 4 showing results obtained from the P-ReFCEV simulations model along an average real driving cycle with initial SOC of 52%

- Hydrogen consumption comparison with SOC and current FEMS state: in this graph it can appreciated the trend of battery charge and fuel consumption along the driving mission and the relative modes used, thanks to the variable "State". 0 is equivalent to vehicle OFF, as is 6 but with the difference that it is subsequent to background battery charging, which is 5. 1 and 2 are BTM and BCM respectively, while 3 and 4 are HTM and HRM respectively. The fuel consumption during the cycle is shown, which obviously increases at times when the FC is ON, with a final value of 30.47 min. For what regards the battery SOC, the initial value of 52% ends in a 45.66%, therefore with a discharge of 6.34 %.

- Produced energy trend and EM torque: the torque trend of the electric motor during the cycle is shown, positive when it is used to drive the vehicle, negative when it is used to create the current needed to recharge the battery. The accumulated output energy of the battery is shown, equal to 2.94 kWh. Wanting to extend this value to a possible complete day time, the average of 8.9h would result in the production (and thus a need for the battery) of 20.38 kWh, while for the maximum peak of 15.1h, would be produced 34.59 kWh.

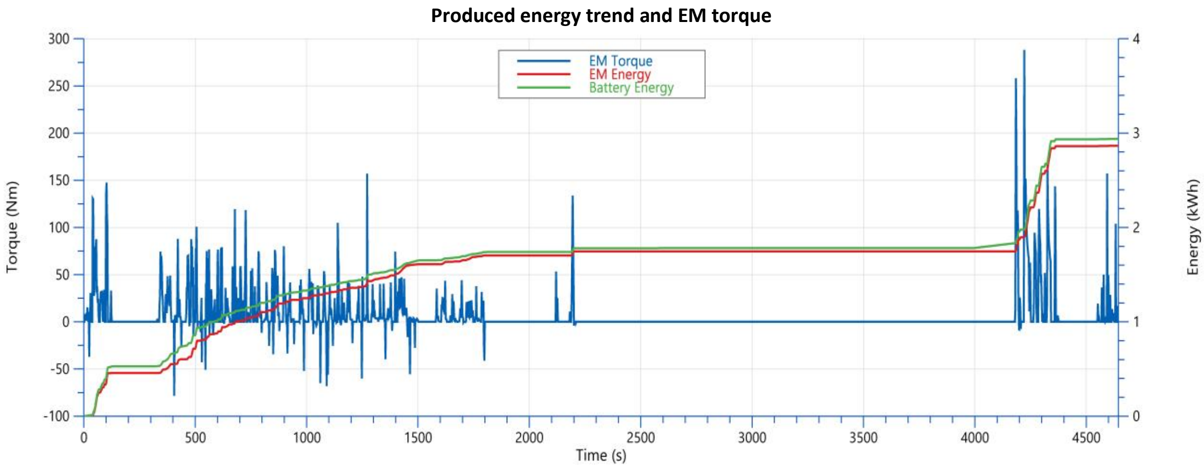

Figure 91: Charts 5 showing results obtained from the P-ReFCEV simulations model along an average real driving cycle with initial SOC of 52%

The following Table 16 shows all relevant numerical data obtained from the realization of the cycle, showing the possibilities that the new FCEV powertrain can hypothetically provide during an average driving cycle for a "Follow me" vehicle.

Data	Value	U.M.
Max vehicle velocity	96.61	km/h
Distance covered	14.48	km
Max demanded power	73.19	kW
Max EM torque traction/braking	288.31/-78.48	Nm
Max EM power traction/braking	54.47/-19.05	kW
Max EM current traction/braking	224.84/-50.81	A
Max EM speed	8126	rpm

EM consumed energy	2.87	kWh
Final SOC	45.66	%
Max battery power discharge/charge	69.05/-17.65	kW
Max battery current discharge/charge	229.69/-51.87	A
Max battery voltage	340.86	V
Min battery voltage	298.80	V
Battery consumed energy	2.94	kWh
Max FC power	13.47	kW
Min FC power	4.19	kW
Max FC compressor power	5.71	kW
Average FC power	7.85	kW
Max FC current	164.26	A
Average FC voltage	88.13	V
Max FC stack efficiency	68.24	%
Min FC stack efficiency	60.59	%
Average FC stack efficiency	65.14	%
Consumed hydrogen	0.37	kg
FC ON time	30.47	min

Table 16: Numerical results of FCEV “Follow me” average cycle simulation

Commenting briefly on these results, the "Follow me" FCEV is able to successfully complete the average drive cycle of the original vehicle. The electric motor proves to be perfectly sized to have some margin over the cycle requirements, never reaching its maximum torque, power or speed for velocities of about 100 km/h. The battery is the element that is certainly required to exert more effort with respect to its own characteristics, arriving close to maximum discharge current and power, while these values for charging are lower by being able to take advantage of the energy coming from the FC. Its charge decreases by 6.34% and uses 7.35% of its energy. This would imply that with such a battery, assuming a hydrogen tank of 4 or 5 kg, it would be possible to run such a cycle 13 times, for a total of 17 hours of use. Obviously, such a hydrogen capacity could hardly be installed on such a vehicle, but in any case, it should be able to operate for a full operative day without recharging/refueling even under the worst conditions. The FC can effectively help the battery both in traction and regeneration, allowing a higher range and being used 39.5% of the time and consuming 0.37 kg, operating at satisfactory efficiency in the range of 65%.

Further results obtained by simulation, running the driving cycle related to the average operating day, lasting 9h, with an initial state of charge of 70%, with included the ON/OFF vehicle dynamic, are presented below.

- FC power, SOC and hydrogen consumption trends: from that Figure 90, the CD-CS discharge profile typical of a hybrid vehicle can be appreciated. The FC power profile stays within the high efficiency window, following the cycle demand while charging the battery, consuming 1.74 kg of fuel and operating for 248.82 minutes, which is the 46% of the cycle time. The final SOC is 44.59%, a decrease of 24.44%.

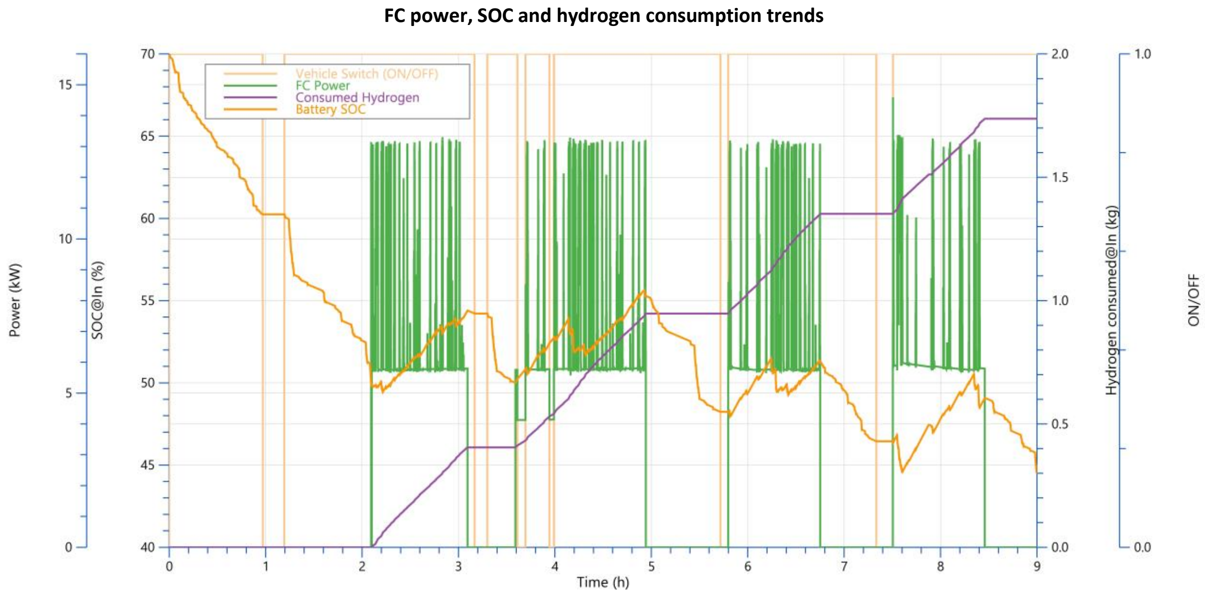

Figure 92: Charts 1 showing results obtained from the P-ReFCEV simulations model along an average real driving operative day cycle with initial SOC of 70%

- Velocity profile with SOC and battery energy trend: from that Figure 91, is possible to see the speed profile of this average operative day cycle, for its 129.66 km. The vehicle is able to follow the cycle in a satisfactory way, excluding some peaks of velocity (above 100 km/h) when is not available the power of the FC. The battery uses 20.81 kWh, which is the 52% of its capacity. This means that the vehicle should be able to travel 250 km with full battery capacity, with an estimated hydrogen consumption of 3.4 kg. This means that this FCEV "Follow me" vehicle should be able to travel the maximum expected 300 km range in one operating day with full use of a 4kg tank.

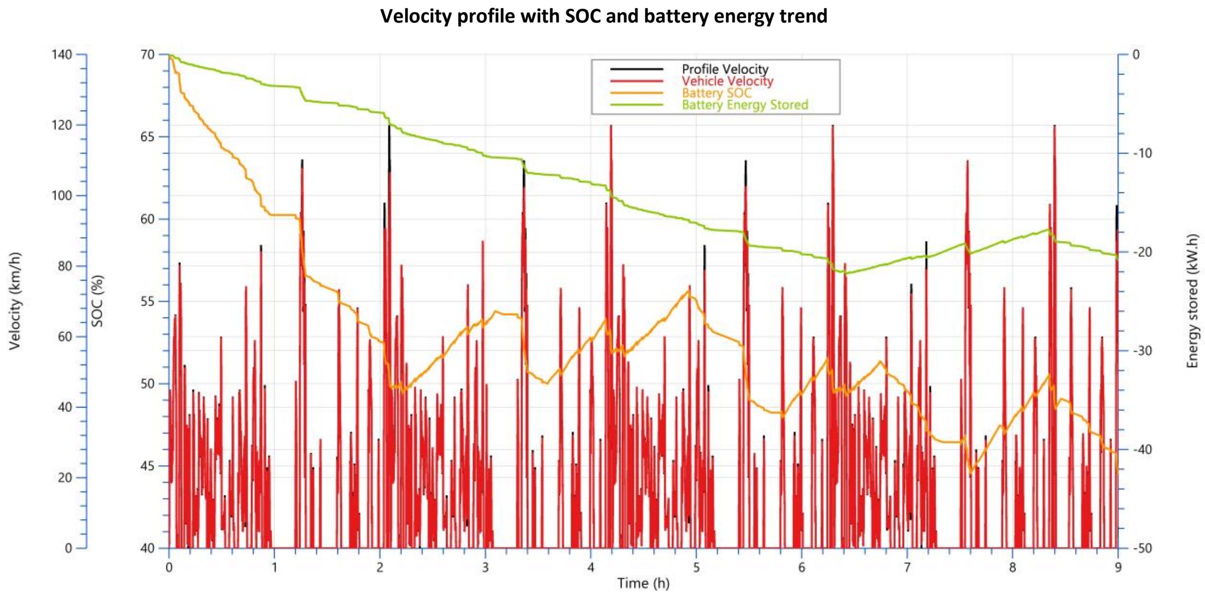

Figure 93: Charts 2 showing results obtained from the P-ReFCEV simulations model along an average real driving operative day cycle with initial SOC of 70%

6.1.2. "Follow me" BEV results

As analysed in Chapter 2, the currently most popular solution for the electrification of the "Follow me" is the BEV, as it is commercially more widespread and economical. Consequently, it is interesting to make a comparison between the powertrain with FC, the results of which were shown in the previous section, and a full electric powertrain with the battery as the sole source of energy and power. This is possible because the same components that make up the FCEV powertrain can be repurposed as BEV architecture, since the same battery and electric motor can provide the power and energy required to satisfactorily complete the average cycle shown above, while keep the same other elements. The model used is the longitudinal dynamic model created in Chapter 4, representing a BEV powertrain, in which are used the 120 kW and 500 Nm Cascadia iM-225W motor and the Leclanché INT-39 Energy LV battery, capable of providing a capacity of 40 kWh and power limits of 80 kW. The HV bus voltage is kept identical, dictated by the battery voltage (330 V nominal).

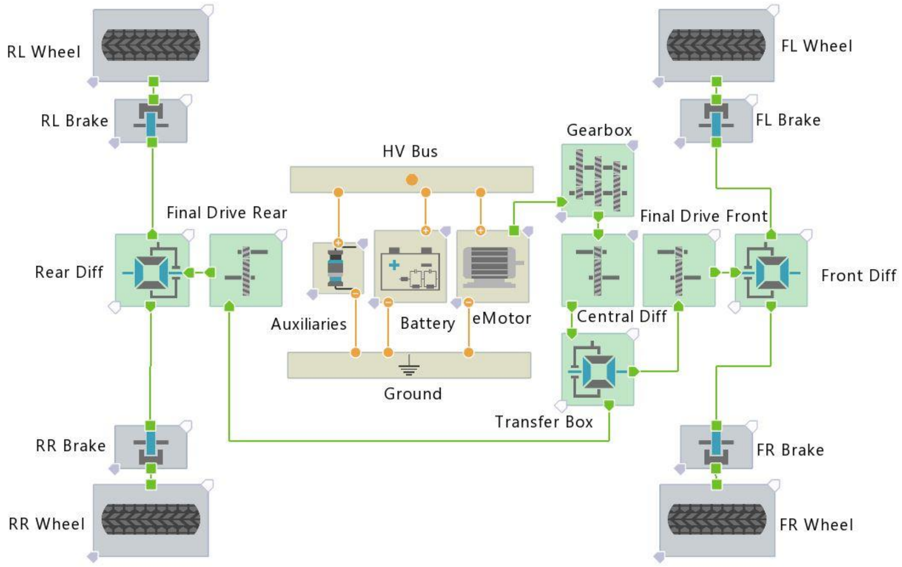

Figure 94: AVL Cruise™ M model to simulate the behavior of the BEV "Follow me" vehicle

In order to establish the comparison, the same results obtained in the previous paragraph are analysed in the same way. The graphs on the following pages are shown, related to the realisation of the same average cycle in Figure 81, in Chapter 5, of 77 minutes with included the ON/OFF vehicle dynamic and same initial SOC was supposed as 52%.

- Velocity profile with SOC trend and switch ON/OFF reference: the vehicle follows the reference speed profile very well in the same way as what obtained with the FCEV. The state of charge of the battery decreases over the cycle with greater intensity, in fact the final SOC is 41.50%, which represent a decrease of 4.16% compared to what can be achieved with the RE hybrid powertrain.
- Power trend of powertrain, and battery: the overall powertrain demanded power is shown as a reference (is the sum of EM and LV auxiliaries power request) and is fully satisfied along the cycle by the battery. As far as the battery is concerned, the power for discharging and for recharging can be appreciated positively and negatively, respectively. The battery, although within its own charging and discharging limits, must reach power peaks in traction much more frequently and in recharging more frequently and with greater intensity, about 250% more. This is because FC power is not present, which when active allows battery not to supply 100% of the demand, especially during regeneration.

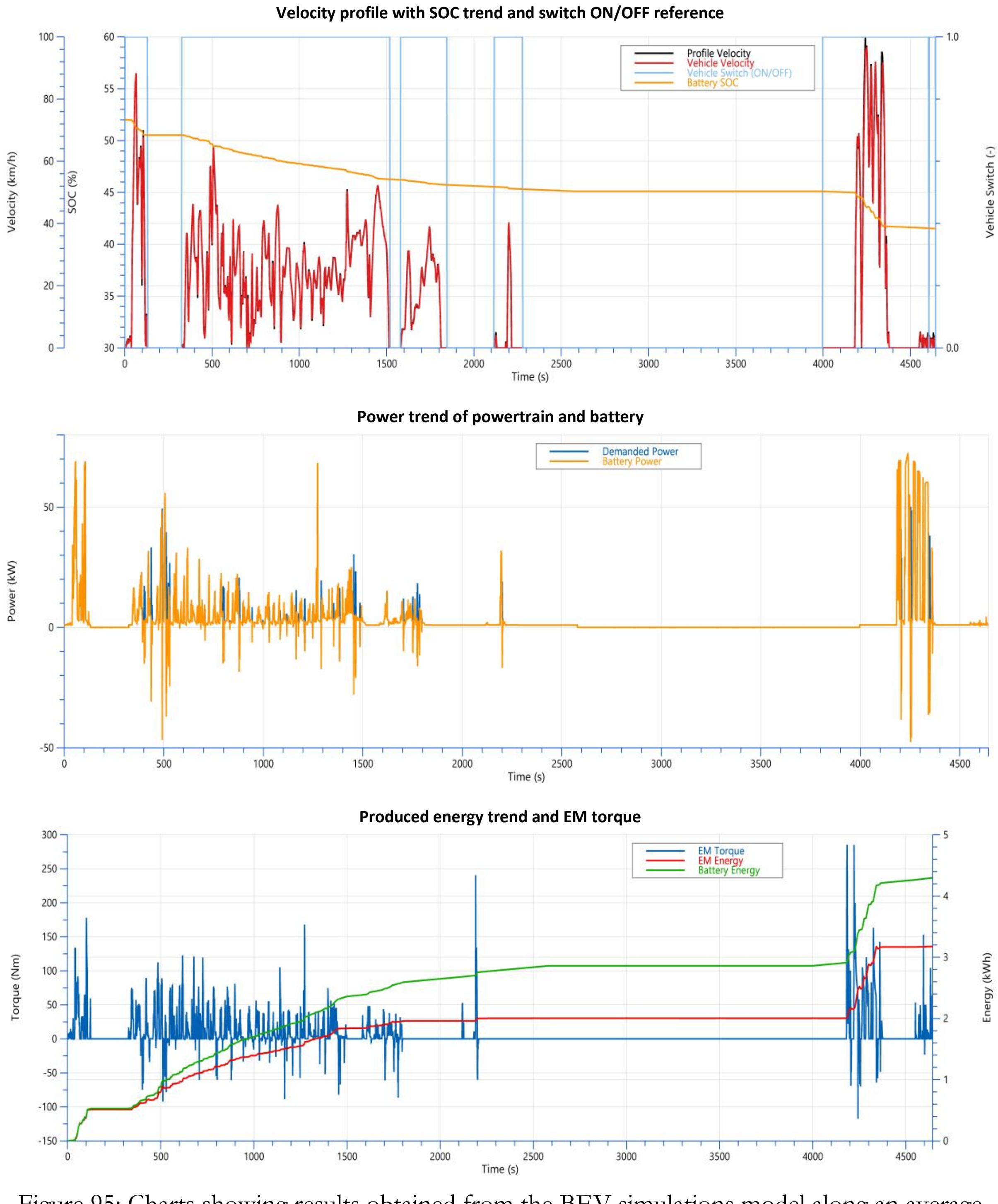

Figure 95: Charts showing results obtained from the BEV simulations model along an average real driving cycle with initial SOC of 52%

- Produced energy trend and EM torque: the torque trend of the electric motor during the cycle is shown, with the accumulated output energy of the battery, equal to 4.29 kWh, compared to the EM ones. As can be seen, the difference between the two is higher in this case, since the battery is the only source of energy which must satisfy the whole demand of the vehicle. As what was done for the FCEV, wanting to extend this value to a possible complete day time, the average of 8.9h would result in the production (and thus a need for the battery) of 29.75 kWh, while for the maximum peak of 15.1h, would be produced 50.48 kWh. This means that 46% more energy is used to perform the same cycle with the same performance.

As done before, the following Table 17 shows all relevant numerical data obtained from the realization of the cycle, showing the possibilities that the BEV powertrain can hypothetically provide and its differences with the FCEV during an average driving cycle for a "Follow me" vehicle.

Data	Value	U.M.	Difference
Max vehicle velocity	96.61	km/h	-
Distance covered	14.49	km	-
Max demanded power	72.09	kW	-
Max EM torque traction/braking	285.34/-117.41	Nm	-/1.6 times
Max EM power traction/braking	59.62/-55.39	kW	-/2.9 times
Max EM current traction/braking	228.44/-141.05	A	-/2.8 times
Max EM speed	8182	rpm	-
EM consumed energy	3.18	kWh	+11 %
Final SOC	41.50	%	+9 %
Max battery power discharge/charge	72.09/-47.67	kW	-/2.7 times
Max battery current discharge/charge	233.20/-137.51	A	-/2.7 times
Max battery voltage	348.68	V	-
Min battery voltage	298.57	V	-
Battery consumed energy	4.29	kWh	+46 %

Table 17: Numerical results of BEV “Follow me” average cycle simulation

What is immediately noticeable is how both the EM and the battery have to be used more in regeneration (and thus charging) than in the case of FCEV. This is due to the fact that, without the FC, the charging current for the battery must come from the motor itself during braking. Otherwise the performance is the same, with obvious higher energy and SOC consumption: its charge decreases by 10.5% and uses 10.9% of its energy. This would imply that with such a battery it would be possible to run such an average cycle 9 times, for a total of 11.5 hours of use, which is only the 60% of what can be done with the FCEV. This means that this type of BEV vehicle will not be capable of operate a full operative day in any condition, with the risk of not be available in some situations, with long recharging time needed to go back to the runaways. In fact, considering a FCEV, the time spent to putting the vehicle back to work, considering the faster recharging of hydrogen fuel, would not lead to such a major problem of non-availability.

In the same way as with the FCEV, Further results obtained by simulation, running the driving cycle related to the average operating day, lasting 9h, with an initial state of charge of 70%, with included the ON/OFF vehicle dynamic, are presented below.

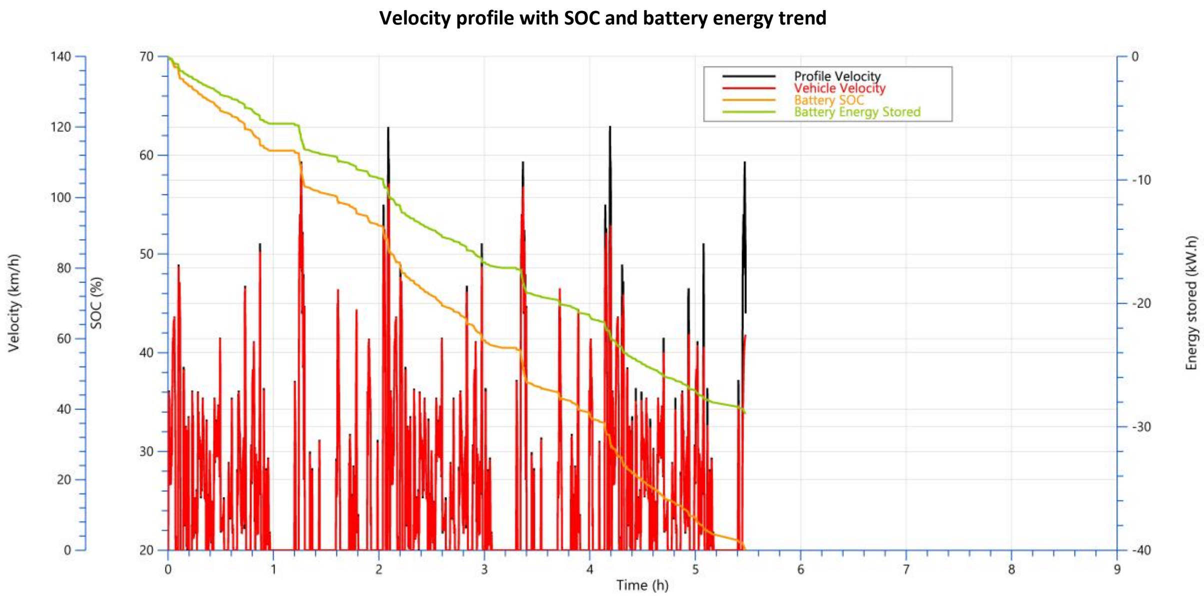

Figure 96: Charts showing results obtained from the BEV simulations model along an average real driving operative day cycle with initial SOC of 70%

From that Figure 94, is possible to see the speed profile of this average operative day cycle, for its 79.88 km, which is the 66% of the FCEV case. The simulation is settled to stop whenever the lower SOC limit of 20% was reached, threshold to not to pass in order to avoid the damaging of the battery. The vehicle is able to follow the cycle in a satisfactory way, excluding some peaks of velocity (above 100 km/h), but only for 5.48 hours, starting to losing performance also before 5 hours of operations, with the EMS imposing limitations in current capacity of the battery, to preserve its operation. The battery uses 28.96 kWh, which is the 72% of its capacity, a +20% respect to the FCEV case. This means that the vehicle should be able to travel 110 km with full battery capacity, less than 1/2 of the hybrid case. This means that this BEV "Follow me" vehicle should be able to travel only the range for a short operative day, with the same problem presented above: the risk of not be available in some situations, with long recharging time needed to go back to the runaways.

6.1.3. "Follow me" FCEV and BEV comparison

Thanks to the results obtained and the analysis of the data obtained, a more in-depth comparison of the two solutions can be established. The hypothesis was to use the same vehicle with a different powertrain, for a BEV and a FCEV. Both solutions are able to perform satisfactorily the operations of a "Follow me", completing the driving missions, acceleration and slope cycles. However, they have several differences and although this comparison is purely theoretical and approximate, it can provide an idea of what are the characteristics, advantages and disadvantages of the two solutions. The following Figure 95 shows the trend of the battery SOC for the two, achieving the same 77-minute average cycle of the original "Follow me". As commented above, the difference is near 9%, which can be reflected in reaching, in an average operative day, from 60 to 70 % of the distance achievable with the FCEV solution, depending on the availability of hydrogen on board.

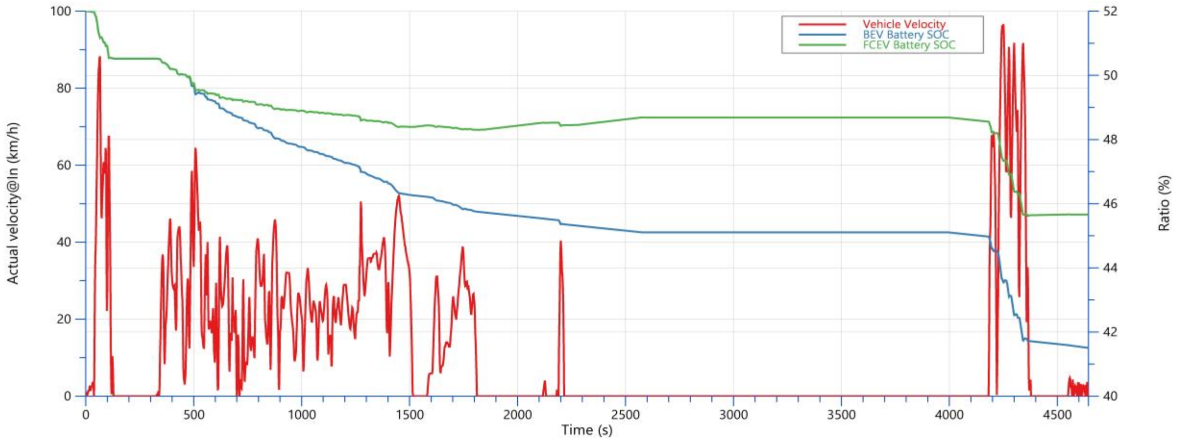

Figure 97: Comparison between BEV and FCEV "Follow me" SOC trend for an average driving cycle of 77 minutes and an initial SOC of 52%

Figure 96 below shows the same but for the case of an average operating day cycle, showing the advantage that FC can bring to the vehicle's autonomy. The BEV is only able to cover 66% of the cycle, stopping when the 20% SOC is reached. From the figure is possible to perfectly distinguish the two battery discharge profiles: CD for the BEV case, and CD-CS (from SOC = 50% onwards) for the FCEV one, in a window of nearly 12% SOC.

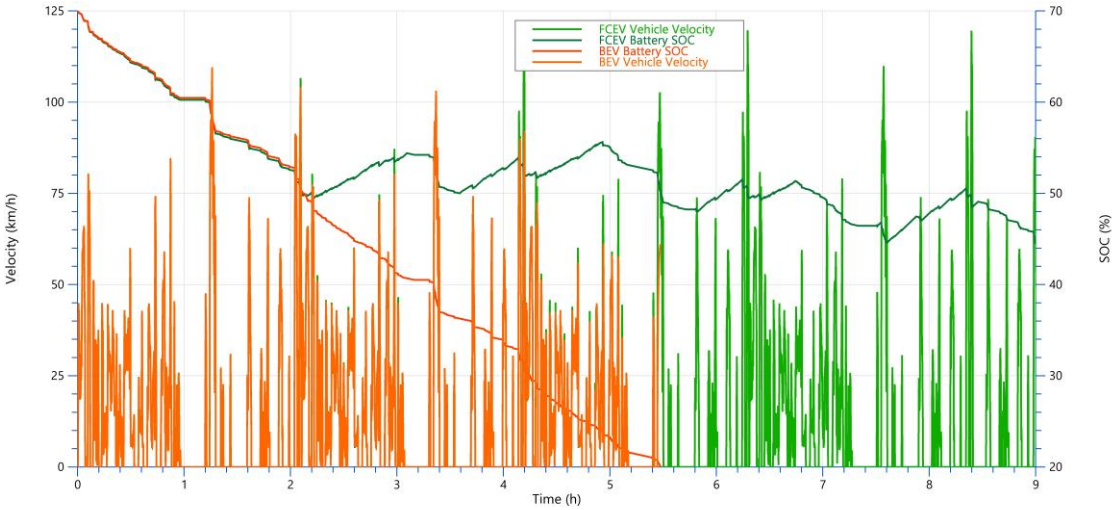

Figure 98: Comparison between BEV and FCEV "Follow me" SOC trend for an average operative day cycle of 9h and an initial SOC of 70%

In addition to the results of longitudinal dynamic simulations, other comparations can be done. For what regards the power demand:

- BEV: battery must satisfy the whole power demand of the cycle, respecting its limitation for discharging and charging power and currents. In this case, talking of 80 kW and 250 A, both for charge and discharge, for driving mission with higher peak powers than the average value the battery could be insufficient. This would imply to have a "Follow me" with more limited performance, or better to find another solution for the battery, with higher power limits, increasing the cost.
- FCEV: fuel cell can help the battery peak power limitations, reaching a 95 kW of overall installed power, in moments when it is ON. This means that this "Follow me" could have better performance in certain conditions, and also the battery and the EM could be preserved thank to its utilization at lower performance, increasing life expectations and reduce maintenance.

For what regards the architecture and management:

- BEV: the architecture is simpler, less components are needed, as well the complexity of the EMS, which is less relevant with respect to ones used for a hybrid vehicle. The only two part which must be implemented are the regeneration of the battery controlling the EM and the control of overcharge/discharge currents basing on SOC and temperature.
- FCEV: the architecture is more complex, with the addition of the FC system, its BoP and the monodirectional DC/DC converter. This implies a higher management of the available space inside the vehicle in design phase, as well the design of electrical connections. In the same way, the EMS for this kind of solution is extremely more complex and crucial, not only for the fuel cell itself but also for the management of EM and battery.

For what regards the fuel cost:

- BEV: in general, charging an EV can cost between 0.10 and 0.20€ per kWh, depending on the area. Therefore, basing on data provided from the results obtained with the average cycle, for the BEV "Follow me" with the 40 kWh battery, the cost of a full charge could be 4 to 8€. For an average driving mission, the cost would be 0.4 to 0.8€, while for an average operational day, will be 2.9 to 5.7€.
- FCEV: the cost of filling up with hydrogen is higher by now. Currently, the price of hydrogen varies greatly depending on the area and can be between 10 and 20€ per kg. Therefore, considering the same 40 kWh battery, the full price of a complete refilling of all the installed energy onboard of the FCEV will be between 14 to 28€, with a 1 kg of H_2 tank, increasing of 70% for each additional kg of H_2. For an average driving mission, the hydrogen cost is 5.5 to 11€, thus 5.8 to 11.5€ for the whole vehicle energy. For an average operational day, the hydrogen cost is 17.4 to 34.8€, thus 19.5 to 39€ for the whole vehicle energy. To fill the vehicle with all the installed energy, between battery and FC, therefore are need between 32.5 to 65€. In any case, the price of this solution is similar to the cost of refuelling of conventional fuel used in combustion engines, taking into account the idea to reach the same distance.

For what regards the range:

- BEV: along the average cycle, with a travelled distance of 14.49 km, were consumed 4.29 kWh, therefore the expected range is at least 135 km. Wanting to express a value of convenience for this solution, this "Follow me" could be addressed to a consumption of 0.02 to 0.04 €/km. This would imply to have a "Follow me" with a lower cost for energy refilling but with more limited range or better to find another solution for the battery, with higher capacity, increasing the cost of this component and the weight of the vehicle.

- FCEV: along the average cycle, with the same distance travelled, were consumed 2.9 kWh, therefore the expected range is at least 250 km, which is the 1.8 times higher with respect to the other solution. Adding the cost for the hydrogen fuel, this "Follow me" could be addressed to a consumption of 0.13 to 0.26 €/km, which is 6.5 times higher with respect the BEV case. These values are also smaller or similar to what can be found in conventional combustion engine solution, considering a low price hydrogen refuelling this solution is beneficial with respect the original "Follow me".

6.2. Resume of the activity and achieved goals

6.2.1. Completed objectives for each chapter

The work carried out during the initial 6 months of the “GreenH2” project allowed us to proceed with the complete product specification of the powertrain for an FCEV for airport use with a “Follow me” function, including a detailed list of its requirements, the dimensioning of the elements that make up its traction system and reliable results from simulation software, such as AVL Cruise™ M and MATLAB® Simulink. Specifically, the following objectives were achieved along the five chapters discussed in the thesis. The main results obtained will be now presented, otherwise for an in-depth analysis, is necessary to refer to the information in the relative chapter.

- **Chapter 1 & 2**: by conducting a detailed literature and market analysis in Chapters 1 and 2, it was possible to derive all the information necessary to define the profile of a “Follow me” vehicle and of a FCEV. Their characteristics, their usual and hypothetical context of use, their local and global environmental impacts and their current and actual solutions were outlined. To summarize the main considerations, it can be assumed that the use of an FCEV, in a future when this type of vehicle will be more efficient and widespread, as will be the infrastructure to allow easy hydrogen refueling, can be a solution to reduce the environmental implications of the airport environment, together with the use of conventional electric vehicles. These benefits can be achieved both locally and globally by transforming a vehicle that is used for many parts of its operational time in an extremely inefficient and polluting manner, into a vehicle using a 0-emission fuel at TTW level and a low impact fuel (although currently only in the best of assumptions and production processes) at WTT level. The direction of decarbonization in recent years at a global level is evident and very rapid, due to the large number of initiatives and projects such as the one concerning this activity. It is necessary to continue with the study on hydrogen powertrains, collection of information and development of hydrogen technologies to make FC solutions from simple and limited experiments used in a few airports around the world into solid, economical, viable and reliable solutions.
- **Chapter 3**: the large amount of powertrain data made available by the onboard instrumentation of a real “Follow me” GSE vehicle operating at the Madrid-Barajas airport was analysed in various ways, with the aim of relating each data collected to

defined characteristics, whether of actual use, driving cycles or energy requirements. The data obtained during the 30 days of acquisition was effectively processed both for individual driving missions and united into operational days, in order to verify what the actual utilisation of the vehicle had been at the airport, whether the hypotheses outlined up to that point were correct, and to enable the definition of objectives for subsequent phases. Already in the data analysis phase, thanks to previous engineering experience and the study of literature and the market, it was possible from the outset to direct the focus of the activity towards a more defined FCEV architecture, with more or less hypothetical elements, awaiting however the various confirmations only with subsequent analyses and simulations, proper to Chapter 4. As presented in the same chapter, wanting to create a general summary of the results obtained through the analysis of the data available from the real "Follow me" vehicle, both with regard to a single driving mission and an entire operational day, the following Table 18 is created. It summarizes and evaluates which characteristics are required and provided by the airport vehicle under examination and thus which will be those to be replicated in the FCEV.

Feature	**Evaluation**
Time of utilization	Average operating time of 80’ for driving mission and 9h for an operative day with strong variability (delta from 8% to 300%), prevalent (55%) idle use with respect to motion
Distance covered	High distances travelled, medium of 117 km with great variability according to needs (delta from 12% to 218%)
Altitude variation	Use of the vehicle on almost flat routes with very limited gradients
Maximum vehicle speed	Average of 80 km/h, moderately high speed (100 km/h) reached in 1/6 of the driving mission, while real peaks (> 120 km/) only less than 5% of cases
Average vehicle speed	Low average speed (30 km/h), almost similar to what expected in urban use
Maximum power needed	High average power of 106 kW, peak values (> 150 kW) achieved in 1/3 of the cases
Average power needed	Low average power for vehicle movement, near 13 kW, with peaks of 40 kW, because of the low average vehicle speed

Average energy needed	High amount of energy required each day (average of 44 kWh), equivalent to the whole capacity of a standard EVs battery
Fuel consumption	High fuel consumption (average of < 10 km/l), higher than the vehicle would have in an urban use and with respect to what shown in its technical sheet
Energy consumption	High energy consumption (average of 0.53 kWh/km), higher than what a normal EV would have, even in the worst energy-demanding cases

Table 18: Summary of results obtained through the analysis of the data available from the powertrain of the real "Follow me" vehicle in Chapter 3

- **Chapter 4**: Starting from what was obtained in the data analysis, it was possible to define a list of precise requirements for the new hybrid propulsion system. The line to be followed was to ensure that, by using a prototype vehicle at the INSIA research centre, a conventional hybrid with a heat engine, combined with the new components to make it FCEV, replacing those currently present, it would be possible to guarantee the same performance as the original vehicle. In some of them was possible, at least in theory, while in others (maximum speed, maximum power, autonomy) obvious compromises had to be made, considering time, engineering and budget limitations. Wanting to create a general summary of the FCEV expected requirements, obtained through the data analysis, theoretical evaluation, experience and market research, the following Table 19 was created:

Component	Requirement
High voltage battery	Li-ion battery with expected nominal 400 VDC (in the range 250 – 500 Vdc) with an energy in the order of 30 – 50 kWh
High voltage DC bus	Expected nominal 400 Vdc (in the range 250 – 500 Vdc)
Electric motor	Synchronous with permanent magnets, expected peak power in the range 100 – 120 kW, maximum torque in the range 300 – 500 Nm, maximum rpm in the range 8000 - 10000
DC/AC power inverter	Possibility to deal with 400 Vdc of the HV bus line and with the peak power of the EM

DC/DC boost converter	Possibility to increase the output voltage of FC to the 400 V of the DC bus
On-board charger	Possibility to deal with 400 Vdc of the HV bus line
Fuel Cell system	Expected output power in the range 10 – 20 kW
Hydrogen tank	Non-refillable and theoretical capacity of at least 1 kg
Vehicle architecture	Very likely Range Extender, very unlikely Load Follower

Table 19: Summary of "Follow me" FCEV powertrain expected requirements in Chapter 4

The most important part of this chapter was the creation, adaptation and use of models for simulations of longitudinal dynamics with AVL Cruise™ M, in an iterative and recursive manner. With these models, it was possible to obtain the above-mentioned requirements and verify that they were sufficient. In addition, the simulations made it possible to find out how the dimensioned components worked with each other, applied to standardised real driving cycles in order to meet certain operating cycles. This chapter achieved the creation of a BEV model on the architecture of the prototype vehicle in INSIA, shown below:

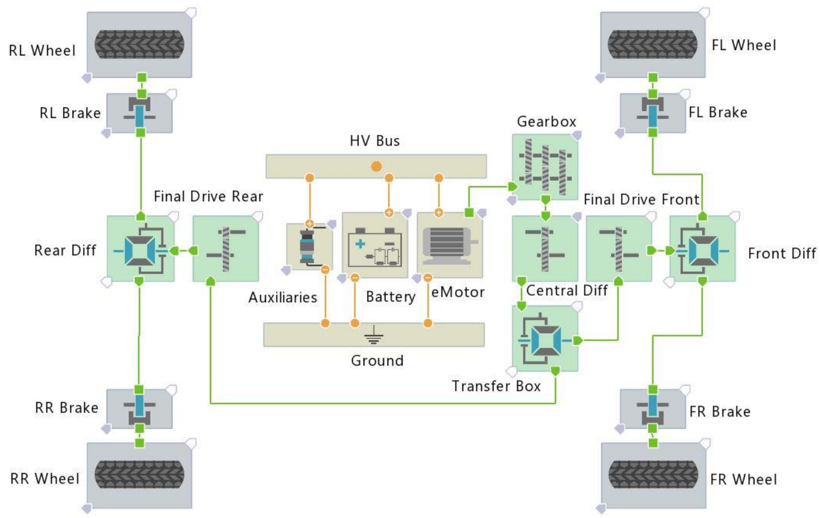

Figure 99: Vehicle model in AVL Cruise™ M obtained in the Chapter 4 to simulate the longitudinal behavior

Finally, the previously dimensioned components were selected from the market, through careful market analysis and a lengthy process of contacting various providers, for their purchase and final future use within the FCEV. The final vehicle structure (called P-ReFCEV), as well as the selected components, are shown below:

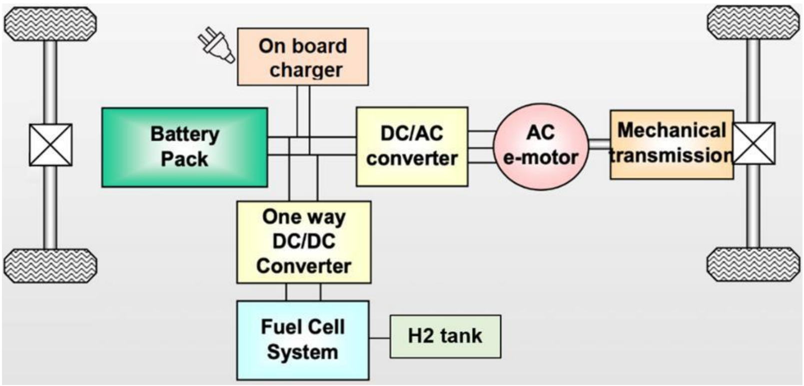

Figure 100: Representative diagram of the FCEV architecture with its main elements obtained at the end of the Chapter 4

Component	**Selection**	**Technical features**
High voltage battery	Leclanché INT-39 Energy LV	Module configuration: 10s2p Pack nominal voltage: 330 VDC Pack nominal capacity: 120 Ah Nominal energy: 40 kWh Maximum discharge/charge current: 200 A
Electric motor	Cascadia HVH250	Peak toque: 500 Nm Continuous torque: 275 Nm Peak power: 210 kW (@700 VDC) Continuous power: 75 kW Maximum speed: 12000 rpm Voltage operating range: 300 – 700 VDC
DC/AC power inverter	Cascadia CM200-DX	Operating voltage: 50-480 VDC Maximum EM current continuous: 300 A Output peak power: 225 kW DC overvoltage trip: 500 VDC
DC/DC boost converter	Horizon VL DC-DC converter	Input voltage: 35 – 120 V Output voltage: 200 – 400 V

		Rated power: 4 – 30 kW Efficiency: 98%
Fuel Cell system	Horizon VL15kW	Cells number: 115 Rated power: 15 kW Output voltage: 80 VDC Operating temperature: 60 – 70 °C Operating pressure: 1 bar
Hydrogen tank	Air Liquide Alphagaz 1	Operating pressure: 200 bar Volume size: 1.8 – 2.8 – 10 m^2 Mass of hydrogen: 0.163 – 0.901 kg

Table 20: Summary of “Follow me” FCEV powertrain final selected components

- **Chapter 5**: In the most elaborate phase of the activity, an energy management strategy (called FEMS) was created and refined to control the powertrain of the FCEV that had been dimensioned and modelled up to that point. The selected strategy for this vehicle was a PFC, with higher complexity with respect to a TC, but more interesting for control algorithm and research. This EMS made it possible to achieve the results shown in the previous paragraph, meeting the performance requirements of the original “Follow me” vehicle. The following image shows the simulation platform in AVL Cruise™ M where is possible to analyze in real time the functioning of the longitudinal model and EMS.

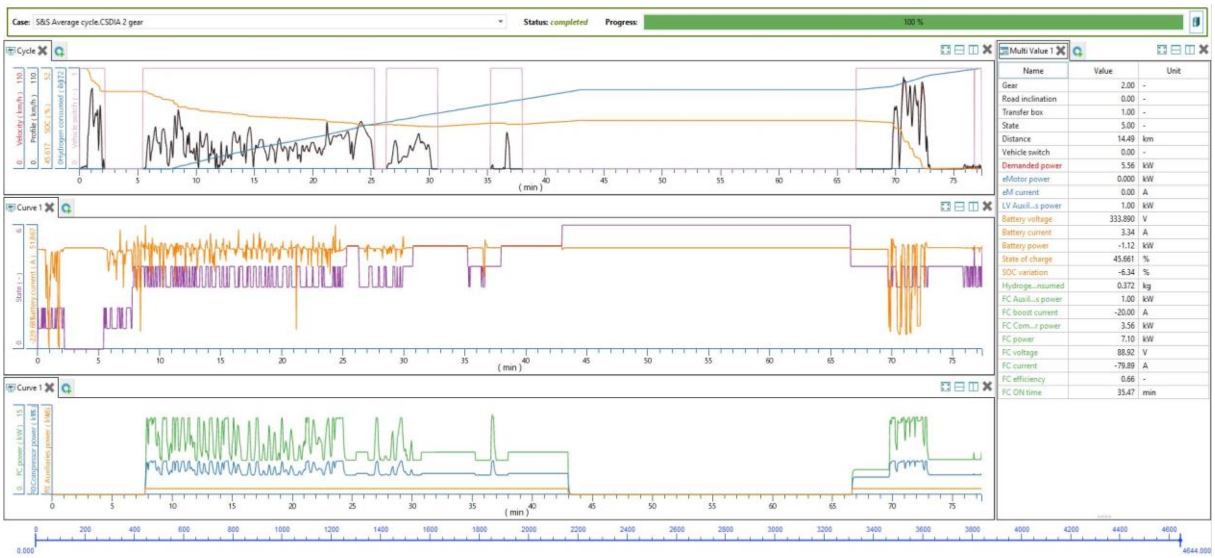

Figure 101: Example of the simulation process panel developed in as AVL Cruise™ M

This activity required a great deal of time, in comparison to the other chapters, as it was an iteratively complex process, in which all the results obtained up to before the creation of the EMS had to be joined together and adjusted several times as the control strategy was developed, and new algorithms added. Having to manage the flows of energy, power, current and voltage of various elements between them, it was possible to deepen our knowledge of the function of the various components that make up the powertrain of an FCEV. This chapter achieved the creation of an FCEV model on the architecture of the prototype vehicle in INSIA, shown below:

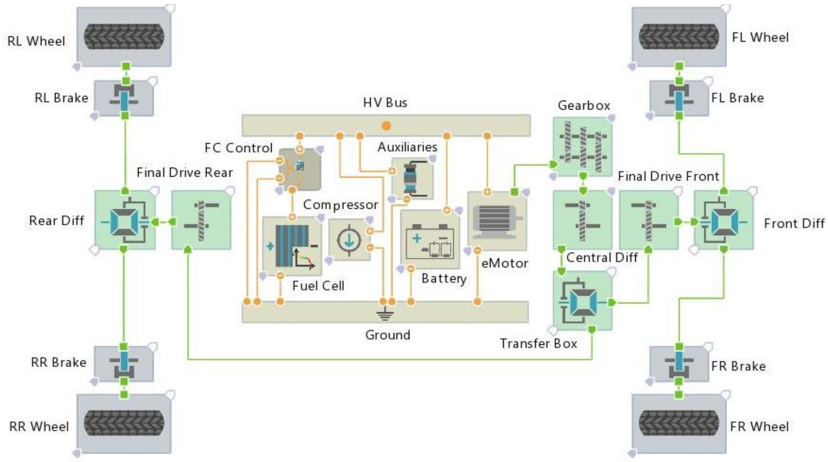

Figure 102: FCEV Vehicle model used in AVL Cruise™ M in chapter 5

In addition, the creation of an EMS made it possible to learn how to use the Stateflow functionality of MATLAB® Simulink for control logic that can be implemented within the ECU of a vehicle. In addition, having to manage the operation of a critical element such as a fuel cell, due to its disadvantages (slow dynamics, limited power, fuel consumption, degradation as a function of use), a long series of algorithms for safeguarding its state were learnt and added to the EMS. Specifically, following the control strategy in this thesis, when dealing with a hybrid vehicle with FC, in addition to the classical dynamics to be considered more related to an electric drive system, the following aspects should always be considered:

- The power window of use of a FC is very limited due to the need to work only in the high efficiency area, so coupling it with a DC-DC boost/buck converter is essential for controlling its current and voltage.
- It is necessary to extend the temporal utilisation of FC as far as possible within the relevant driving mission, inside certain limits, since it is disadvantageous to

use recurring ON/OFF dynamics due to the degradation of FC and the required start-up energy.

- The dynamics in FC power generation must be kept under control from the point of view of certain kW/s generation thresholds, to avoid reactant (hydrogen and air) starvation.
- In addition to the control of battery overcharge/discharge currents (and powers), which can normally be implemented within an electrified vehicle strategy, it must be considered that the FC, at certain times in the driving mission, also delivers current to the battery without it being spent on traction. Consequently, the EMS must be able to predict that the battery will always be able to accept the surplus current from the FC, in addition to the braking regeneration one. Moreover, the battery must also be able to provide current for sustaining the start-up dynamics of the fuel cell, which require power in the order of kW and a determined capability in C-rate terms.
- The FC is self-sustaining during its operation: a portion of the power produced is used to power its BoP. This implies providing a dynamic in an EMS whereby the FC never has to produce less than the power required for its self-support, resulting in a higher fuel consumption but a shorter life and performance degradation.
- It is necessary to implement logics in the EMS that allow, on the one hand, not activating the FC for driving missions of very limited duration or energy demand (parking, switching ON without movement, etc.), as well as preventing it from being switched OFF shortly after its activation, with logics such as background battery charging.

- **Chapter 6**: All the previous realized phases find their union and verification in dynamic simulations whose results are presented in this Chapter. The "Follow me" with the new propulsion system proves to be adequate to operate in satisfactory way all the conduction cycles of the original vehicle, both for single driving missions and operative days, as well as acceleration and grade tests. For what regards convenience with respect the conventional vehicle, thanks to the new hybrid powertrain is possible to have these advantages:
  - Same performance within the runaways.

- Net zero TTW emissions.
- Highly reduced noise pollution.
- Daily operation without energy recharging problems, even in more demanding conditions from the point of view of covered distance and time.
- Vehicle functioning remains unchanged from the point of view of the operator.
- Weight of the vehicle remains the same.
- Vehicle operating with a higher overall efficiency.
- As far as the price of filling up with hydrogen is concerned, the solution is beneficial compared to a diesel or petrol combustion engine.

In order to achieve these advantages, it is clear that other issues must be faced:

- Reduced autonomy, decreasing to only 1/3 of the original availability.
- Higher frequency in recharging/refuelling along its useful life, from every 3÷6 days to 1÷3 days.
- When energy runs out, longer time for recharging the battery respect to what needed to refuel, excluding the presence of fast-charging stations.
- Increased complexity of the powertrain, and number of components and management of their interaction.
- Higher maintenance operations and costs.

Furthermore, in order to present what may be the advantages of having a hybrid unit RE solution in addition to a normal BEV, the same simulations were performed on such an architecture and the results analysed, showing that a FC hybrid unit accounting for the 15% of the total installed power:

- Allows a 40% more range and time of utilization, while keeping the other components unchanged.
- Allows the EM and battery to be operated further away from their constructive power and current limits, increasing their useful life and reducing their need for maintenance.
- Although it costs more to refuel, allows additional range to be obtained in emergency situations or without interrupting vehicle operation.

- A battery with more energy and power must be added to the powertrain, increasing the weight of the vehicle, to achieve the same range.
- The advantages just presented are, however, achieved only as consequence of increased powertrain, propulsion system and management complexity, higher refuelling prices, reduced overall efficiency and higher cost of the complete solution.

In conclusion, the "Follow me" solution with a fuel cell hybrid propulsion system proves to be a feasible, viable and reliable solution that can lead to advantages over other possible solutions, while having to deal with a number of disadvantages and complexities that are far greater than the same other solutions. Some of them, such as the cost of the technology and fuel, the high initial investment, the lack of infrastructure and the significant WTT emissions, can be considerably decreased in the future, increasing the convenience of the solution presented in this project. Until then, this solution will undoubtedly remain a prototype with promising results, but for obvious technological and economic reasons it is unlikely to be preferred to BEV or HEV with combustion engines.

6.2.2. Critical analysis and future phases

In what has been achieved so far, some general critical considerations can be expressed on how it has been achieved, how it could have been done better, what could be modified and what experience can bring for the future. In this way, this may can be useful to understand the complexities and difficulties that can be encountered in the realisation of a certain type of project, as well as to keep some points open for later stages of the project or future similar ones:

- The price of components and the *budget available is a strong limitation* to what is possible to achieve certain performance, sometimes even more crippling than the possibilities and engineering skills possessed.
- In the same way, the *lack of information possessed on commercial elements* or the unavailability of their communication of by direct suppliers, most often due to confidentiality, can be a source of errors and constant changes.
- In the real choice phase of the elements that make up the powertrain, considering the budget and time constraints, it is necessary to look for a *consequential logic in the selection*

of the components, which cannot only come directly from the analysis of the requirements from the data analysis. In fact, the best thing to do turns out to be to first define the vehicle's traction motor, whose power, torque, speed, current and voltage characteristics make it possible to choose the elements that provide it with sufficient energy to make maximum use of its characteristics. The power generation elements of the vehicle must be selected before the conversion elements, due to the same logic presented for the traction motor. More details can be analysed in advance when selecting the actual components, e.g. geometry, volume and weight, can greatly simplify more advanced stages of the project.

- It is advantageous for the performance of the vehicle to have the powertrain look for a *higher voltage for the HV bus*, as it allows lower current values, making it easier to comply with overcharge and discharge limits keeping the same power. It also allows better characteristic curves to be obtained from the same EM, as well as allowing wiring with less cross-sectional area for the same current, also decreasing losses.
- A complete and thorough *prior knowledge of how a CF works is fundamental* to the realisation of a hybrid vehicle that utilises this type of power, even better if this knowledge is at a chemical level. Lacking the ability to know and understand at each stage of the activity what conditions need to be conceived, designed and engineered for the optimal functioning of the FC can lead to often having to modify things at later stages of the activity, increasing the time and complexity of operations.
- It will probably be necessary in later stages of the project to *evaluate an EMS for the FC that is TC*, as it could lead to a higher efficiency of the system, considering its limited power level. Until now, only a PFC strategy has been studied because it was more complex and engineering-wise interesting, but this does not necessarily imply that it is the most efficient for any type of powertrain and driving mission characteristics.
- The validity of the results of *software simulations of vehicle dynamics must be validated by experimental tests* in order to allow a greater degree of confidence in the realisation of vehicle models, knowing what influence they may have on the final realisation of a real prototype. Similarly, it is important to make software models as realistic as possible, to the limits of perfection, as approximations even if small can add up and lead to more substantial differences.

Having presented the activity in all its phases so far, for the sake of completeness the next phases of the project will now be presented, which will lead to its completion in 2025 with the realisation of the prototype of the airport vehicle and real tests in the research centre:

1. Technical drawing of the *powertrain design*: once the various elements of the hybrid propulsion system have been acquired, and the complete list of components to be added to the architecture and all their measurements are available, the powertrain must be created and designed. Either as a theoretical draft or as a drawing via software, all elements must be positioned within the vehicle chassis in an efficient and safe manner, drawing all supports and fastening elements useful for positioning them (These supports and fastening elements will be produced directly in the research centre). During this phase, the Power Distribution Box (PDB), which is the unit that combines and allows the delivery of power to all critical traction and auxiliary electric components, while protecting electronic components and vehicle occupants, will also be designed.
2. *Testing of real components*: once the various elements of the hybrid powertrain have been purchased and are available in INSIA, each of them will be put through their paces in dedicated engine benches and test platforms to obtain real data on their operation at various operating regimes. This will be necessary to obtain more precise data on the various elements in order to understand the most correct way to manage them and their physical and electrical connection with the correct current and voltage values.
3. *Hardware-in-the-loop realisation*: knowing all the characteristics of the elements, the EMS is refined and exported for the creation of the Hardware-in-the-loop (HIL), a method of testing and validating the strategy software on specially equipped test platform, simulating the ECU of the vehicle, which receives data inputs from physical devices such as throttle and braking pedals. This step is necessary to adapt the EMS to an implementable version in the control unit of the real vehicle.
4. *Composed powertrain testing*: once the powertrain design has been realised and the elements have been tested individually, they are assembled in a test platform recreating the layout within the vehicle, to simulate the joint and actual operation. At this stage the EMS is used for the actual control of the real vehicle elements, resulting in a strategy that can be physically evaluated, corrected in the HIL and ready to be actually installed in the vehicle ECU.

5. *Installation of components*: the hybrid architecture designed to date is officially realised by placing the powertrain elements inside the chassis and joining them together for final operation. The elements of the old hybrid combustion propulsion system are removed to make room for the new ones, while all physical, mechanical and electrical connections are made between them and between them and the driveline to enable prototype operation.
6. *Chassis dynamometer test*: the physically realised prototype is placed on the chassis dynamometer to simulate the vehicle's operation in various road conditions in a controlled environment, to assess its operation in a safe manner, without using it outdoors.
7. *On-road testing*: finally, the prototype is used in real-life operation tests inside the research centre's track, testing its real-life use in an actual environment, albeit not the airport, but able to validate its usefulness. The results obtained will be able to define the final characteristics obtainable from the new “Follow me” FCEV thus conceived, designed and realised, drawing conclusions and concluding the project.

Bibliography

[1]. *Madrid Barajas International Airport - Airport Information and Guide*. Barajas. (n.d.). Retrieved October 13, 2022, from https://www.aeropuertomadrid-barajas.com/eng/home.html

[2]. *Plan de Acción Climática 2021-2030 - Aena*. AENA. (n.d.). Retrieved October 17, 2022, from https://www.aena.es/sites/Satellite?blobcol=urldata&blobkey=id&blobtable=MungoBlobs&blobwhere=1576856428662&ssbinary=true

[3]. *CANmod.gps: GPS-to-can with 3D inertial sensor and UDR*. CSS Electronics. (n.d.). Retrieved October 17, 2022, from https://www.csselectronics.com/products/gps-to-can-bus-gnss-imu

[4]. *The 17 goals | Sustainable Development*. (n.d.). Retrieved October 17, 2022, from https://sdgs.un.org/goals

[5]. Sreenath, S., Sudhakar, K., & Yusop, A. F. (2021). *Sustainability at airports: Technologies and best practices from ASEAN countries*. Journal of Environmental Management, 299, 1–12. https://doi.org/10.1016/j.jenvman.2021.113639

[6]. Benito, F. J. (2021, April 27). *Los Aeropuertos Españoles Avanzan hacia su Descarbonización*. Verde y Azul. Retrieved October 13, 2022, from https://verdeyazul.diarioinformacion.com/los-aeropuertos-espanoles-avanzan-hacia-su-descarbonizacion.html

[7]. Navarro, D. (2018, January 31). *Innvextran: todoterreno hibrido enchiufable Eléctrica fabricado en España*. Retrieved October 18, 2022, from https://www.autofacil.es/coches-electricos-e-hibridos/innvextran-todoterreno-hibrido-enchufable-hecho-espana/86573.html

[8]. Ravello, V. (2021, May 9) CRF-STELLANTIS. E-Powertrain Components *Lecture 18: Applications and vehicle integration in Simple-Series HEVs*.

[9]. Wikimedia Foundation. (2022, August 26). *Aircraft marshalling*. Retrieved October 17, 2022, from https://en.wikipedia.org/wiki/Aircraft_marshalling

[10]. Mercedes-Benz Group Media. (n.d.). *Smart versatility: Putting in a smart appearance with the police and Fire Brigade*. Mercedes-Benz Group AG. Retrieved October 19, 2022, from https://media.daimler.com/marsMediaSite/en/instance/ko/smart-versatility-Putting-in-a-smart-appearance-with-the-police-and-fire-brigade.xhtml?oid=9361620

[11]. *Höchster Sicherheitsstandard am Flughafen: Hamburg Airport Führt Innovatives System zur Bewertung des pistenzustands ein*. Innovatives System zur Bewertung des Pistenzustands - Hamburg Airport. (n.d.). Retrieved October 19, 2022, from https://hha-prod-waf.cms.hamburg-airport.de:8443/blueprint/servlet/de/unternehmen/presse/pressemitteilungen/archiv/innovatives-system-zur-bewertung-des-pistenzustands-35498?userVariant

[12]. *Huracán Evo is the new follow-me car at Bologna Airport*. Lamborghini.com. (n.d.). Retrieved October 19, 2022, from https://www.lamborghini.com/en-en/news/huracan-evo-is-the-new-follow-me-car-at-bologna-airport

[13]. Zhao, X., Wang, L., Zhou, Y., Pan, B., Wang, R., Wang, L., & Yan, X. (2022). *Energy Management Strategies for fuel cell hybrid electric vehicles: Classification, comparison, and outlook.* Energy Conversion and Management, 270, 116179. https://doi.org/10.1016/j.enconman.2022.116179

[14]. Bauman, J., & Kazerani, M. (2008). *A comparative study of fuel-cell–battery, fuel-cell–ultracapacitor, and fuel-cell–battery–ultracapacitor vehicles*. IEEE Transactions on Vehicular Technology, *57*(2), 760–769. https://doi.org/10.1109/tvt.2007.906379

[15]. Daud, W. R. W., Rosli, R. E., Majlan, E. H., Hamid, S. A. A., Mohamed, R., & Husaini, T. (2017). *PEM fuel cell system control: A Review.* Renewable Energy, 113, 620–638. https://doi.org/10.1016/j.renene.2017.06.027

[16]. Blunier, Benjamin, et al. *Proton Exchange Membrane Fuel Cells Modeling*, John Wiley & Sons, Incorporated, 2012. *ProQuest Ebook Central*, https://ebookcentral.proquest.com/lib/polito-ebooks/detail.action?docID=1124648

[17]. Alternative Fuel Data Center. (n.d.). *How do fuel cell electric vehicles work using hydrogen?* U.S. Departament of Energy. Retrieved October 27, 2022, from https://afdc.energy.gov/vehicles/how-do-fuel-cell-electric-cars-work

[18]. Hussain, M. M., & Dincer, I. (2010). *Life cycle assessment of hydrogen fuel cell and gasoline vehicles.* Electric and Hybrid Vehicles, 275–286. https://doi.org/10.1016/b978-0-444-53565-8.00011-7

[19]. Ren, L., Zhou, S., & Ou, X. (2020). *Life-cycle energy consumption and greenhouse-gas emissions of hydrogen supply chains for fuel-cell vehicles in China.* Energy, 209, 118482. https://doi.org/10.1016/j.energy.2020.118482

[20]. Liu, X., Reddi, K., Elgowainy, A., Lohse-Busch, H., Wang, M., & Rustagi, N. (2020). *Comparison of well-to-wheels energy use and emissions of a hydrogen fuel cell electric vehicle relative to a conventional gasoline-powered internal combustion engine vehicle.* International Journal of Hydrogen Energy, 45(1), 972–983. https://doi.org/10.1016/j.ijhydene.2019.10.192

[21]. Colella, W. G., Jacobson, M. Z., & Golden, D. M. (2005). *Switching to a U.S. hydrogen fuel cell vehicle fleet: The resultant change in emissions, energy use, and greenhouse gases.* Journal of Power Sources, 150, 150–181. https://doi.org/10.1016/j.jpowsour.2005.05.092

[22]. Ahmadi, P., & Khoshnevisan, A. (2022). *Dynamic simulation and lifecycle assessment of hydrogen fuel cell electric vehicles considering various hydrogen production methods.* International Journal of Hydrogen Energy, *47*(62), 26758–26769. https://doi.org/10.1016/j.ijhydene.2022.06.215

[23]. Evangelisti, S., Tagliaferri, C., Brett, D. J. L., & Lettieri, P. (2017). *Life cycle assessment of a polymer electrolyte membrane fuel cell system for passenger vehicles*. Journal of Cleaner Production, 142, 4339–4355. https://doi.org/10.1016/j.jclepro.2016.11.159

[24]. Kannangara, M., Bensebaa, F., & Vasudev, M. (2021). *An adaptable life cycle greenhouse gas emissions assessment framework for electric, hybrid, fuel cell and conventional vehicles: Effect of electricity mix, mileage, battery capacity and battery chemistry in the context of Canada.* Journal of Cleaner Production, 317, 128394. https://doi.org/10.1016/j.jclepro.2021.128394

[25]. Greer, F., Rakas, J., & Horvath, A. (2020). *Airports and environmental sustainability: A comprehensive review.* Environmental Research Letters, 15(10), 103007. https://doi.org/10.1088/1748-9326/abb42a

[26]. Overton, J. (Author), Bresette, D. (Editor), Werner, C. (Editor), & McGann, A. (Editor), (2022, June 9). *Issue Brief | The Growth in Greenhouse Gas Emissions from Commercial Aviation*. EESI Environmental and Energy Study Institute. Retrieved October 22, 2022, from https://www.undp.org/publications/issue-brief-just-transition

[27]. *Future of aviation*. ICAO - Uniting Aviation, A United Nation Specialised Agency. (2022). Retrieved October 22, 2022, from https://www.icao.int/Meetings/FutureOfAviation/Pages/default.aspx

[28]. Hájnik, A., Harantová, V., & Kalašová, A. (2021). *Use of electromobility and autonomous vehicles at airports in Europe and worldwide.* Transportation Research Procedia, 55, 71–78. https://doi.org/10.1016/j.trpro.2021.06.008

[29]. CDM Federal Programs Corporation, KB Environmental Sciences, Inc., & Ricondo & Associates, Inc. (2012). *Airport Ground Support Equipment (GSE): Emission reduction strategies, inventory, and tutorial.* ACRP Report 78. https://doi.org/10.17226/22681

[30]. Testa, E., Giammusso, C., Bruno, M., & Maggiore, P. (2013). *Analysis of environmental benefits resulting from use of hydrogen technology in handling operations at airports.* Clean Technologies and Environmental Policy, 16(5), 875–890. https://doi.org/10.1007/s10098-013-0678-3

[31]. Published by N. Sönnichsen, & 3, A. (2022, August 3). *Number of hydrogen fuel stations by country (2021)*. Statista. Retrieved October 22, 2022, from https://www.statista.com/statistics/1026719/number-of-hydrogen-fuel-stations-by-country/

[32]. Martín, R. (2011, May 31). *Aena intruduce el vehículo eléctrico en sus aeropuertos*. Motor.es. Retrieved October 24, 2022, from https://www.motor.es/noticias/aena-intruduce-el-vehiculo-electrico-en-sus-aeropuertos.php

[33]. *More electric GSE at Stuttgart airport.* Ground Handling International. (n.d.). Retrieved October 24, 2022, from https://magazine.groundhandling.com/news/stuttgart-airport-reinforces-its-green-credentials/

[34]. *Electric Mobility Action Plan in LAirA airport FUAs*. Interreg central europe. (n.d.). Retrieved October 24, 2022, from https://www.interreg-central.eu/Content.Node/Electric-Mobility-Action-Plan.pdf

[35]. Dimitrova, M. (2018, April 13). *Autonomous vehicles: Future-proofing the airport environment*. Future Travel Experience. Retrieved October 24, 2022, from https://www.futuretravelexperience.com/2018/04/autonomous-vehicles-future-proofing-the-airport-environment/

[36]. *JetBlue introduces the largest electric ground service equipment (EGSE) fleet at New York's JFK International Airport, cutting four million pounds of greenhouse gas emissions per year*. JetBlue. (n.d.). Retrieved October 24, 2022, from http://mediaroom.jetblue.com/investor-relations/press-releases/2019/09-26-2019-170227350

[37]. Banks, K. (2019, October 11). *Electrification at Canada's airports: Ambitious to uninspired*. Electric Autonomy Canada. Retrieved October 24, 2022, from https://electricautonomy.ca/2019/05/07/electrification-at-canadas-airports/

[38]. Pande, P. (2020, November 10). *Indian airports look to electric vehicles*. Simple Flying. Retrieved October 26, 2022, from https://simpleflying.com/indian-airport-electric-vehicles/

[39]. Director. (2019, May 23). *Primer vehículo follow me Eléctrico Aeropuerto alicante*. Aviación Digital. Retrieved October 24, 2022, from https://aviaciondigital.com/aeropuerto-de-alicante-elche-adquiere-su-primer-coche-follow-me-electrico/

[40]. Editor, S. (2022, October 21). *Citroen Ami as follow-me-car in Genoa: Zero emissions below - electromobility (E-mobility), airports: Information: Vision mobility*. SasaTimes. Retrieved October 24, 2022, from https://sasatimes.com/citroen-ami-as-follow-me-car-in-genoa-zero-emissions-below-electromobility-e-mobility-airports-information-vision-mobility/

[41]. Automotive World. (2015, June 3). *All-electric zoe takes off at Tag Farnborough Airport*. Automotive World. Retrieved October 24, 2022, from https://www.automotiveworld.com/news-releases/electric-zoe-takes-tag-farnborough-airport/

[42]. Elsevier Advanced Technology - Mark Allen Group (MAG). (2006, July). *Fuel cell airport vehicle in series production*. Fuel Cells Bulletin. Retrieved October 26, 2022, from https://www.journals.elsevier.com/fuel-cells-bulletin

[43]. Burmeister, W. (2017, August). *Hydrogen Project at Munich Airport*. ARGEMUC. Retrieved October 26, 2022, from https://www.semanticscholar.org/paper/HYDROGEN-PROJECT-AT-MUNICH-AIRPORT/3480a0990b1426b82e598648843d697cd0b5a74e

[44]. Elsevier Advanced Technology - Mark Allen Group (MAG). (2019, October 10). *Plug power showcases fuel cell powered GSE project at Local Airport*. Fuel Cells Bulletin. Retrieved October 26, 2022, from https://www.sciencedirect.com/science/article/pii/S1464285919303633

[45]. Gauchia, L., Fontela, P., Soria, A., Mielgo, J., Sierra, J. F., de Blas, J., & Martinez, J. M. (2014, April 22). *Airport electric vehicle powered by Fuel Cell*. Journal of Power Sources. Retrieved October 26, 2022, from https://www.academia.edu/298895/Airport_Electric_Vehicle_Powered_by_Fuel_Cell

[46]. IEA. (n.d.). *How much will renewable hydrogen production drive demand for new renewable energy capacity by 2027? – analysis*. IEA - International Energy Agency. Retrieved January 28, 2023, from

https://www.iea.org/reports/how-much-will-renewable-hydrogen-production-drive-demand-for-new-renewable-energy-capacity-by-2027

[47]. Paternostro, M. (2022, June 28). *Auto a idrogeno, Tipologia, Prezzi, Caratteristiche e Quali in Vendita*. newsauto.it. Retrieved October 27, 2022, from https://www.newsauto.it/guide/auto-idrogeno-caratteristiche-prezzi-autonomia-2022-258855/

[48]. *CANmod.gps: GPS-to-can with 3D inertial sensor and UDR*. CSS Electronics. (n.d.). Retrieved October 17, 2022, from https://www.csselectronics.com/products/gps-to-can-bus-gnss-imu

[49]. *New Ford Ranger – technical specifications*. Ford Media Center. (n.d.). Retrieved November 12, 2022, from https://media.ford.com/

[50]. Wu, X., Freese, D., Cabrera, A., & Kitch, W. A. (2015*). Electric vehicles' energy consumption measurement and estimation.* Transportation Research Part D: Transport and Environment, 34, 52–67. https://doi.org/10.1016/j.trd.2014.10.007

[51]. *Energy consumption of full electric vehicles*. EV Database. (n.d.). Retrieved November 26, 2022, from https://ev-database.org/cheatsheet/energy-consumption-electric-car

[52]. *Iveco Massif specifications*. Massif in detail. (n.d.). Retrieved December 3, 2022, from https://www.iveco.com/en-us/press-room/kit/pages/massif_in_detail.aspx

[53]. Zhao, X., Wang, L., Zhou, Y., Pan, B., Wang, R., Wang, L., & Yan, X. (2022). *Energy Management Strategies for fuel cell hybrid electric vehicles: Classification, comparison, and outlook.* Energy Conversion and Management, 270, 116179. https://doi.org/10.1016/j.enconman.2022.116179

[54]. Tran, D.-D., Vafaeipour, M., El Baghdadi, M., Barrero, R., Van Mierlo, J., & Hegazy, O. (2020). *Thorough state-of-the-art analysis of electric and hybrid vehicle powertrains: Topologies and Integrated Energy Management Strategies.* Renewable and Sustainable Energy Reviews, 119, 109596. https://doi.org/10.1016/j.rser.2019.109596

[55]. Melero-Perez, A., Wenzhong Gao, & Fernandez-Lozano, J. J. (2009). *Fuzzy Logic Energy Management Strategy for fuel cell/Ultracapacitor/Battery hybrid vehicle with multiple-input DC/DC converter.* 2009 IEEE Vehicle Power and Propulsion Conference. https://doi.org/10.1109/vppc.2009.5289851

[56]. Sarvaiya, S., Ganesh, S., & Xu, B. (2021). *Comparative analysis of hybrid vehicle energy management strategies with optimization of fuel economy and battery life.* Energy, 228, 120604. https://doi.org/10.1016/j.energy.2021.120604

[57]. Peng, J., He, H., & Xiong, R. (2017). Rule based Energy Management Strategy for a series–parallel plug-in hybrid electric bus optimized by Dynamic Programming. *Applied Energy*, *185*, 1633–1643. https://doi.org/10.1016/j.apenergy.2015.12.031

[58]. Zheng, chunhua, Zhang, D., Xiao, Y., & Li, W. (2022). Reinforcement learning-based energy management strategies of fuel cell hybrid vehicles with multi-objective control. *SSRN Electronic Journal*. https://doi.org/10.2139/ssrn.4129106

[59]. Boekel, J. J. P. V., Besselink, I. J. M., & Nijmeijer, H. (2015, June 26). *Design and realization of a one-pedal-driving algorithm for the TU/e Lupo El*. MDPI. Retrieved December 27, 2022, from https://www.mdpi.com/2032-6653/7/2/226

[60]. *Alternative fuels data center. Charging Electric Vehicles at Home*. U.S. Department of Energy. Energy Efficiency & Renewable Energy. Retrieved Januaty 22, 2023, from https://afdc.energy.gov/fuels/electricity_charging_home.html

[61]. Iea. (n.d.). *Executive summary – Global hydrogen review 2021 – Analysis*. IEA. Retrieved January 22, 2023, from https://www.iea.org/reports/global-hydrogen-review-2021/executive-summary

[62]. Iea. (n.d.). *Trends in charging infrastructure – Global EV Outlook 2022 – analysis*. IEA. Retrieved January 22, 2023, from https://www.iea.org/reports/global-ev-outlook-2022/trends-in-charging-infrastructure

[63]. Ravello, V. (2021, May 9) CRF-STELLANTIS. E-Powertrain Components *Lecture 22: Applications and vehicle integration in Fuel Cell Electric Vehicles*.

[64]. Harris, T. P., Nix, A. C., Perhinschi, M. G., Wayne, W. S., Diethorn, J. A., & Mull, A. R. (2021). Implementation of radial basis function artificial neural network into an adaptive equivalent consumption minimization strategy for optimized control of a hybrid electric vehicle. *Journal of Transportation Technologies*, *11*(04), 471–503. https://doi.org/10.4236/jtts.2021.114031

[65]. Hryshchenko, T. (2021, August 10). *What are fuel cells/how do they work?* Turbomachinery blog. Retrieved February 1, 2023, from https://blog.softinway.com/an-introduction-to-fuel-cells-what-are-they-how-do-they-work-and-how-can-we-improve-their-efficiency/

[66]. Tsakyridis, G., Xiros, N. I., Scharringhausen, M., & Witte, L. (2020). Design and control of a DC boost converter for fuel-cell-powered marine vehicles. *Journal of Marine Science and Application*, *19*(2), 246–265. https://doi.org/10.1007/s11804-020-00140-8

[67]. Three-dimensional PEM fuel cells modeling using COMSOL multiphysics. (2017). *The International Journal of Multiphysics*, *11*(4). https://doi.org/10.21152/1750-9548.11.4.427

[68]. Thounthong, P., Pierfederici, S., Martin, J.-P., Hinaje, M., & Davat, B. (2010). Modeling and control of Fuel Cell/supercapacitor hybrid source based on differential flatness control. *IEEE Transactions on Vehicular Technology*, *59*(6), 2700–2710. https://doi.org/10.1109/tvt.2010.2046759

[69]. Thounthong, P., Raël, S., & Davat, B. (2009). Energy Management of fuel cell/battery/supercapacitor hybrid power source for vehicle applications. *Journal of Power Sources*, *193*(1), 376–385. https://doi.org/10.1016/j.jpowsour.2008.12.120

[70]. Raceanu, M., Marinoiu, A., Culcer, M., Varlam, M., & Bizon, N. (2014). Preventing reactant starvation of a 5 kW PEM fuel cell stack during sudden load change. *Proceedings of the 2014 6th International Conference on Electronics, Computers and Artificial Intelligence (ECAI)*. https://doi.org/10.1109/ecai.2014.7090147

Acknowledgments

It is my duty to dedicate this space of my thesis to the people and institutions that contributed, with their support, possibilities, help and knowledge, to the path of these months in the activity and realization of the elaborate.

First and foremost, special thanks to my supervisor Andrea Tonoli for his patience, advice, guidance and knowledge conveyed throughout the realization of the thesis. In general, I would like to thank the Politecnico di Torino and all the professors I met during the Master's course for all the knowledge transmitted, bringing me closer to and immersing me in the automotive world, what I can now say is one of my greatest passions and a means of pursuing my personal and professional dreams. The commitment put in despite and after the pandemic situation, which characterised the entire first year of teaching, was a demonstration of professionalism and seriousness, which in times of difficulty are never taken for granted qualities.

Asimismo, mi agradecimiento a mi co-relator José María López Martínez, también por darme la oportunidad de ser acogido en la familia INSIA y la posibilidad de realizar mi Tesis en este centro de investigación. En general, también me gustaría dar las gracias a la Universidad Politécnica de Madrid, a todos los profesores que conocí a lo largo del camino, y especialmente al centro de investigación INSIA, que en poco tiempo me acogió con inmenso respeto y fraternidad, a pesar de ser de otro País, haciéndome sentir parte de esta gran familia y apasionándome por el mundo de la investigación. Quiero agradecer especialmente a mi equipo de DISPIMA, Enrique Alcalà, Jaime Alvarez, Victor Del Pozo, Nuria Flores y Juan Pastor, que compartieron conmigo sus conocimientos y me ayudaron generosamente en la realización de la actividad en todas sus fases.

Ringrazio infinitamente la mia famiglia, Elisa, Massimo, Daniele e Cesare, che mi ha sempre sostenuto, appoggiando ogni mia decisione, fornendomi insegnamenti di vita preziosi nelle più svariate occasioni nel corso di questi due anni. Riconosco ed apprezzo soprattutto l'enorme appoggio datomi nel momento in cui decisi di allontanarmi da casa, per il mio percorso Erasmus prima e successivamente quando decisi di proseguire la mia vita in Spagna per la attività lavorativa.

Finally, special thanks also to the all the students and colleagues I have met during my studies, both in Italy and in Spain, whose knowledge and skills have allowed me to grow and develop my own, inside and outside the university classroom. I would also like to thank all my friends enormously, who during these two years have always been supportive and provided me with important advice for my academic and personal life.